This is to certify that the
dissertation entitled

INVESTIGATING A NOVEL FUNCTION OF HISTONE H3 IN MITOTIC CHECKPOINT CONTROL IN *SACCHAROMYCES CEREVISIAE*

presented by

Jianjun Luo

has been accepted towards fulfillment
of the requirements for the

Ph.D. degree in Biochemistry and Molecular Biology

Major Professor's Signature

7/15/2010

Date

INVESTIGATING A NOVEL FUNCTION OF HISTONE H3 IN MITOTIC CHECKPOINT CONTROL IN *SACCHAROMYCES CEREVISIAE*

By

Jianjun Luo

A DISSERTATION

Submitted to
Michigan State University
in partial fulfillment of the requirements
for the degree of

DOCTOR OF PHILOSOPHY

Biochemistry and Molecular Biology

2010

ABSTRACT

INVESTIGATING A NOVEL FUNCTION OF HISTONE H3 IN MITOTIC CHECKPOINT CONTROL IN *SACCHAROMYCES CEREVISIAE*

By

Jianjun Luo

Erroneous segregation of eukaryotic genome causes aneuploidy that is the leading cause of first-trimester miscarriages and is also intimately linked to certain developmental defects and cancers. To prevent missegregation, dividing cells monitor both kinetochore-spindle attachment and the tension between sister chromatids. Mitotic tension is a result of bipolar attachment, that is, spindles emanating from opposite spindle pole bodies attach to and pull each of the two sister kinetochores. Although it has been firmly established that many interphase nuclear functions, including transcriptional regulation, are regulated by chromatin and histones, how mitotic progression and quality control might be influenced by histones is still less well characterized. Our studies indicated that histone H3 plays a crucial role in activating the spindle assembly checkpoint in response to a defect in mitosis. Lack of tension due to erroneous attachment activates the spindle assembly checkpoint, which corrects the mistakes and ensures segregation fidelity. A histone H3 mutation (Gly44 to Ser) impairs the ability of yeast cells to activate the checkpoint in a tensionless crisis, leading to missegregation and aneuploidy. The defects in tension sensing result directly from an attenuated H3-Sgo1p interaction essential for pericentric recruitment of Sgo1p. Reinstating the pericentric enrichment of Sgo1p alleviates the mitotic

defects. Histone H3, and hence the chromatin, is thus a key factor transmitting the tension status to the spindle assembly checkpoint.

Further studies on characterizing the interaction between H3 and Sgo1p led to the discovery that the tension sensing function depends critically on a unique "tension sensing motif", or TSM, of histone H3. Lys42, Gly44, and Thr45 of H3 form a core of a motif executing a mitotic function that is pivotal for cells to respond to the lack of tension between sister chromatids. This motif functions through physically recruiting or retaining Sgo1p at the pericentromeres. Intriguingly, the histone acetyltransferase activity of Gcn5p likely plays a negative role in H3 TSM-Sgo1p function. These results reveal that a TSM of histone H3 is a key player in faithful segregation of mitotic chromosomes, and that interaction with a chromatin modifying enzyme may be an important part of the mitotic quality control process.

ACKNOWLEDGMENTS

I gratefully acknowledge my advisor, Dr. Min-Hao Kuo, for his years of advice, supervision, and contribution to my research. This work would not have been possible without his encouragement and support. I would also like to acknowledge my committee members, Dr. Dean DellaPenna, Dr. R. William Henry, Dr. Laura R. McCabe, and Dr. John L. Wang, for their continuous guidance and support. Many thanks go in particular to Xinjing Xu, our previous lab manager/research scientist, for her selfless assistance in my research and life. I would like to thank many Kuo lab members, Dr. Yang Liu, Dr. Asha Acharya, David Almy, Xiaobo Li, for their valuable discussion and help in my research. I also want to thank Dr. David N. Arnosti, Dr. Zachary Burton, and Dr. Colleen Doherty for their comments and suggestions in my research. I would like to indicate my gratitude to Dr. Pamela J. Fraker, Dr. Louis King, and Dr. Joseph Leykam for their guidance and technical assistance. I also want to thank the Department of Biochemistry and Molecular Biology and the GEDD group for the financial support. Finally, I want to express my gratitude wholeheartedly to my wife Xiangyi Wang, my son Gerald Yanming Luo, my parents and parents-in-law for their support and love.

TABLE OF CONTENTS

Images in this thesis/dissertation are presented in color

LIST OF TABLES

LIST OF FIGURES

CHAPTER II: Histone H3 Exerts a Key Function in Mitotic Checkpoint Control

CHAPTER I

Literature Review

Literature Review

Part I: Nucleosome structure and roles of histones in cell cycle progression

Nucleosome composition, positioning and centromeric nuclesome

In eukaryotes, the enormous length of genomic DNA needs to be packaged into a higher order nucleoprotein complex termed chromatin, whose basic repeat unit is the nucleosome. The nucleosome core particle consists of 146 base pairs (bp) of DNA wrapped in 1.65 left-handed superhelical turns around a histone octamer, which is formed by four histone partners: an H3-H4 tetramer and two H2A-H2B dimers (99). Histones are small basic proteins consisting of a globular domain and a more flexible and charged NH_2-terminal tail that protrudes from the nucleosome. The distinct levels of chromatin organization are dependent on the dynamic higher order structuring of nucleosomes (65). Nucleosomes are connected to each other via a linker DNA of characteristic length. Linker histone H1 is bound to the nucleosome at the point where the DNA enters and exits the core, and to the linker DNA. The internucleosomal associations also can be mediated by direct interactions between histone H4 amino-terminal tail and the acid patch of the H2A/H2B (25, 141).

Due to the organization into nucleosome and the highly compacted chromatin structure, genomic DNA sequences can be more or less accessible to

transcription, DNA repair or DNA recombination machinery (9, 42, 70, 135). Recently, genomic technologies have been widely used to map nucleosome positioning across genomes, and results similarly point out that nucleosomes are highly phased near the 5' end of genes, a nucleosome-depleted region close to the transcriptional start site is flanked on both sides by positioned nucleosomes. The depletion of nucleosome at the promoter region favors the assembly of transcriptional machinery and the initiation of transcription (67, 106, 168, 176).

In the centromeres of the eukaryotic chromosome, the H3 variant CENP-A (Cse4p in budding yeast) is assembled into the centromere specific nucleosome (109, 143). Cse4p shares 64% identity to canonical H3 and exhibits similar DNA-binding characteristics as H3 (75, 147). Recently, Camahort and colleagues examined the composition of Cse4p-containing nucleosome and their results further supported the notion that Cse4p simply replaces H3 in an octameric nucleosome that contains Cse4p, H2A, H2B, and H4 (14). A kinetochore protein, Scm3p, originally thought to form a unique centromere specific hexameric nucleosome with Cse4p and H4 (112), may just be required when Cse4p protein levels are limited. Scm3p is not an essential component of Cse4p-containing centromeric chromatin (14).

Known histone alleles and chromatin function

So far, many histone mutations have been identified, and studies on these histone mutants have rapidly expanded our understanding of a variety of chromatin functions. The *sin* (switch-independent) alleles [H3 E105K (Glu105 to Lys mutation), H3 R116H, H3 T118I, H4 V43I, H4 R45H, H4 R45C], which sufficiently alter nucleosome mobility, nucleosome structure or higher order chromatin folding, partially bypass the need for the SWI/SNF chromatin remodeling complex in transcriptional regulation (33, 52, 88, 116, 133). The *lrs* (Loss of rDNA Silencing) alleles (H3 72-83, H4 78-81) cause a loss of repression of genes specifically embedded in transcriptionally silent regions of the genome (e.g., ribosomal DNA locus or telomeres) (122, 142). Although each of SIN and LRS domain consists of histone H3 and H4 L1 and L2 loops that form a DNA-binding surface at either superhelical location (SHL) ± 2.5 (LRS) or SHL ± 0.5 (SIN), these two domains are functionally distinct. Indeed, mutations in the LRS domain do not cause the *sin* phenotypes, and vice versa (35).

In addition to *sin* and *lrs* alleles which mainly affect the globular domain of histones, studies with deletions or single mutations on the flexible histone tail region have also provided evidence for chromatin functions in cell cycle progression. For instance, deleting the N-terminal domain of H3 or H4 delays progression through the G_2/M periods (114). Four lysine residues in the N-terminal domain of histone H4 (K5, K8, K12, K16), which are subjected to reversible acetylation, are required for the maintenance of genome integrity, and are important for DNA replication and nuclear division (107, 108). In an endeavor

to explore essential functions of H3 and H4 amino terminus, Ma *et al.* (102) carried out a genetic screen for second-site mutations that are lethal when combined with a H3 amino-terminal deletion, and identified *HSL1* and *HSL7* (histone synthetic-lethal gene). Hsl1p and Hsl7p are negative regulators of Swe1p (the *S. Cerevisiae* homolog of Wee1p) kinase. The Swe1p kinase inhibits mitotic Cdc28p kinase activity and destroys the function of morphogenesis checkpoint required for delaying mitosis when bud formation is impaired. Therefore, these cell cycle regulators function in a pathway upstream of H3 to modulate histone functions in the cell cycle (102).

Moreover, a histone H4 allele, *hhf1-20* (H4 T82I A89V double mutant), compromises the interaction between H4 and the centromere specific H3 variant Cse4p, thus impeding the functions of centromere and mitotic progression at the restrictive temperature (144). Two alleles of histone H2A (H2A S20F, H2A G30D) cause cold-sensitive growth defects, a significant increase in ploidy, increased chromosome loss rate, and altered chromatin structure over centromeric DNA, suggesting a critical role for histone H2A in centromere function (127). The hyperploidy phenotype can be suppressed by mutations affecting a histone deacetylases, *HDA1* (71). Together, these studies suggest a prominent role for histones in chromosome segregation; however, little is known about how histones proactively regulate the mitotic progression and cell cycle regulation.

Part II: Histone post-translational modifications

Each core histone contains an accessible N-terminal tail that is subjected to different post-translational modifications including methylation, phosphorylation, acetylation, ubiquitination, etc. (20, 64, 140, 148). Changes in chromatin structure and dynamics by histone post-translational modifications, chromatin remodeling, and DNA methylation, are correlatively associated with transcriptional regulation. The reversible acetylation of histones by histone acetyltransferases (HATs) and deacetylases (HDACs) regulates the accessibility of DNA and recruits select proteins for regulating transcription. Histone methylation, catalyzed by histone methyltransferases (HMTs) and cleared by a variety of demethylases (23, 82), acts primarily as docking sites for different proteins whose recruitment regulates the biochemical and structural characteristics of the underlying chromatin loci. DNA methylation exerts mighty effects, both locally and spanning an expansive chromatin locus, on gene activity (123).

Histone methylation

The majority of biological methylation reactions are catalyzed by methyltransferases that transfer the methyl group from S-adenosyl methionine (SAM, SAMe, or AdoMet) to the acceptor molecules including DNA, RNA, and selective arginine or lysine residues in proteins. Methylation of DNA and histones

has tremendous impacts on local and global gene activities, DNA repair, and epigenetic inheritance (17, 132, 151, 157). Synthesis of SAM involves the methionine adenosyltransferases (MATs), ATP, and methionine. Epigenetic regulation involving SAM includes methylation of DNA, histones, and several nonhistone transcriptional regulators, such as the tumor suppressor protein p53 and the general transcriptional factor TAF10 (55). DNA methylation represses transcription, and is essential for the maintenance of chromatin structure and genomic stability. Alterations of the promoter methylation have been associated with changes of transcription profiles of cancers. Consistently, transgenic mice with one of the two methionine adenosyltransferase genes (*MAT1A*) deleted revealed stunning development of hepatocellular cancer (HCC) by 18 months of age (97). Deleting *MAT1A* leads to drastic decrease of the liver SAM level and increase of serum methionine concentration. However, it should be noted that, it is unclear whether the cancerous development was ascribed to misregulation of DNA or histone methylation, or both. In this regard, it is interesting to note that the budding yeast *Saccharomyces cerevisiae* does not have DNA methylation, and hence may be a good model to delineate the effect of deleting the methionine adenosyltransferase genes (*SAM1* and *SAM2*) on protein methylation and gene expression (100).

In higher eukaryotes, H3 K4, K9, K27, K36, K79, and H4 K20 can be methylated (17). In general, methylation at H3 K4, K36, and K79 is associated with transcriptional activation, whereas methylation of H3 K9, K27, and H4 K20 are

marks of repressive chromatin states (110, 130). *In vitro* studies showed that tri-methylation of H4 at lysine 20 increased the ability of nucleosomal arrays to fold and condense, suggesting that histone methylation not only creates binding sites for proteins, but also likely affects higher order chromatin structure directly (98). Studies carried out in HeLa cells indicated that trimethylation on H3 K9 and H4 K20 in late G_2 is necessary for proper pericentric heterochromatin formation and chromosome segregation during mitosis (50). In fission yeast, H3 K9 methylation provides binding sites for heterochromatin protein (HP1) in RNAi-dependent heterochromatin assembly processes (44). In budding yeast, only H3 K4, K36, and K79 are known to be methylated by histone lysine methyltransferase enzymes, Set1p, Set2p, and Dot1p, respectively (111).

Histone phosphorylation

Phosphorylation of histone H3 plays an important role in the regulation of gene expression and in chromosome condensation. The long standing mystery for H3 serine 10 (S10) phosphorylation is that this modification appears to be involved in two structurally opposite processes: transcriptional activation (21, 61) which requires chromatin fiber decondensation, and chromosome compaction during cell division in which chromatin condensation is indispensible (48, 54, 160). H3 S10 phosphorylation begins during prophase, with peak levels detected during metaphase, and a general decrease in the amount of phosphorylation during the progression through the telophase (46). A similar correlation can be observed

during meiosis and a lack of H3 S10 phosphorylation inhibits meiosis in *Tetrahymena thermophila* (166, 167). Surprisingly, in budding yeast, mutation of S10A does not result in a major defect in chromosome transition, suggesting phosphorylation of H3 at S10 is not indispensible for cell-cycle progression in yeast (54).

Since the first discovery that phosphorylation of histone H3 S10 was associated with chromosome condensation and segregation during mitosis and meiosis (46), mitosis-specific phosphorylation of H3 has also been observed at H3 S28 (38) and at H3 threonine 11 (129). Although the H3 S31 residue exists only in histone variant H3.3, phosphorylation of H3 S31 occurs at centromeric regions of metaphase chromosomes (47). Interestingly, *S. cerevisiae* contains only one type of canonical H3, which is most similar to mammalian H3.3, and also contains serine 31 (10).

Mitosis-specific phosphorylation of H3 S10 starts in late G_2 phase on pericentromeric chromatin only. As mitosis proceeds, phosphorylation of H3 spreads along the chromosome arms and completes its coating on the entire chromosome at prophase (39, 51). The dephosphorylation process starts at anaphase and finishes at telophase (39, 51). Members of the Aurora serine/threonine kinase family have been found to govern histone H3 phosphorylation at H3 S10 during mitosis in several organisms (37, 54). In addition, Aurora B phosphorylates H3 S28 *in vitro* (149) and *in vivo* in

mammalian cells (39). In *S. cerevisiae*, the sole Aurora kinase encoded by the *IPL1* gene (18) is required for high-fidelity chromosome segregation (34). Cells bearing only a temperature-sensitive allele (*ipl1-2*) of *IPL1* show a reduction in the level of H3 S10 phosphorylation when grown at restrictive temperature (54).

14-3-3 proteins

14-3-3 proteins are a family of highly conserved, ubiquitously expressed, abundant acidic proteins in all eukaryotes studied (11). 14-3-3s were first recognized to interact with a discrete phosphoserine or phosphothreonine motif by forming homo- or heterodimers (174). While there are seven 14-3-3 isoforms in mammals, Bmh1p and Bmh2p are the only two 14-3-3 proteins in *S. cerevisiae*. Bmh1p and Bmh2p share 91% overall identity and >97% identity over their first 256 residues (36, 159). Simultaneous knockout of these two functionally redundant isoforms in *S. cerevisiae* is lethal (158). Bmh1p and Bmh2p are also required for a timely G_1/S transition, DNA damage checkpoints and genomic stability (95, 96). Recently, Macdonald and colleagues reported that three human 14-3-3 isoforms (ε, ζ, γ) bind H3 (aa 1-20) peptides in a phosphorylation dependent fashion (103). Our data also showed that Bmh1p binds preferentially to phosphorylated H3 (Luo and Kuo, unpublished data).

Histone acetylation

Acetyl coA (Ac-coA) is the acetate donor for acetylation reactions, in which the acetyl group is transferred from Ac-coA to the lysine ε-amino group on the N-terminal tail of histones. In mammalian cells, Ac-coA can be synthesized via two routes. Ac-coA synthetase, like many fungal cells, condenses acetate and coenzyme A into Ac-coA. In the second pathway, the ATP-citrate lyase (ACL) uses energy from ATP hydrolysis to convert citrate, a TCA cycle product/intermediate, and coenzyme A into Ac-coA and oxaloacetate. Boeke and colleagues used the budding yeast as the model to show that one of two Ac-coA synthetases in yeast, Acs2p, also regulates the global acetylation of histones, and that synthetic lethality results from deleting a key histone acetyltransferase (HAT), Gcn5p, in an *acs2*-conditional mutant (153).

Acetylation of core histones has been shown to enhance the affinity of transcription factors for nucleosomal DNA (69, 91, 163) and may cause a conformational change in nucleosome structure (3, 121). The acetylation of histones by HATs is thought to affect chromatin function through two different mechanisms. First, it neutralizes the positive charge of the lysine ε-amino groups on the N-terminal tail of histones, which to some extent changes the structural characteristics of the histone or the binding to the DNA (3, 121). Second, this epigenetic mark serves as recognition sites for the binding of transcriptional factors to promote transcription (5, 16, 57). Histone acetylation is a reversible process, acetyl groups can be removed by histone deacetylases to reestablish the positive charge in the histones (84).

Histone acetylation has been linked to transcriptional activation. Studies showed that histone acetylation sites and HATs are indispensible for gene expression (29, 84, 86, 134). Genome-wide analyses on histone acetylation indicated that acetylation at a majority of lysine residues in histone H3 and H4 tails correlates positively with gene transcription (87, 94, 128). Since the identification of yeast transcriptional adaptor Gcn5p as catalytic subunit of type A histone acetyltransferase (13), Gcn5p has been shown the capability to acetylate H3 (at K9,14,18), H4 (K8, K16), and H2B (K11, 16) (85, 114, 150, 165, 178). The modulation of transcription by Gcn5p is independent of its known coactivator function (58). Recently, H3 K36 has also been identified as an acetylation site by Gcn5p, and ChIP-chip experiments demonstrated that H3K36 acetylation predominantly localized to the promoters of RNA polymerase II transcribed genes. This pattern is similar to that of other acetylation sites including H3 K9 and K14 but completely inversely related to that of H3 K36 methylation, suggesting the existence of an acetyl/methyl switch that governs chromatin function during transcription process (115). In addition, 28% of H3 in yeast contains acetylated K56 (172). H3 K56 acetylation by Rtt109 correlates with actively transcribed genes and associates with the elongating form of polymerase II in yeast (137).

The temporal acetylation on N-terminal tails of H3 and H4 is important for newly synthesized histones to be assembled into nucleosomes (145). For example, acetylation on H3 K56, which resides within the globular core domain of histone

H3, was demonstrated to be critical in nucleosome assembly following DNA replication and repair, implying the importance of H3 K56 acetylation on genomic stability (19, 27, 93, 177). Similarly, histone acetylation on H3 and H4 tails is also required for efficient origin activation during S phase, probably facilitating the loading of replication factor(s) at origins (155).

Histone acetyltransferase Gcn5p

The conserved histone acetyltransferase Gcn5p is present in multiple HAT complexes in yeast, including ADA and SAGA, each of which contains both unique and shared protein subunits (12, 30, 41, 138). SAGA (Spt-Ada-Gcn5-Acetyltransferase), a TAF (II)-containing multiprotein complex, is involved in transcription regulation in *S. cerevisiae* (41). The SAGA complex preferentially acetylates H3 K14, followed by H3 K18, and to lesser extents H3 K9 and H3 K23 within nucleosomes. The ADA complex is similar to SAGA, preferentially acetylating H3 K14 followed by H3 K18 (53).

Studies indicated that Gcn5p is not essential for maintaining the integrity of SAGA complex, the absence of Gcn5p does not affect the association of any other proteins within SAGA, suggesting a peripheral location of Gcn5p in the complex (171). The mutation of *gcn5* E173Q is not defective in Ac-coA binding and that substitution has no gross effect on Gcn5p protein structure, but dramatically affect the HAT activity of Gcn5p (90, 154).

Although *GCN5* is not an essential gene in yeast, Gcn5p is required for mitotic gene expression (83). In the absence of *GCN5*, cells accumulate at G_2/M phase, indicating important roles of Gcn5p in cell cycle progression (178). Aside from Gcn5p, Sas3p is required for both the HAT activity and the integrity of the NuA3 complex, which preferentially acetylates H3 in nucleosomes (53, 68). The combined functional loss of *GCN5* and *SAS3* results in an extensive, global loss of H3 acetylation and arrests cells at G_2/M phase (53), suggesting that histone acetylation is critical for cell cycle progression. Recently, Vernarecci and colleagues reported that Gcn5p is physically localized to the centromere and it might epigenetically regulate the functions of centromere/kinetochore in mitosis (162). Consistent with this observation, components of histone deacetylases complex (Hda1p, Hda2p, Hda3p) are also involved in the regulation of histone function at centromere and chromosome segregation (71).

Cross-talk between histone modifications

Different kinds of modifications on histones can cross-talk to act in concert to modulate gene expression. For example, monoubiquitination at K123 of histone H2B mediated by Rad6p is a prerequisite for trimethylation of both H3 K4 and H3 K79 by COMPASS and Dot1p methyltransferases, respectively, which then lead to the silencing of genes located near telomeres (26, 118, 120, 152). Asymmetric di-methylation of histone H3 R2 prevents the methylation of H3 K4 as well as binding to the H3 tail by MLL thereby inhibiting the transcriptional activation (45,

56). Moreover, effects of combinatorial histone modifications on protein binding were also observed. For instance, the 14-3-3 proteins bind to phosphorylated H3 (S10) with higher affinity when H3 K14 becomes acetylated (164, 170), whereas the double modifications of H3 (S10 phosphorylation and K14 acetylation) are required to dissociate heterochromatin protein 1 from the methylated H3 tail (105).

Modifications of histone tails considerably extend the information potential of the DNA code and gene regulation. Histone modifications can influence each other in synergistic or antagonistic ways, thus mediating gene regulation.

Part III: Budding yeast mitotic spindle checkpoint and tension sensing mechanism

To maintain genomic stability during cell division, the spindle assembly checkpoint (SAC) ensures that all chromosomes make proper bipolar attachment to microtubules arising from opposite spindle pole bodies and come under tension before the transition from metaphase to anaphase (124, 146, 179). When cells encounter a problem of lack of tension between sister chromatids, or when the kinetochore is not attached to spindles, the mitotic checkpoint complex binds and inhibits cdc20p, the substrate adapter for the anaphase-promoting complex (APC). The APC is a ubiquitin ligase complex required for the destruction of the securin (Pds1p in yeast). Pds1p inhibits the activity of the separase (Esp1p in yeast), which is the protease required for the cleavage of cohesin and the separation of sister chromatids (6). Thus, SAC inhibits the APC activity, and blocks cell cycle at G_2/M phase until the spindle/kinetochore defect is corrected.

It has been controversial and difficult to determine whether signals of tension and microtubule attachment are separate or interdependent, and which one is the primary checkpoint signal (119, 124). Aurora B kinase, the enzymatically active component of the chromosomal passenger complex (CPC), appears to be able to distinguish these two checkpoint activators (7, 124).

CPC and Aurora B kinase/Ipl1p

The budding yeast CPC consists of Ipl1p (Aurora B), Sli15p (INCENP), Bir1p (Survivin), and Nbl1p (Borealin-like protein) (4, 117, 156). In metazoans, INCENP, Survivin and Borealin twin together and form a three-helix bundle before it recruits Aurora B. The localization of Aurora B thus depends on all the other CPC components (66). Upon entry into mitosis, the CPC starts to associate with the inner centromere, a region located between sister kinetochores. After the separation of sister chromatids in anaphase, CPC relocates to the spindle midzone (4, 15, 76, 136). During metaphase, the CPC plays vital roles in recruiting kinetochore proteins and those that are responsible for kinetochore-microtubule interactions (1, 24, 31, 73, 89, 92). Thus, the CPC is thought to be one of the most upstream regulators of centromere/kinetochore function (76).

Indeed, the analysis of a temperature-sensitive *ipl1* mutant, showed that Ipl1p is required to activate the spindle checkpoint in response to defects in the tension between sister chromatids (7, 8, 125). Sli15p provides the binding sites for Ipl1p, and their association increases the kinase activity of Ipl1p. Consistent with that, *sli15* mutant cells exhibit similar phenotypes as *ipl1* cells (79). Although Bir1p and Nbl1p have little effect on the kinase activity of Ipl1p, they might contribute to its substrate specificity; accordingly, mutant cells of *bir1* and *ndl1* also have problems in achieving accurate segregation (117, 139). One possible mechanism by which Ipl1p activates the spindle checkpoint in response to the absence of tension is that Ipl1p promotes the bi-orientation by destabilizing improper kinetochore-microtubule interactions (125).

Shuogshin/Sgo1p

Another protein required for checkpoint activation in a tensionless crisis is Shugoshin (60). The Shugoshin proteins were originally reported to be important for centromeric protection of cohesin in meiosis I (72, 80, 104, 131), although in vertebrate cells Shugoshin proteins also protect centromeric cohesin in the pre-anaphase stage of mitosis. The sole budding yeast Shugoshin protein, Sgo1p, is required for cohesin protection only in meiosis I but not in mitosis (60, 72, 104). The protection of the cohesin complex by Sgo1p requires the recruitment of a protein phosphatase 2A (PP2A) to centromeric region. PP2A functions by counteracting the phosphorylation process on cohesin subunit and prevents its untimely degradation (81, 126, 173). In meiosis II and mitosis, the tension between two sister chromatids might force the Shugoshin-PP2A complex to be relocated from inner centromeric region to the inner kinetochore, consequently permitting cohesion degradation and chromosome segregation (43).

Mitotic roles of Sgo1p in budding yeast were revealed by studies on a particular *sgo1* mutant, which was defective in activating spindle checkpoint because of the loss of tension between sister chromatids, and yet, mutant cells responded normally to microtubule depolymerization (60), implied that Sgo1p, like Ipl1p, plays a critical role in tension specific checkpoint activation.

Fission yeast contains two Shugoshin proteins, Sgo1p and Sgo2p, Sgo1p is specifically expressed in meiosis and functions in the protection of cohesin, whereas Sgo2p is expressed in both mitotic and meiotic cell cycle (80, 81) and is required to ensure bipolar kinetochore-microtubule attachments by promoting the localization of Aurora B to kinetochores (73, 161). Whether budding yeast Sgo1p directs Ipl1p to kinetochore for tension sensing is unclear, but studies on budding yeast indicated that in meiosis I, Sgo1p recruits Ipl1p to centromeric region for the continued presence of PP2A and the protection of cohesin (113, 175). Additionally, the loss of *sgo1* in budding yeast causes the inability of cells to reorient misattached chromatids, suggesting that Sgo1p is required for the kinetochore biorientation (59, 77).

The localization of Sgo1p to the centromere relies on a spindle checkpoint protein Bub1p (32, 78, 80). In fission yeast, studies suggested that Bub3p, along with its binding partner Bub1p, are required to promote the conversion from chromosome mono-orientation to bi-orientation (169). Recent studies in fission yeast indicated that Bub1p phosphorylates histone H2A at a conserved residue serine 121 and that this phosphorylation is important for the centromeric localization of Sgo1p. H2A S121A mutation phenocopies Bub1p kinase-inactive mutant *bub1-KD* in defects of kinetochore-microtubule attachment and centromeric protection. And the double mutant of H2A S121A and *bub1-KD* show no additive defects in chromosome segregation, suggesting that the

phosphorylation of H2A and Bub1p kinase activity function in the same pathway for the centromeric localization of Sgo1p (32, 74).

Part IV: Research interests and significance

Failures in the detection of bipolar attachment and the tension between two sister chromatids can lead to aneuploidy and genomic instability. H3 Ser10 phosphorylation occurs in all eukaryotes examined thus far. Defects in H3 phosphorylation are associated with chromosome missegregation (167). Such errors in chromosome segregation might result in aneuploidy (6), which is a hallmark of many cancers and might contribute to tumorigenesis (28, 63). Expression of the Aurora kinases is well coordinated with H3 phosphorylation during G_2/M transition (22). Aberrant regulation of Aurora kinases also has been associated with chromosome missegregation and tumor progression (49). So far, little is known about how chromatin proactively participates in mitotic progression and cell cycle regulation.

Shugoshin protein family was recently identified as a cohesin protector in meiosis I (40, 81). It also contributes to the tension sensing function in mitosis by promoting the biorientation of kinetochore (73, 77). It has been observed that the downregulation of human Sgo1p leads to chromosome instability in colorectal cancer cells (62). The build-up of tension on all pairs of sister chromatids signals the successful establishment of bipolar attachment, which is the prerequisite for cells to initiate anaphase and maintain accurate chromosome segregation (2). However, the mechanism of tension sensing and how Sgo1p is recruited and functioned in mitotic tension sensing is less understood.

Uneven partitioning of duplicated genomes is associated with many devastating medical conditions, including cancers and trisomy. Faithful segregation requires that each of the two sister kinetochores attach to spindles emanating from opposite spindle pole bodies, resulting in tension between sisters. My studies uncovered a surprising tension-sensing function of histone H3. By recruiting the Shugoshin protein to pericentromeres, H3 plays an early and pivotal role in ensuring chromosome biorientation. This novel function of H3 appears to be independent of epigenetic marks, i.e., posttranslational modifications, hence underscoring the flexibility of histone H3 in exerting selective nuclear functions (101).

REFERENCES

1. **Andrews, P. D., Y. Ovechkina, N. Morrice, M. Wagenbach, K. Duncan, L. Wordeman, and J. R. Swedlow.** 2004. Aurora B regulates MCAK at the mitotic centromere. Dev Cell **6**:253-68.

2. **Ault, J. G., and R. B. Nicklas.** 1989. Tension, microtubule rearrangements, and the proper distribution of chromosomes in mitosis. Chromosoma **98**:33-9.

3. **Bauer, W. R., J. J. Hayes, J. H. White, and A. P. Wolffe.** 1994. Nucleosome structural changes due to acetylation. J Mol Biol **236**:685-90.

4. **Beardmore, V. A., L. J. Ahonen, G. J. Gorbsky, and M. J. Kallio.** 2004. Survivin dynamics increases at centromeres during G2/M phase transition and is regulated by microtubule-attachment and Aurora B kinase activity. J Cell Sci **117**:4033-42.

5. **Berger, S. L.** 2007. The complex language of chromatin regulation during transcription. Nature **447**:407-12.

6. **Bharadwaj, R., and H. Yu.** 2004. The spindle checkpoint, aneuploidy, and cancer. Oncogene **23**:2016-27.

7. **Biggins, S., and A. W. Murray.** 2001. The budding yeast protein kinase Ipl1/Aurora allows the absence of tension to activate the spindle checkpoint. Genes Dev **15**:3118-29.

8. **Biggins, S., F. F. Severin, N. Bhalla, I. Sassoon, A. A. Hyman, and A. W. Murray.** 1999. The conserved protein kinase Ipl1 regulates microtubule binding to kinetochores in budding yeast. Genes Dev **13**:532-44.

9. **Boeger, H., J. Griesenbeck, and R. D. Kornberg.** 2008. Nucleosome retention and the stochastic nature of promoter chromatin remodeling for transcription. Cell **133**:716-26.

10. **Brandt, W. F., and C. von Holt.** 1982. The primary structure of yeast histone H3. Eur J Biochem **121**:501-10.

11. **Bridges, D., and G. B. Moorhead.** 2005. 14-3-3 proteins: a number of functions for a numbered protein. Sci STKE **2005**:re10.

12. **Brown, C. E., T. Lechner, L. Howe, and J. L. Workman.** 2000. The many HATs of transcription coactivators. Trends Biochem Sci **25**:15-9.

13. **Brownell, J. E., J. Zhou, T. Ranalli, R. Kobayashi, D. G. Edmondson, S. Y. Roth, and C. D. Allis.** 1996. Tetrahymena histone acetyltransferase A: a homolog to yeast Gcn5p linking histone acetylation to gene activation. Cell **84**:843-51.

14. **Camahort, R., M. Shivaraju, M. Mattingly, B. Li, S. Nakanishi, D. Zhu, A. Shilatifard, J. L. Workman, and J. L. Gerton.** 2009. Cse4 is part of an octameric nucleosome in budding yeast. Mol Cell **35**:794-805.

15. **Carmena, M., S. Ruchaud, and W. C. Earnshaw.** 2009. Making the Auroras glow: regulation of Aurora A and B kinase function by interacting proteins. Curr Opin Cell Biol **21**:796-805.

16. **Carrozza, M. J., R. T. Utley, J. L. Workman, and J. Cote.** 2003. The diverse functions of histone acetyltransferase complexes. Trends Genet **19**:321-9.

17. **Cedar, H., and Y. Bergman.** 2009. Linking DNA methylation and histone modification: patterns and paradigms. Nat Rev Genet **10**:295-304.

18. **Chan, C. S., and D. Botstein.** 1993. Isolation and characterization of chromosome-gain and increase-in-ploidy mutants in yeast. Genetics **135**:677-91.

19. **Chen, C. C., J. J. Carson, J. Feser, B. Tamburini, S. Zabaronick, J. Linger, and J. K. Tyler.** 2008. Acetylated lysine 56 on histone H3 drives chromatin assembly after repair and signals for the completion of repair. Cell **134**:231-43.

20. **Cheung, P., C. D. Allis, and P. Sassone-Corsi.** 2000. Signaling to chromatin through histone modifications. Cell **103**:263-71.

21. **Cheung, P., K. G. Tanner, W. L. Cheung, P. Sassone-Corsi, J. M. Denu, and C. D. Allis.** 2000. Synergistic coupling of histone H3 phosphorylation and acetylation in response to epidermal growth factor stimulation. Mol Cell **5**:905-15.

22. **Crosio, C., G. M. Fimia, R. Loury, M. Kimura, Y. Okano, H. Zhou, S. Sen, C. D. Allis, and P. Sassone-Corsi.** 2002. Mitotic phosphorylation of histone H3: spatio-temporal regulation by mammalian Aurora kinases. Mol Cell Biol **22**:874-85.

23. **Culhane, J. C., and P. A. Cole.** 2007. LSD1 and the chemistry of histone demethylation. Curr Opin Chem Biol **11**:561-8.

24. **Ditchfield, C., V. L. Johnson, A. Tighe, R. Ellston, C. Haworth, T. Johnson, A. Mortlock, N. Keen, and S. S. Taylor.** 2003. Aurora B couples chromosome alignment with anaphase by targeting BubR1, Mad2, and Cenp-E to kinetochores. J Cell Biol **161**:267-80.

25. **Dorigo, B., T. Schalch, K. Bystricky, and T. J. Richmond.** 2003. Chromatin fiber folding: requirement for the histone H4 N-terminal tail. J Mol Biol **327**:85-96.

26. **Dover, J., J. Schneider, M. A. Tawiah-Boateng, A. Wood, K. Dean, M. Johnston, and A. Shilatifard.** 2002. Methylation of histone H3 by COMPASS requires ubiquitination of histone H2B by Rad6. J Biol Chem **277**:28368-71.

27. **Downs, J. A.** 2008. Histone H3 K56 acetylation, chromatin assembly, and the DNA damage checkpoint. DNA Repair (Amst) **7**:2020-4.

28. **Draviam, V. M., S. Xie, and P. K. Sorger.** 2004. Chromosome segregation and genomic stability. Curr Opin Genet Dev **14**:120-5.

29. **Durrin, L. K., R. K. Mann, P. S. Kayne, and M. Grunstein.** 1991. Yeast histone H4 N-terminal sequence is required for promoter activation in vivo. Cell **65**:1023-31.

30. **Eberharter, A., D. E. Sterner, D. Schieltz, A. Hassan, J. R. Yates, 3rd, S. L. Berger, and J. L. Workman.** 1999. The ADA complex is a distinct histone acetyltransferase complex in Saccharomyces cerevisiae. Mol Cell Biol **19**:6621-31.

31. **Emanuele, M. J., W. Lan, M. Jwa, S. A. Miller, C. S. Chan, and P. T. Stukenberg.** 2008. Aurora B kinase and protein phosphatase 1 have opposing roles in modulating kinetochore assembly. J Cell Biol **181**:241-54.

32. **Fernius, J., and K. G. Hardwick.** 2007. Bub1 kinase targets Sgo1 to ensure efficient chromosome biorientation in budding yeast mitosis. PLoS Genet **3**:2312-2325.

33. **Flaus, A., C. Rencurel, H. Ferreira, N. Wiechens, and T. Owen-Hughes.** 2004. Sin mutations alter inherent nucleosome mobility. Embo J **23**:343-53.

34. **Francisco, L., W. Wang, and C. S. Chan.** 1994. Type 1 protein phosphatase acts in opposition to IpL1 protein kinase in regulating yeast chromosome segregation. Mol Cell Biol **14**:4731-40.

35. **Fry, C. J., A. Norris, M. Cosgrove, J. D. Boeke, and C. L. Peterson.** 2006. The LRS and SIN domains: two structurally equivalent but functionally distinct nucleosomal surfaces required for transcriptional silencing. Mol Cell Biol **26:**9045-59.

36. **Gelperin, D., J. Weigle, K. Nelson, P. Roseboom, K. Irie, K. Matsumoto, and S. Lemmon.** 1995. 14-3-3 proteins: potential roles in vesicular transport and Ras signaling in Saccharomyces cerevisiae. Proc Natl Acad Sci U S A **92:**11539-43.

37. **Giet, R., and D. M. Glover.** 2001. Drosophila aurora B kinase is required for histone H3 phosphorylation and condensin recruitment during chromosome condensation and to organize the central spindle during cytokinesis. J Cell Biol **152:**669-82.

38. **Goto, H., Y. Tomono, K. Ajiro, H. Kosako, M. Fujita, M. Sakurai, K. Okawa, A. Iwamatsu, T. Okigaki, T. Takahashi, and M. Inagaki.** 1999. Identification of a novel phosphorylation site on histone H3 coupled with mitotic chromosome condensation. J Biol Chem **274:**25543-9.

39. **Goto, H., Y. Yasui, E. A. Nigg, and M. Inagaki.** 2002. Aurora-B phosphorylates Histone H3 at serine28 with regard to the mitotic chromosome condensation. Genes Cells **7:**11-7.

40. **Goulding, S. E., and W. C. Earnshaw.** 2005. Shugoshin: a centromeric guardian senses tension. Bioessays **27:**588-91.

41. **Grant, P. A., L. Duggan, J. Cote, S. M. Roberts, J. E. Brownell, R. Candau, R. Ohba, T. Owen-Hughes, C. D. Allis, F. Winston, S. L. Berger, and J. L. Workman.** 1997. Yeast Gcn5 functions in two multisubunit complexes to acetylate nucleosomal histones: characterization of an Ada complex and the SAGA (Spt/Ada) complex. Genes Dev **11:**1640-50.

42. **Green, C. M., and G. Almouzni.** 2002. When repair meets chromatin. First in series on chromatin dynamics. EMBO Rep **3:**28-33.

43. **Gregan, J., M. Spirek, and C. Rumpf.** 2008. Solving the shugoshin puzzle. Trends Genet **24:**205-7.

44. **Grewal, S. I.** 2010. RNAi-dependent formation of heterochromatin and its diverse functions. Curr Opin Genet Dev.

45. **Guccione, E., C. Bassi, F. Casadio, F. Martinato, M. Cesaroni, H. Schuchlautz, B. Luscher, and B. Amati.** 2007. Methylation of histone

H3R2 by PRMT6 and H3K4 by an MLL complex are mutually exclusive. Nature **449**:933-7.

46. **Gurley, L. R., J. A. D'Anna, S. S. Barham, L. L. Deaven, and R. A. Tobey.** 1978. Histone phosphorylation and chromatin structure during mitosis in Chinese hamster cells. Eur J Biochem **84**:1-15.

47. **Hake, S. B., B. A. Garcia, M. Kauer, S. P. Baker, J. Shabanowitz, D. F. Hunt, and C. D. Allis.** 2005. Serine 31 phosphorylation of histone variant H3.3 is specific to regions bordering centromeres in metaphase chromosomes. Proc Natl Acad Sci U S A **102**:6344-9.

48. **Hans, F., and S. Dimitrov.** 2001. Histone H3 phosphorylation and cell division. Oncogene **20**:3021-7.

49. **Harrington, E. A., D. Bebbington, J. Moore, R. K. Rasmussen, A. O. Ajose-Adeogun, T. Nakayama, J. A. Graham, C. Demur, T. Hercend, A. Diu-Hercend, M. Su, J. M. Golec, and K. M. Miller.** 2004. VX-680, a potent and selective small-molecule inhibitor of the Aurora kinases, suppresses tumor growth in vivo. Nat Med **10**:262-7.

50. **Heit, R., J. B. Rattner, G. K. Chan, and M. J. Hendzel.** 2009. G2 histone methylation is required for the proper segregation of chromosomes. J Cell Sci **122**:2957-68.

51. **Hendzel, M. J., Y. Wei, M. A. Mancini, A. Van Hooser, T. Ranalli, B. R. Brinkley, D. P. Bazett-Jones, and C. D. Allis.** 1997. Mitosis-specific phosphorylation of histone H3 initiates primarily within pericentromeric heterochromatin during G2 and spreads in an ordered fashion coincident with mitotic chromosome condensation. Chromosoma **106**:348-60.

52. **Horn, P. J., K. A. Crowley, L. M. Carruthers, J. C. Hansen, and C. L. Peterson.** 2002. The SIN domain of the histone octamer is essential for intramolecular folding of nucleosomal arrays. Nat Struct Biol **9**:167-71.

53. **Howe, L., D. Auston, P. Grant, S. John, R. G. Cook, J. L. Workman, and L. Pillus.** 2001. Histone H3 specific acetyltransferases are essential for cell cycle progression. Genes Dev **15**:3144-54.

54. **Hsu, J. Y., Z. W. Sun, X. Li, M. Reuben, K. Tatchell, D. K. Bishop, J. M. Grushcow, C. J. Brame, J. A. Caldwell, D. F. Hunt, R. Lin, M. M. Smith, and C. D. Allis.** 2000. Mitotic phosphorylation of histone H3 is governed by Ipl1/aurora kinase and Glc7/PP1 phosphatase in budding yeast and nematodes. Cell **102**:279-91.

55. **Huang, J., and S. L. Berger.** 2008. The emerging field of dynamic lysine methylation of non-histone proteins. Curr Opin Genet Dev **18:**152-8.

56. **Hyllus, D., C. Stein, K. Schnabel, E. Schiltz, A. Imhof, Y. Dou, J. Hsieh, and U. M. Bauer.** 2007. PRMT6-mediated methylation of R2 in histone H3 antagonizes H3 K4 trimethylation. Genes Dev **21:**3369-80.

57. **Iizuka, M., and M. M. Smith.** 2003. Functional consequences of histone modifications. Curr Opin Genet Dev **13:**154-60.

58. **Imoberdorf, R. M., I. Topalidou, and M. Strubin.** 2006. A role for gcn5-mediated global histone acetylation in transcriptional regulation. Mol Cell Biol **26:**1610-6.

59. **Indjeian, V. B., and A. W. Murray.** 2007. Budding yeast mitotic chromosomes have an intrinsic bias to biorient on the spindle. Curr Biol **17:**1837-46.

60. **Indjeian, V. B., B. M. Stern, and A. W. Murray.** 2005. The centromeric protein Sgo1 is required to sense lack of tension on mitotic chromosomes. Science **307:**130-3.

61. **Ivaldi, M. S., C. S. Karam, and V. G. Corces.** 2007. Phosphorylation of histone H3 at Ser10 facilitates RNA polymerase II release from promoter-proximal pausing in Drosophila. Genes Dev **21:**2818-31.

62. **Iwaizumi, M., K. Shinmura, H. Mori, H. Yamada, M. Suzuki, Y. Kitayama, H. Igarashi, T. Nakamura, H. Suzuki, Y. Watanabe, A. Hishida, M. Ikuma, and H. Sugimura.** 2009. Human Sgo1 downregulation leads to chromosomal instability in colorectal cancer. Gut **58:**249-60.

63. **Jallepalli, P. V., and C. Lengauer.** 2001. Chromosome segregation and cancer: cutting through the mystery. Nat Rev Cancer **1:**109-17.

64. **Jason, L. J., S. C. Moore, J. D. Lewis, G. Lindsey, and J. Ausio.** 2002. Histone ubiquitination: a tagging tail unfolds? Bioessays **24:**166-74.

65. **Jenuwein, T., and C. D. Allis.** 2001. Translating the histone code. Science **293:**1074-80.

66. **Jeyaprakash, A. A., U. R. Klein, D. Lindner, J. Ebert, E. A. Nigg, and E. Conti.** 2007. Structure of a Survivin-Borealin-INCENP core complex reveals how chromosomal passengers travel together. Cell **131:**271-85.

67. **Jiang, C., and B. F. Pugh.** 2009. Nucleosome positioning and gene regulation: advances through genomics. Nat Rev Genet **10:**161-72.

68. **John, S., L. Howe, S. T. Tafrov, P. A. Grant, R. Sternglanz, and J. L. Workman.** 2000. The something about silencing protein, Sas3, is the catalytic subunit of NuA3, a yTAF(II)30-containing HAT complex that interacts with the Spt16 subunit of the yeast CP (Cdc68/Pob3)-FACT complex. Genes Dev **14:**1196-208.

69. **Juan, L. J., R. T. Utley, C. C. Adams, M. Vettese-Dadey, and J. L. Workman.** 1994. Differential repression of transcription factor binding by histone H1 is regulated by the core histone amino termini. Embo J **13:**6031-40.

70. **Kamakaka, R. T., and J. O. Thomas.** 1990. Chromatin structure of transcriptionally competent and repressed genes. Embo J **9:**3997-4006.

71. **Kanta, H., L. Laprade, A. Almutairi, and I. Pinto.** 2006. Suppressor analysis of a histone defect identifies a new function for the hda1 complex in chromosome segregation. Genetics **173:**435-50.

72. **Katis, V. L., M. Galova, K. P. Rabitsch, J. Gregan, and K. Nasmyth.** 2004. Maintenance of cohesin at centromeres after meiosis I in budding yeast requires a kinetochore-associated protein related to MEI-S332. Curr Biol **14:**560-72.

73. **Kawashima, S. A., T. Tsukahara, M. Langegger, S. Hauf, T. S. Kitajima, and Y. Watanabe.** 2007. Shugoshin enables tension-generating attachment of kinetochores by loading Aurora to centromeres. Genes Dev **21:**420-35.

74. **Kawashima, S. A., Y. Yamagishi, T. Honda, K. I. Ishiguro, and Y. Watanabe.** 2009. Phosphorylation of H2A by Bub1 Prevents Chromosomal Instability Through Localizing Shugoshin. Science.

75. **Keith, K. C., and M. Fitzgerald-Hayes.** 2000. CSE4 genetically interacts with the Saccharomyces cerevisiae centromere DNA elements CDE I and CDE II but not CDE III. Implications for the path of the centromere dna around a cse4p variant nucleosome. Genetics **156:**973-81.

76. **Kelly, A. E., and H. Funabiki.** 2009. Correcting aberrant kinetochore microtubule attachments: an Aurora B-centric view. Curr Opin Cell Biol **21:**51-8.

77. **Kiburz, B. M., A. Amon, and A. L. Marston.** 2008. Shugoshin promotes sister kinetochore biorientation in Saccharomyces cerevisiae. Mol Biol Cell **19:**1199-209.

78. **Kiburz, B. M., D. B. Reynolds, P. C. Megee, A. L. Marston, B. H. Lee, T. I. Lee, S. S. Levine, R. A. Young, and A. Amon.** 2005. The core centromere and Sgo1 establish a 50-kb cohesin-protected domain around centromeres during meiosis I. Genes Dev **19:**3017-30.

79. **Kim, J. H., J. S. Kang, and C. S. Chan.** 1999. Sli15 associates with the ipl1 protein kinase to promote proper chromosome segregation in Saccharomyces cerevisiae. J Cell Biol **145:**1381-94.

80. **Kitajima, T. S., S. A. Kawashima, and Y. Watanabe.** 2004. The conserved kinetochore protein shugoshin protects centromeric cohesion during meiosis. Nature **427:**510-7.

81. **Kitajima, T. S., T. Sakuno, K. Ishiguro, S. Iemura, T. Natsume, S. A. Kawashima, and Y. Watanabe.** 2006. Shugoshin collaborates with protein phosphatase 2A to protect cohesin. Nature **441:**46-52.

82. **Klose, R. J., K. E. Gardner, G. Liang, H. Erdjument-Bromage, P. Tempst, and Y. Zhang.** 2007. Demethylation of histone H3K36 and H3K9 by Rph1: a vestige of an H3K9 methylation system in Saccharomyces cerevisiae? Mol Cell Biol **27:**3951-61.

83. **Krebs, J. E., C. J. Fry, M. L. Samuels, and C. L. Peterson.** 2000. Global role for chromatin remodeling enzymes in mitotic gene expression. Cell **102:**587-98.

84. **Kuo, M. H., and C. D. Allis.** 1998. Roles of histone acetyltransferases and deacetylases in gene regulation. Bioessays **20:**615-26.

85. **Kuo, M. H., J. E. Brownell, R. E. Sobel, T. A. Ranalli, R. G. Cook, D. G. Edmondson, S. Y. Roth, and C. D. Allis.** 1996. Transcription-linked acetylation by Gcn5p of histones H3 and H4 at specific lysines. Nature **383:**269-72.

86. **Kuo, M. H., J. Zhou, P. Jambeck, M. E. Churchill, and C. D. Allis.** 1998. Histone acetyltransferase activity of yeast Gcn5p is required for the activation of target genes in vivo. Genes Dev **12:**627-39.

87. **Kurdistani, S. K., S. Tavazoie, and M. Grunstein.** 2004. Mapping global histone acetylation patterns to gene expression. Cell **117:**721-33.

88. **Kurumizaka, H., and A. P. Wolffe.** 1997. Sin mutations of histone H3: influence on nucleosome core structure and function. Mol Cell Biol **17**:6953-69.

89. **Lan, W., X. Zhang, S. L. Kline-Smith, S. E. Rosasco, G. A. Barrett-Wilt, J. Shabanowitz, D. F. Hunt, C. E. Walczak, and P. T. Stukenberg.** 2004. Aurora B phosphorylates centromeric MCAK and regulates its localization and microtubule depolymerization activity. Curr Biol **14**:273-86.

90. **Langer, M. R., K. G. Tanner, and J. M. Denu.** 2001. Mutational analysis of conserved residues in the GCN5 family of histone acetyltransferases. J Biol Chem **276**:31321-31.

91. **Lee, D. Y., J. J. Hayes, D. Pruss, and A. P. Wolffe.** 1993. A positive role for histone acetylation in transcription factor access to nucleosomal DNA. Cell **72**:73-84.

92. **Lens, S. M., and R. H. Medema.** 2003. The survivin/Aurora B complex: its role in coordinating tension and attachment. Cell Cycle **2**:507-10.

93. **Li, Q., H. Zhou, H. Wurtele, B. Davies, B. Horazdovsky, A. Verreault, and Z. Zhang.** 2008. Acetylation of histone H3 lysine 56 regulates replication-coupled nucleosome assembly. Cell **134**:244-55.

94. **Liu, C. L., T. Kaplan, M. Kim, S. Buratowski, S. L. Schreiber, N. Friedman, and O. J. Rando.** 2005. Single-nucleosome mapping of histone modifications in S. cerevisiae. PLoS Biol **3**:e328.

95. **Lottersberger, F., A. Panza, G. Lucchini, S. Piatti, and M. P. Longhese.** 2006. The Saccharomyces cerevisiae 14-3-3 Proteins Are Required for the G1/S Transition, Actin Cytoskeleton Organization and Cell Wall Integrity. Genetics **173**:661-75.

96. **Lottersberger, F., F. Rubert, V. Baldo, G. Lucchini, and M. P. Longhese.** 2003. Functions of Saccharomyces cerevisiae 14-3-3 proteins in response to DNA damage and to DNA replication stress. Genetics **165**:1717-32.

97. **Lu, S. C., and J. M. Mato.** 2008. S-Adenosylmethionine in cell growth, apoptosis and liver cancer. J Gastroenterol Hepatol **23 Suppl 1**:S73-7.

98. **Lu, X., M. D. Simon, J. V. Chodaparambil, J. C. Hansen, K. M. Shokat, and K. Luger.** 2008. The effect of H3K79 dimethylation and H4K20 trimethylation on nucleosome and chromatin structure. Nat Struct Mol Biol **15**:1122-4.

99. **Luger, K., A. W. Mader, R. K. Richmond, D. F. Sargent, and T. J. Richmond.** 1997. Crystal structure of the nucleosome core particle at 2.8 A resolution. Nature **389**:251-60.

100. **Luo, J., and M. H. Kuo.** 2009. Linking nutrient metabolism to epigenetics. Cell Science Reviews **6**:49-54.

101. **Luo, J., X. Xu, H. Hall, E. M. Hyland, J. D. Boeke, T. Hazbun, and M. H. Kuo.** 2009. Histone H3 Exerts Key Function in Mitotic Checkpoint Control. Mol Cell Biol.

102. **Ma, X. J., Q. Lu, and M. Grunstein.** 1996. A search for proteins that interact genetically with histone H3 and H4 amino termini uncovers novel regulators of the Swe1 kinase in Saccharomyces cerevisiae. Genes Dev **10**:1327-40.

103. **Macdonald, N., J. P. Welburn, M. E. Noble, A. Nguyen, M. B. Yaffe, D. Clynes, J. G. Moggs, G. Orphanides, S. Thomson, J. W. Edmunds, A. L. Clayton, J. A. Endicott, and L. C. Mahadevan.** 2005. Molecular basis for the recognition of phosphorylated and phosphoacetylated histone h3 by 14-3-3. Mol Cell **20**:199-211.

104. **Marston, A. L., W. H. Tham, H. Shah, and A. Amon.** 2004. A genome-wide screen identifies genes required for centromeric cohesion. Science **303**:1367-70.

105. **Mateescu, B., P. England, F. Halgand, M. Yaniv, and C. Muchardt.** 2004. Tethering of HP1 proteins to chromatin is relieved by phosphoacetylation of histone H3. EMBO Rep **5**:490-6.

106. **Mavrich, T. N., I. P. Ioshikhes, B. J. Venters, C. Jiang, L. P. Tomsho, J. Qi, S. C. Schuster, I. Albert, and B. F. Pugh.** 2008. A barrier nucleosome model for statistical positioning of nucleosomes throughout the yeast genome. Genome Res **18**:1073-83.

107. **Megee, P. C., B. A. Morgan, B. A. Mittman, and M. M. Smith.** 1990. Genetic analysis of histone H4: essential role of lysines subject to reversible acetylation. Science **247**:841-5.

108. **Megee, P. C., B. A. Morgan, and M. M. Smith.** 1995. Histone H4 and the maintenance of genome integrity. Genes Dev **9**:1716-27.

109. **Meluh, P. B., P. Yang, L. Glowczewski, D. Koshland, and M. M. Smith.** 1998. Cse4p is a component of the core centromere of Saccharomyces cerevisiae. Cell **94**:607-13.

110. **Mikkelsen, T. S., M. Ku, D. B. Jaffe, B. Issac, E. Lieberman, G. Giannoukos, P. Alvarez, W. Brockman, T. K. Kim, R. P. Koche, W. Lee, E. Mendenhall, A. O'Donovan, A. Presser, C. Russ, X. Xie, A. Meissner, M. Wernig, R. Jaenisch, C. Nusbaum, E. S. Lander, and B. E. Bernstein.** 2007. Genome-wide maps of chromatin state in pluripotent and lineage-committed cells. Nature **448:**553-60.

111. **Millar, C. B., and M. Grunstein.** 2006. Genome-wide patterns of histone modifications in yeast. Nat Rev Mol Cell Biol **7:**657-66.

112. **Mizuguchi, G., H. Xiao, J. Wisniewski, M. M. Smith, and C. Wu.** 2007. Nonhistone Scm3 and histones CenH3-H4 assemble the core of centromere-specific nucleosomes. Cell **129:**1153-64.

113. **Monje-Casas, F., V. R. Prabhu, B. H. Lee, M. Boselli, and A. Amon.** 2007. Kinetochore orientation during meiosis is controlled by Aurora B and the monopolin complex. Cell **128:**477-90.

114. **Morgan, B. A., B. A. Mittman, and M. M. Smith.** 1991. The highly conserved N-terminal domains of histones H3 and H4 are required for normal cell cycle progression. Mol Cell Biol **11:**4111-20.

115. **Morris, S. A., B. Rao, B. A. Garcia, S. B. Hake, R. L. Diaz, J. Shabanowitz, D. F. Hunt, C. D. Allis, J. D. Lieb, and B. D. Strahl.** 2007. Identification of histone H3 lysine 36 acetylation as a highly conserved histone modification. J Biol Chem **282:**7632-40.

116. **Muthurajan, U. M., Y. Bao, L. J. Forsberg, R. S. Edayathumangalam, P. N. Dyer, C. L. White, and K. Luger.** 2004. Crystal structures of histone Sin mutant nucleosomes reveal altered protein-DNA interactions. Embo J **23:**260-71.

117. **Nakajima, Y., R. G. Tyers, C. C. Wong, J. R. Yates, 3rd, D. G. Drubin, and G. Barnes.** 2009. Nbl1p: a Borealin/Dasra/CSC-1-like protein essential for Aurora/Ipl1 complex function and integrity in Saccharomyces cerevisiae. Mol Biol Cell **20:**1772-84.

118. **Nakanishi, S., J. S. Lee, K. E. Gardner, J. M. Gardner, Y. H. Takahashi, M. B. Chandrasekharan, Z. W. Sun, M. A. Osley, B. D. Strahl, S. L. Jaspersen, and A. Shilatifard.** 2009. Histone H2BK123 monoubiquitination is the critical determinant for H3K4 and H3K79 trimethylation by COMPASS and Dot1. J Cell Biol **186:**371-7.

119. **Nezi, L., and A. Musacchio.** 2009. Sister chromatid tension and the spindle assembly checkpoint. Curr Opin Cell Biol **21:**785-95.

120. **Ng, H. H., R. M. Xu, Y. Zhang, and K. Struhl.** 2002. Ubiquitination of histone H2B by Rad6 is required for efficient Dot1-mediated methylation of histone H3 lysine 79. J Biol Chem **277:**34655-7.

121. **Norton, V. G., B. S. Imai, P. Yau, and E. M. Bradbury.** 1989. Histone acetylation reduces nucleosome core particle linking number change. Cell **57:**449-57.

122. **Park, J. H., M. S. Cosgrove, E. Youngman, C. Wolberger, and J. D. Boeke.** 2002. A core nucleosome surface crucial for transcriptional silencing. Nat Genet **32:**273-9.

123. **Phalke, S., O. Nickel, D. Walluscheck, F. Hortig, M. C. Onorati, and G. Reuter.** 2009. Retrotransposon silencing and telomere integrity in somatic cells of Drosophila depends on the cytosine-5 methyltransferase DNMT2. Nat Genet **41:**696-702.

124. **Pinsky, B. A., and S. Biggins.** 2005. The spindle checkpoint: tension versus attachment. Trends Cell Biol **15:**486-93.

125. **Pinsky, B. A., C. Kung, K. M. Shokat, and S. Biggins.** 2006. The Ipl1-Aurora protein kinase activates the spindle checkpoint by creating unattached kinetochores. Nat Cell Biol **8:**78-83.

126. **Pinsky, B. A., C. R. Nelson, and S. Biggins.** 2009. Protein phosphatase 1 regulates exit from the spindle checkpoint in budding yeast. Curr Biol **19:**1182-7.

127. **Pinto, I., and F. Winston.** 2000. Histone H2A is required for normal centromere function in Saccharomyces cerevisiae. Embo J **19:**1598-612.

128. **Pokholok, D. K., C. T. Harbison, S. Levine, M. Cole, N. M. Hannett, T. I. Lee, G. W. Bell, K. Walker, P. A. Rolfe, E. Herbolsheimer, J. Zeitlinger, F. Lewitter, D. K. Gifford, and R. A. Young.** 2005. Genome-wide map of nucleosome acetylation and methylation in yeast. Cell **122:**517-27.

129. **Preuss, U., G. Landsberg, and K. H. Scheidtmann.** 2003. Novel mitosis-specific phosphorylation of histone H3 at Thr11 mediated by Dlk/ZIP kinase. Nucleic Acids Res **31:**878-85.

130. **Psathas, J. N., S. Zheng, S. Tan, and J. C. Reese.** 2009. Set2-dependent K36 methylation is regulated by novel intratail interactions within H3. Mol Cell Biol **29:**6413-26.

131. **Rabitsch, K. P., J. Gregan, A. Schleiffer, J. P. Javerzat, F. Eisenhaber, and K. Nasmyth.** 2004. Two fission yeast homologs of Drosophila Mei-

S332 are required for chromosome segregation during meiosis I and II. Curr Biol **14:**287-301.

132. **Radman-Livaja, M., C. L. Liu, N. Friedman, S. L. Schreiber, and O. J. Rando.** 2010. Replication and active demethylation represent partially overlapping mechanisms for erasure of H3K4me3 in budding yeast. PLoS Genet **6:**e1000837.

133. **Recht, J., and M. A. Osley.** 1999. Mutations in both the structured domain and N-terminus of histone H2B bypass the requirement for Swi-Snf in yeast. Embo J **18:**229-40.

134. **Reid, J. L., V. R. Iyer, P. O. Brown, and K. Struhl.** 2000. Coordinate regulation of yeast ribosomal protein genes is associated with targeted recruitment of Esa1 histone acetylase. Mol Cell **6:**1297-307.

135. **Roth, D. B., and S. Y. Roth.** 2000. Unequal access: regulating V(D)J recombination through chromatin remodeling. Cell **103:**699-702.

136. **Ruchaud, S., M. Carmena, and W. C. Earnshaw.** 2007. Chromosomal passengers: conducting cell division. Nat Rev Mol Cell Biol **8:**798-812.

137. **Schneider, J., P. Bajwa, F. C. Johnson, S. R. Bhaumik, and A. Shilatifard.** 2006. Rtt109 is required for proper H3K56 acetylation: a chromatin mark associated with the elongating RNA polymerase II. J Biol Chem **281:**37270-4.

138. **Sendra, R., C. Tse, and J. C. Hansen.** 2000. The yeast histone acetyltransferase A2 complex, but not free Gcn5p, binds stably to nucleosomal arrays. J Biol Chem **275:**24928-34.

139. **Shimogawa, M. M., P. O. Widlund, M. Riffle, M. Ess, and T. N. Davis.** 2009. Bir1 is required for the tension checkpoint. Mol Biol Cell **20:**915-23.

140. **Sims, R. J., 3rd, K. Nishioka, and D. Reinberg.** 2003. Histone lysine methylation: a signature for chromatin function. Trends Genet **19:**629-39.

141. **Sinha, D., and M. A. Shogren-Knaak.** 2010. The role of direct interactions between the histone H4 tail and the H2A core in long-range nucleosome contacts. J Biol Chem.

142. **Smith, J. S., E. Caputo, and J. D. Boeke.** 1999. A genetic screen for ribosomal DNA silencing defects identifies multiple DNA replication and chromatin-modulating factors. Mol Cell Biol **19:**3184-97.

143. **Smith, M. M.** 2002. Centromeres and variant histones: what, where, when and why? Curr Opin Cell Biol **14:**279-85.

144. **Smith, M. M., P. Yang, M. S. Santisteban, P. W. Boone, A. T. Goldstein, and P. C. Megee.** 1996. A novel histone H4 mutant defective in nuclear division and mitotic chromosome transmission. Mol Cell Biol **16:**1017-26.

145. **Sobel, R. E., R. G. Cook, C. A. Perry, A. T. Annunziato, and C. D. Allis.** 1995. Conservation of deposition-related acetylation sites in newly synthesized histones H3 and H4. Proc Natl Acad Sci U S A **92:**1237-41.

146. **Stern, B. M., and A. W. Murray.** 2001. Lack of tension at kinetochores activates the spindle checkpoint in budding yeast. Curr Biol **11:**1462-7.

147. **Stoler, S., K. C. Keith, K. E. Curnick, and M. Fitzgerald-Hayes.** 1995. A mutation in CSE4, an essential gene encoding a novel chromatin-associated protein in yeast, causes chromosome nondisjunction and cell cycle arrest at mitosis. Genes Dev **9:**573-86.

148. **Strahl, B. D., and C. D. Allis.** 2000. The language of covalent histone modifications. Nature **403:**41-5.

149. **Sugiyama, K., K. Sugiura, T. Hara, K. Sugimoto, H. Shima, K. Honda, K. Furukawa, S. Yamashita, and T. Urano.** 2002. Aurora-B associated protein phosphatases as negative regulators of kinase activation. Oncogene **21:**3103-11.

150. **Suka, N., Y. Suka, A. A. Carmen, J. Wu, and M. Grunstein.** 2001. Highly specific antibodies determine histone acetylation site usage in yeast heterochromatin and euchromatin. Mol Cell **8:**473-9.

151. **Sun, Y., X. Jiang, Y. Xu, M. K. Ayrapetov, L. A. Moreau, J. R. Whetstine, and B. D. Price.** 2009. Histone H3 methylation links DNA damage detection to activation of the tumour suppressor Tip60. Nat Cell Biol **11:**1376-82.

152. **Sun, Z. W., and C. D. Allis.** 2002. Ubiquitination of histone H2B regulates H3 methylation and gene silencing in yeast. Nature **418:**104-8.

153. **Takahashi, H., J. M. McCaffery, R. A. Irizarry, and J. D. Boeke.** 2006. Nucleocytosolic acetyl-coenzyme a synthetase is required for histone acetylation and global transcription. Mol Cell **23:**207-17.

154. **Trievel, R. C., J. R. Rojas, D. E. Sterner, R. N. Venkataramani, L. Wang, J. Zhou, C. D. Allis, S. L. Berger, and R. Marmorstein.** 1999. Crystal

structure and mechanism of histone acetylation of the yeast GCN5 transcriptional coactivator. Proc Natl Acad Sci U S A **96:**8931-6.

155. **Unnikrishnan, A., P. R. Gafken, and T. Tsukiyama.** 2010. Dynamic changes in histone acetylation regulate origins of DNA replication. Nat Struct Mol Biol.

156. **Vagnarelli, P., and W. C. Earnshaw.** 2004. Chromosomal passengers: the four-dimensional regulation of mitotic events. Chromosoma **113:**211-22.

157. **Vaillant, I., and J. Paszkowski.** 2007. Role of histone and DNA methylation in gene regulation. Curr Opin Plant Biol **10:**528-33.

158. **van Heusden, G. P., D. J. Griffiths, J. C. Ford, A. W. T. F. Chin, P. A. Schrader, A. M. Carr, and H. Y. Steensma.** 1995. The 14-3-3 proteins encoded by the BMH1 and BMH2 genes are essential in the yeast Saccharomyces cerevisiae and can be replaced by a plant homologue. Eur J Biochem **229:**45-53.

159. **van Heusden, G. P., and H. Y. Steensma.** 2006. Yeast 14-3-3 proteins. Yeast **23:**159-71.

160. **Van Hooser, A., D. W. Goodrich, C. D. Allis, B. R. Brinkley, and M. A. Mancini.** 1998. Histone H3 phosphorylation is required for the initiation, but not maintenance, of mammalian chromosome condensation. J Cell Sci **111 (Pt 23):**3497-506.

161. **Vanoosthuyse, V., S. Prykhozhij, and K. G. Hardwick.** 2007. Shugoshin 2 regulates localization of the chromosomal passenger proteins in fission yeast mitosis. Mol Biol Cell **18:**1657-69.

162. **Vernarecci, S., P. Ornaghi, A. Bagu, E. Cundari, P. Ballario, and P. Filetici.** 2008. Gcn5p plays an important role in centromere kinetochore function in budding yeast. Mol Cell Biol **28:**988-96.

163. **Vettese-Dadey, M., P. A. Grant, T. R. Hebbes, C. Crane- Robinson, C. D. Allis, and J. L. Workman.** 1996. Acetylation of histone H4 plays a primary role in enhancing transcription factor binding to nucleosomal DNA in vitro. Embo J **15:**2508-18.

164. **Walter, W., D. Clynes, Y. Tang, R. Marmorstein, J. Mellor, and S. L. Berger.** 2008. 14-3-3 interaction with histone H3 involves a dual modification pattern of phosphoacetylation. Mol Cell Biol **28:**2840-9.

165. **Wang, L., C. Mizzen, C. Ying, R. Candau, N. Barlev, J. Brownell, C. D. Allis, and S. L. Berger.** 1997. Histone acetyltransferase activity is conserved between yeast and human GCN5 and is required for complementation of growth and transcriptional activation. Mol Cell Biol **17:**519-27.

166. **Wei, Y., C. A. Mizzen, R. G. Cook, M. A. Gorovsky, and C. D. Allis.** 1998. Phosphorylation of histone H3 at serine 10 is correlated with chromosome condensation during mitosis and meiosis in Tetrahymena. Proc Natl Acad Sci U S A **95:**7480-4.

167. **Wei, Y., L. Yu, J. Bowen, M. A. Gorovsky, and C. D. Allis.** 1999. Phosphorylation of histone H3 is required for proper chromosome condensation and segregation. Cell **97:**99-109.

168. **Whitehouse, I., O. J. Rando, J. Delrow, and T. Tsukiyama.** 2007. Chromatin remodelling at promoters suppresses antisense transcription. Nature **450:**1031-5.

169. **Windecker, H., M. Langegger, S. Heinrich, and S. Hauf.** 2009. Bub1 and Bub3 promote the conversion from monopolar to bipolar chromosome attachment independently of shugoshin. EMBO Rep **10:**1022-8.

170. **Winter, S., E. Simboeck, W. Fischle, G. Zupkovitz, I. Dohnal, K. Mechtler, G. Ammerer, and C. Seiser.** 2008. 14-3-3 proteins recognize a histone code at histone H3 and are required for transcriptional activation. Embo J **27:**88-99.

171. **Wu, P. Y., C. Ruhlmann, F. Winston, and P. Schultz.** 2004. Molecular architecture of the S. cerevisiae SAGA complex. Mol Cell **15:**199-208.

172. **Xie, W., C. Song, N. L. Young, A. S. Sperling, F. Xu, R. Sridharan, A. E. Conway, B. A. Garcia, K. Plath, A. T. Clark, and M. Grunstein.** 2009. Histone h3 lysine 56 acetylation is linked to the core transcriptional network in human embryonic stem cells. Mol Cell **33:**417-27.

173. **Xu, Z., B. Cetin, M. Anger, U. S. Cho, W. Helmhart, K. Nasmyth, and W. Xu.** 2009. Structure and function of the PP2A-shugoshin interaction. Mol Cell **35:**426-41.

174. **Yaffe, M. B., K. Rittinger, S. Volinia, P. R. Caron, A. Aitken, H. Leffers, S. J. Gamblin, S. J. Smerdon, and L. C. Cantley.** 1997. The structural basis for 14-3-3:phosphopeptide binding specificity. Cell **91:**961-71.

175. **Yu, H. G., and D. Koshland.** 2007. The Aurora kinase Ipl1 maintains the centromeric localization of PP2A to protect cohesin during meiosis. J Cell Biol **176:**911-8.

176. **Yuan, G. C., Y. J. Liu, M. F. Dion, M. D. Slack, L. F. Wu, S. J. Altschuler, and O. J. Rando.** 2005. Genome-scale identification of nucleosome positions in S. cerevisiae. Science **309:**626-30.

177. **Yuan, J., M. Pu, Z. Zhang, and Z. Lou.** 2009. Histone H3-K56 acetylation is important for genomic stability in mammals. Cell Cycle **8:**1747-53.

178. **Zhang, W., J. R. Bone, D. G. Edmondson, B. M. Turner, and S. Y. Roth.** 1998. Essential and redundant functions of histone acetylation revealed by mutation of target lysines and loss of the Gcn5p acetyltransferase. Embo J **17:**3155-67.

179. **Zhou, J., J. Yao, and H. C. Joshi.** 2002. Attachment and tension in the spindle assembly checkpoint. J Cell Sci **115:**3547-55.

CHAPTER II

Histone H3 Exerts a Key Function in Mitotic Checkpoint Control

Published in *Mol. Cell. Biol.* 2010 January; 30(2): 537-549.

Histone H3 Exerts a Key Function in Mitotic Checkpoint Control

Jianjun Luo, Xinjing Xu, Hana Hall[2], Edel M. Hyland[3], Jef D. Boeke[3], Tony Hazbun[2], and Min-Hao Kuo[1]*

Department of Biochemistry and Molecular Biology, and [1]Programs in Genetics and in Cell and Molecular Biology, Michigan State University, East Lansing, MI 48824

[2]Department of Medicinal Chemistry and Molecular Pharmacology, 575 Stadium Mall Drive, West Lafayette, IN 47907-2091

[3]High Throughput Biology Center, Johns Hopkins University School of Medicine, Baltimore, MD 21205

Received 24 July 2009 / Accepted 3 November 2009

*Corresponding author. Mailing address: 401 BCH Building, Department of Biochemistry and Molecular Biology, Michigan State University, East Lansing, MI 48824. Phone: (517) 355-0163. FAX: (517) 353-9334. E-mail: kuom@msu.edu.

ABSTRACT

It has been firmly established that many interphase nuclear functions, including transcriptional regulation, are regulated by chromatin and histones. How mitotic progression and quality control might be influenced by histones is less well characterized. We show that histone H3 plays a crucial role in activating the spindle assembly checkpoint in response to a defect in mitosis. Prior to anaphase, all chromosomes must attach to spindles emanating from the opposite spindle pole bodies. The tension between sister chromatids generated by the poleward pulling force is an integral part of chromosome biorientation. Lack of tension due to erroneous attachment activates the spindle assembly checkpoint, which corrects the mistakes and ensures segregation fidelity. A histone H3 mutation impairs the ability of yeast cells to activate the checkpoint in a tensionless crisis, leading to missegregation and aneuploidy. The defects in tension sensing result directly from an attenuated H3-Sgo1p interaction essential for pericentric recruitment of Sgo1p. Reinstating the pericentric enrichment of Sgo1p alleviates the mitotic defects. Histone H3, and hence the chromatin, is thus a key factor transmitting the tension status to the spindle assembly checkpoint.

INTRODUCTION

During mitosis, chromatin goes through significant compaction and condensation to form metaphase chromosomes for segregation. While there is a wealth of information on the crucial roles played by chromatin structures and histone modifications in controlling transcription, replication, repair, and recombination (30), much less is known about how individual histones contribute mechanistically to mitotic progression and regulation.

Forward and reverse genetic studies have suggested that histones, rather than being merely a part of the cargo during mitotic segregation, may play key roles in cell cycle progression and regulation. A histone H4 allele, *hhf1-20*, compromises the interaction between H4 and the centromere-specific H3 variant Cse4p, thus impeding centromeric functions and mitosis at the restrictive temperature (50). Two alleles of histone H2A (44) cause cold-sensitive growth defects and a significant increase in ploidy. This hyperploidy phenotype can be suppressed by mutations affecting a histone deacetylase, *HDA1* (19). Similarly, the Gcn5p histone acetyltransferase genetically interacts with several inner kinetochore components and is physically mapped to the centromeric regions (57). Deleting the flexible tail domain of H3 and H4 results in mitotic delay (36) via a mechanism that can be suppressed by inhibiting the spindle assembly checkpoint activity (J.L. and M.H.K., unpublished data). Together, these data

warrant a more thorough examination of how chromatin may proactively regulate the process of mitotic segregation.

The center stage for mitotic segregation and control is the kinetochore, a large proteinaceous complex assembled on centromeres. The ultimate function of the kinetochore is to capture the spindle microtubules during mitosis. The kinetochore-spindle attachment drives the movement of chromatids to daughter cells, and error-free attachment is essential for even partitioning of the entire genetic complement. To prepare for segregation, S-phase cells first establish sister chromatid cohesion by loading the cohesin complex to centromeres, pericentromeres, and selective regions in the chromatin arms (8, 38). Cohesion prevents precocious segregation before alignment of chromosomes at the metaphase midplate. When cells enter the prophase, spindles are assembled in and emanate from the two spindle pole bodies and are captured by kinetochores. The opposing poleward pulling force then generates tension between sisters and causes the congression of bioriented chromosomes toward the midplane (11). Equatorial alignment of all chromosomes leads to activation of the anaphase-promoting complex/cyclosome, which catalyzes polyubiquitylation and degradation of the securin protein Pds1p and cyclins (23, 60), and activation of the separase Esp1p, which cleaves the Mcd1p/Scc1p subunit of the cohesin complex (37), and hence permits sister chromatid segregation.

One of the most critical mitotic control mechanisms for segregation is the spindle assembly checkpoint, SAC (31), which monitors both the kinetochore-spindle attachment and the resultant tension between sisters (43, 61). The tension sensing function of the SAC is critical for cells to detect and correct the so-called syntelic attachment; that is, both sister kinetochores capture spindles emanating from the same spindle pole body. This condition meets the attachment requirement but does not generate tension. Aneuploidy will result if this type of error is not eradicated. One of the factors essential for cells to detect the tensionless crisis is the Shugoshin protein (Sgo) (7, 15, 21). Downregulation of human Sgo1 expression is linked to about half of the colorectal cancer cases analyzed in one study (16). Yeast Sgo1p is localized to the centromeres and pericentromeres (22, 46). Centromeres and pericentromeres are the most likely loci in which tension is generated and monitored (3, 14). Here we show that histone H3 plays a key role in the pericentric recruitment of Sgo1p for the tension sensing function in mitosis.

MATERIALS AND METHODS

Yeast strains and plasmid constructs. The yeast strains and plasmids used in this work are listed in Tables 2-1 and 2-2.

Most of the strains were derived from the W303 background (JHY200) (1). Initially, phenotypic characterization, including cellular responses to various stresses (e.g. see Fig. 1A) and suppression by 2μm *SGO1*, was conducted in parallel with both JHY200 and its S288C counterpart JHY205 (1). Both strains exhibited literally identical phenotypes. Subsequent studies were thus focused on the W303 background strains.

To delete *SGO1*, primers O361 and O362 were used to PCR amplify the *Kluyveromyces lactis TRP1* selective marker from plasmid pBS1479 (47), and the PCR product was transformed into yeast cells for tryptophan prototroph selection.

To tag endogenous Pds1p with 13xMyc, O323 and O324 were used to PCR amplify pFA6a-13Myc-TRP1 for yeast integrative transformation. Integration was verified with *PDS1*- specific primers O325 and O326 and *TRP1*- specific primers O375 and O376. Mcd1p-13Myc was created in a scheme identical to that used for Pds1p-13Myc, except for the use of *MCD1*-specific primers OJL21, OJL22 (for integration), and OJL23 (for verification). To introduce a carboxyl-terminal

six-hemagglutinin (6xHA) tag to Sgo1p, yeast strain A10652 (22) was used for a genomic PCR (primers O363 and O364) that amplified the 6xHA-TRP1 fragment flanked by *SGO1* sequences. The resultant PCR product was transformed into yMK1243 and yJL145 to knock in the HA tag and the *TRP1* marker, creating yJL343 and yJL344, respectively. Contrary to Kitajima et al. (25), who analyzed Myc-tagged *SGO1*, we did not observe discernible phenotypes associated with carboxyl-terminal HA tagging.

To place the *MCD1* gene under the control of the *GAL1,10* promoter (i.e., yJL171 and yJL172), the His3MX6-PGAL1 sequence (42) was amplified with primers O388 and O389. The PCR fragment was agarose gel purified and transformed into yMK1329 for histidine prototroph selection. Yeast genomic PCR was conducted using primers O390 and O391 (derived from the *MCD1* locus) against O392 or O393 (derived from the His3MX6 sequence) for verification. The correct integration of the *GAL* promoter to the *MCD1* 5' untranslated region was further verified by the inability of cells to grow in the presence of glucose.

To introduce the G44S mutation to a green fluorescent protein (GFP)-marked strain, SBY214, the *(hht1-hhf1)*Δ*::KanMX* allele from JHY200 was PCR amplified using primers O396 and O397 and transformed into SBY214 to knock out *HHT1-HHF1* (creating yJL118). Correct integration was verified by genomic PCR using primers O398, O399 (from the *HHT1/HHF1* locus), and mk133 (from KanMX). To replace the remaining copy of H3 and H4, i.e., *HHF2-HHT2*, with either wild-type

(WT) H3 or the G44S mutant with the *URA3* selective marker, plasmid pMK622 (WT or G44S mutant) was cleaved with *Sna*B I and *Eco*R I for integrative transformation. *Ura*$^+$ colonies were isolated for genomic PCR to verify the integration. Genomic PCR using primers O404 and O405 was done to amplify an *HHT2* fragment for *Sca* I digestion (indicative of the G44S mutation) and sequencing to rule out the existence of any unwanted mutations. To create congenic strains that differ only at the *HHT2* locus, both the WT and G44S mutant versions of pMK622 were digested for yJL118 transformation, resulting in yJL292 (*HHT2-HHT2::URA3-KTR5*) and yJL293 (*hht2 G44S-HHF2::URA3-KTR5*).

The yeast chromosomal copy of *HHT2* was mutated by integrating pMK622 bearing the desired mutation. To create pMK622, pMK621 was first generated by PCR to amplify from yeast genomic DNA part of *HHF2* and *KTR5* with primers O400 and O401. The PCR fragment was digested with *Eco*R I and *Sph* I and cloned into the same sites of pJJ244 (18). pMK622 was made by inserting the *Spe* I (blunted) and *Aat* II fragment from pQQ18 bearing the G44S mutation into the *Nar* I (blunted) and *Aat* II sites of pMK621, resulting in pMK622 with two 140-bp direct repeats spanning the *URA3* gene.

Histone mutations were generated by two-step PCR site-directed mutagenesis. Briefly, the desired mutations were incorporated into two complementary oligonucleotides, and each was used for PCR against O17 (downstream of *HHT2*

open reading frame [ORF]) or O19 (downstream of the *HHF2* ORF) that hybridized outside the *HHT2/HHF2* genes in pQQ18. The two PCR fragments (amplified using pQQ18 as the template by *Pfu* Turbo DNA polymerase [Stratagene]) were agarose gel purified and subjected to a second round of PCR. The complementary sequence at the 3' ends of these two PCR fragments allowed annealing and extension. Primers O17 and O19 were included in the reaction mixture to exponentially amplify the entire *HHT2/HHF2* gene with the mutation. The final PCR fragments were then digested with *Sal* I and *Spe* I and used to replace the WT *Sal* I/*Spe* I sequence in pQQ18. The entire H3 and H4 genes were sequenced for verification. This second-step PCR usually did not work well with *Pfu* Turbo polymerase. *Taq* polymerase was used to circumvent this problem. However, *Taq* polymerase frequently introduced unwanted mutations that had to be revealed by sequencing and, if detected, set aside. The original G44S mutation was obtain fortuitously in this manner.

pMK573, a 2μm *URA3 SGO1* plasmid, was created by PCR amplifying the *SGO1* ORF from yeast genomic DNA with primers O329 and O330 that included 42 bp of homology to the vector pMK572 (see below) at the 5' ends. The PCR fragment was cotransformed with *Hind* III- and *Eco*R I-digested pMK572 into yeast strain yMK839 (32). *Ura*$^+$ colonies were subjected to DNA isolation and bacterial transformation. Miniprep DNA was analyzed by restriction digestion and sequencing across the insertion junctions for confirmation of a correct insert.

To create pMK572 (a multicloning sequence flanked by the *ADH1* promoter and terminator), ADH-Ras-ΔBamH I (4) was digested with *Sma* I and self-ligated to remove the Ras sequence. The resultant plasmid, pMK322, then was used as the template for PCR using primers O327 and O328 to amplify the *ADH1* sequence and the multicloning sites. The PCR fragment was cotransformed with *Hind* III- and *Eco*R I-digested YEplac195 (a 2μm *URA3* plasmid [10]), resulting in pMK572. The multicloning sequence contains unique *Hin*d III, *Sma* I, *Sal* I, *Bss*H II, *Mlu* I, *Sac* I, *Not* I, *Eag* I, *Sfi* I, *Bal* I, and *Eco*R I restriction sites.

To create a construct for glutathione *S*-transferase (GST)-HA-Sgo1p in *Escherichia coli*, the *SGO1* ORF was PCR amplified with primers OJL25 and OJL26. The PCR fragment obtained was digested with *Not* I and ligated to *Not* I-linearized pMK595, resulting in in-frame fusion of 3xHA and *SGO1* (pJL51). To further generate a GST fusion of HA-SGO1 for bacterial production, 3xHA-SGO1 was isolated from pJL51 and inserted into pSP72 (Promega) at the *Hind* III and *Xho* I sites. The *BamH* I-*Xho* I fragment was then isolated and ligated to the *BamH* I and *Xho* I sites of pGEX4T-1, generating pJL55.

Yeast methods. Yeast growth media, conditions, and transformation were based on standard procedures (49). When appropriate, a 5% concentration of Casamino Acids (CAA) was used to substitute for synthetic amino acid mixtures as a selective medium for a uracil, tryptophan, or adenine prototroph. Yeast transformation was done by the lithium acetate method (9).

Chromosome stability of the WT and G44S mutant strains was examined according to Spencer et al. (51), using plasmid pYCF1/CEN3.L cut with *Bgl* II and transformed into yMK1243 and yJL145. *Ura*$^+$ transformants were grown in CAA-Ura medium overnight and then plated directly onto yeast extract-peptone-dextrose (YPD) plates to allow colony formation and scoring. A tension sensing test using the *pGAL-MCD1* mutant strains was done precisely to reference 15, using strains yJL171 and yJL172.

For Western analyses of yeast proteins, yeast extracts were prepared by directly boiling cell pellets in appropriate volumes of 2x sodium dodecyl sulfate (SDS)-polyacrylamide gel electrophoresis (PAGE) loading dye for 5 min, followed by vortexing with 1 lysate volume of glass beads (0.45 μm in diameter; Sigma) at room temperature for 5 min. The mixtures were boiled again for 5 min and then centrifuged at 14,000 x *g* at room temperature for 1 min. The supernatant was transferred to another tube for SDS-PAGE.

Suppressor screening. To screen for a multicopy suppressor of the G44S mutation, a YEplac195-based library was constructed by ligating 1 to 3 kb of *Dpn* I-digested yeast genomic DNA (enriched by sucrose gradient ultracentrifugation) to the *Bam*H I site of YEplac195 (10). G44S mutant cells transformed with 0.3 μg of library DNA in each of 20 transformation reactions were plated onto CAA-Ura, and *Ura*$^+$ colonies (estimated to be about 60,000 in total) were then replica plated onto YPD plates supplemented with 20 μg/ml benomyl and incubated at 30°C.

Initial benomyl-resistant colonies were regrown in YPD and streaked onto 5-fluoroorotic acid plates to select for clones that had lost the *URA3* plasmid. Benomyl sensitivity tests were repeated to screen for clones displaying plasmid-dependent benomyl resistance. Candidates were subjected to DNA isolation for *E. coli* transformation. Plasmid DNAs were isolated for restriction digestion and retransformation into the G44S mutant strain to verify the suppression phenotypes, including hypersensitivity to benomyl, heat shock, and cold. The identity of the insert was revealed by DNA sequencing using universal M13 primers.

Chromatin immunoprecipitation (ChIP). ChIP was conducted as previously described (28). To quantify the ChIP results, the semiquantitative PCR products were purified and resolved by 9% PAGE and stained with ethidium bromide. The captured gel images were then quantified by NIH Image. Intensities of the *CEN*/pericentric fragment were compared to that of a common internal control (the *DED1* or, in some cases, the *PGK1* locus). The ratio was further normalized to 0.1% input DNA (set at 1.0) for PCR amplifications carried out in parallel with all of the reactions. The ChIP data were obtained from at least three independent yeast cultures.

Recombinant Sgo1p preparation. To express and purify GST-HA-Sgo1p from *E. coli*, 125 ml of BL21 codon+ cells (Stratagene) were subjected to induction (optical density at 600 nm of 0.5 to 0.6 in LB-ampicillin medium) with 1 mM

isopropyl-β-D-thiogalactopyranoside (IPTG) at 37°C for 4 hours. Cells were pelleted (5,000 x *g* for 5 min) at 4°C and sonicated in 5 ml of HEMGT buffer (25 mM HEPES, pH7.9, 12.5 mM $MgCl_2$, 150 mM KCl, 0.1 mM EDTA, 0.1% Tween 20, 10% Glycerol, 1 mM dithiothreitol, 1 mM phenylmethylsulfonyl fluoride) six times for 20 sec each time with 1-min chilling intervals. The soluble fraction was obtained by centrifugation at 10,000 x *g* for 15 min at 4°C. Sgo1p was purified by incubating the cytosol with 200 µl of reduced glutathione Sepharose 4B beads (Amersham) at 4°C for 1 hour. Bound Sgo1p was washed twice with 5 ml of binding buffer for 5 min each time, followed by another wash with 1.5 ml of binding buffer, and transferred to a microcentrifuge tube. The elution was done by gently rocking beads in 200 µl of 50 mM glutathione in the binding buffer for 30 minutes at 4°C. Eluate was collected, and the elution was repeated once under the same conditions. Two batches of eluate were separately dispensed and stored at -70°C. The yield and purity of GST-HA-Sgo1p were estimated by SDS-PAGE.

Sgo1p interaction with H3, nucleosomal particles, and oligonucleosomes. Histones were prepared according to reference 6. Recombinant yeast histone H3 and reconstituted nucleosomal particles were gifts from K. Luger. For pulldown assays, approximately 5.5 µg of soluble recombinant Sgo1p was incubated with about 3.4 µg of yeast histones or oligonucleosome liberated by micrococcal nuclease digestion from a nuclear preparation with an A_{260} *of* 200 (WT and G44S mutant) in 150 µl of HEMGT buffer at 4°C for 1hour. Six microliters of glutathione

beads and 150 µl of the HEMGT buffer were added to the reaction mixtures, which were rocked gently at 4°C for another hour. Beads were washed with 500 µl of HEMGT buffer three times for 5 min each time, followed by boiling in 2x SDS-PAGE loading buffer for 5 min. Eluate was resolved by 15% SDS-PAGE and blotted for anti-H3 Western analyses. The anti-H3 antibodies were rabbit polyclonal serum made in house and raised against the peptide H_2N-CIQLARRIRGERA-COOH. The Western assay used a 1:2,000 dilution of the primary antibody. For far-western assays, 0.3 µg of yeast histones was first resolved by 15% SDS-PAGE and then blotted onto a polyvinylidene difluoride (PVDF) membrane. Small strips of the membrane were blocked with 10% milk in TTBS (0.9% NaCl, 0.1% [vol/vol] Tween 20, 50 mM Tris, pH7.4) at room temperature for 30 min, followed by two 10-min TTBS washes. For the Sgo1p-histone interaction, the membrane was incubated with 0.3 µg of GST-HA-Sgo1 in 3 ml of TTBS buffer supplemented with 0.1% gelatin. The binding was conducted at 4°C with gentle rocking for 3 to 5 hours. The membrane was then subjected to regular Western blotting procedures using anti-HA monoclonal antibody 12CA5 (Roche) at a 1:750 dilution.

RESULTS

An H3 mutation causes mitotic chromosome instability

To identify histone H3 mutations that affect chromatin metabolism in the budding yeast *Saccharomyces cerevisiae*, we fortuitously encountered a Gly-to-Ser mutation of histone H3 at position 44 (referred to as G44S henceforth) that caused hypersensitivity to benomyl, cold temperature (14°C), heat shock (37°C), and hydroxyurea (HU; Fig. 1A). Mild growth defects were also caused by UV light; however, methyl methanesulfonate did not have an obvious effect. At 26°C, the doubling time of log-phase cultures of the WT and G44S mutant strains are 110.9 ± 7.6 and 129.1 ± 8.8 min/generation, respectively (see Fig. S1 in the supplemental data). Fluorescence-activated cell sorter analyses of cultures grown at 14°C, 26°C, or 37°C did not reveal obvious defects in ploidy or cell cycle control (data not shown). These results demonstrated that the H3 G44S mutation conferred pleiotropic phenotypes and that cells were defective in dealing with certain stresses. It is worth noting that the some of the observed phenotypes, in particular, those related to mitosis (see below), were not specific to the original serine substitution, as an alanine mutation introduced at Gly44 resulted in literally identical phenotypes (data not shown). All of the analyses henceforth were conducted using the G44S allele.

Residue G44 resides at the end of a unique region of H3 (K37-G44) that connects the flexible tail domain (residues 1 to 36) and the well-structured core

(residues 45 to about 130) (Fig. 1B) (34). The small region of K37-G44 inserts through the aligned minor grooves of two DNA gyres and then makes a sharp β turn into the nucleosome core. This conserved β turn structure brings the K42 carbonyl oxygen to a topographically favorable position to form a hydrogen (H) bond with the amide group of T45 (Fig. 1B, right) (58). In addition, the amide group of G44 may also H bond with the DNA phosphate backbone (34). By contrast, P43 does not appear to participate in H bond formation with any nearby atoms of DNA or histones, suggesting that G44 plays unique roles in determining the architecture of H3 as it transitions from the extended flexible tail domain into a rigidly structured nucleosomal core. Given the unique position of G44 and the cellular hypersensitivity of the mutant to such genotoxic insults as benomyl, HU, and UV light, we suspected that some of the observed phenotypes were results of aberrations of chromatin metabolism. This work focused on the mitotic functions of G44.

To examine the role of H3 G44 in mitotic chromosome metabolism, we first measured the chromosome stability by introducing an artificial, non-essential chromosome into WT and G44S mutant cells bearing the *ade2-1* ochre mutant allele (51). *ade2*$^-$ yeast cells accumulate a red pigment and produce red colonies, whereas *Ade*$^+$ colonies are white. The artificial chromosome used in this study contained a mutant *SUP11* tRNA gene that suppresses the ochre mutation. Recipient cells thus formed white colonies. The frequency of first-division chromosome loss of WT and G44S mutant cells was measured (Fig. 2A).

Compared with WT cells, G44S mutant cells lost the indicator chromosome at a much greater rate (71 losses versus <1 loss per 1,000 divisions). In addition, red sectoring of G44S mutant cells was commonly accompanied by indentation of the otherwise round, smooth colonies (see closeups). This phenomenon may be due to slower cellular growth rates arising from aneuploidy of native chromosomes, and is consistent with the notion that the G44S mutation causes stochastic mitotic errors that retard growth (Fig. S1).

We next investigated the molecular defects underlying the benomyl hypersensitivity of G44S mutant cells. Eukaryotes respond to benomyl-triggered microtubule depolymerization by activating the SAC, which stabilizes the securin protein (Pds1p in yeast) and arrests cells at G_2/M phase (31). When G44S mutant and WT cells were examined for the budding index and the Pds1p level after benomyl treatment, we observed a similar efficiency of G_2/M arrest (Fig. 3A) and upregulation of Pds1p for up to 180 minutes (Fig. 3B), indicating that dissolving microtubules by benomyl was sufficient to trigger the normal spindle checkpoint responses. However, if yeast cells were plated on drug-free YPD medium to assess viability after 2, 4, or 6 hours of benomyl treatment, mutant cells lost viability more quickly (Fig. 2B). These results suggested that a lethal error, most likely missegregation (47), occurred when cells resumed mitosis after benomyl removal. To examine whether the segregation fidelity of G44S mutant cells was impaired after the brief benomyl shock, we used a GFP-marked haploid strain in which a *lac* operator array was integrated to the *TRP1* locus 12 kb from

CEN4 (53). In this background, one of the two copies of H3 was deleted and the remaining one was replaced with the G44S allele. This new GFP-marked G44S mutant strain exhibited phenotypes comparable to those seen with the original, non-GFP-marked strain, including sensitivity to benomyl, cold, and heat (data not shown).

When GFP-marked yeast cells were allowed to recover from the 2-hr benomyl shock, the WT strain exhibited a low rate of missegregation (1.1% ± 0.2% of the G1-phase cells showed two GFP dots), whereas the G44S mutant cells showed 11.3% ± 0.7% co-segregation of both Chromosome IV sister chromatids (Fig. 2C). Without benomyl treatment, both strains had a low incidence of missegregation, although there seemed to be a mild elevation in the G44S background (1.5% ± 0.6% versus 3.3% ± 0.2%). These data suggested that the G44S mutant cells were unable to either detect or to correct the erroneous kinetochore-spindle attachment that frequently happens during recovery from benomyl toxicity (56). Together, the results in Fig. 2 strongly suggested that the G44S mutation caused chromosome instability by impairing a cellular control mechanism that ensured the bipolar microtubule-kinetochore attachment before committing to anaphase.

G44S mutant cells are defective in tension sensing

Prior to the anaphase onset, sister chromatids are held together by the cohesin complex (27, 39). Cohered chromatids resist the poleward pulling force from

bipolar spindles, hence generating tension. The SAC can be activated by attachment errors or by the lack of tension. Given that G44S mutant cells exhibited normal SAC activation upon microtubule depolymerization (Fig. 3), and that attachment errors likely eluded cellular scrutiny (Fig. 2C), we tested whether the SAC was activated in G44S mutant cells under a tensionless condition.

To examine the tension-sensing function, we used a method (15) whereby the *MCD1* gene encoding an essential cohesin component was placed under the repressible control of the *GAL1* promoter (*pGAL*). Shifting cells from galactose to glucose medium represses *MCD1* expression and hence perturbs the formation of sister cohesion, which consequently prevents tension establishment but does not influence the spindle-kinetochore attachment (2). This tensionless crisis activates the SAC. Using this approach, we compared the SAC activation of the WT and G44S mutant strains. Yeast cells bearing the *pGAL-MCD1* gene were grown to log phase in YPgal medium and synchronized at G1 by α-factor. Cells were then released into either YPgal (Gal to Gal) or YPD (Gal to Glc) and harvested at different time points before the cells were again arrested at the next G1 stage by α-factor. Western blotting was conducted to compare the level of Pds1p to see whether the tensionless crisis triggered the activation of SAC in G44S mutant cells (Fig. 4). Gal-to-Gal treatment allowed yeast cells to continue dividing, as evidenced by the degradation of Pds1p when cells finished the first round of mitosis. In contrast, shifting WT cells from galactose to glucose (Gal to Glc) stabilized Pds1p, demonstrating the activation of the SAC. On the other

hand, G44S mutant cells degraded Pds1p about 60 minutes after release from the first G_1 block under both Gal-to-Gal and Gal-to-Glc conditions, indicating that the G44S mutation impaired the ability of cells to detect or to respond correctly to the tensionless condition.

Shugoshin is a high-copy-number suppressor of G44S tension-sensing defects

The above results revealed that the G44S mutation of H3 caused a defect in the tension-sensing function in mitosis. To further delineate the molecular mechanism underlying this new function of histone H3, we conducted a high-copy-number suppressor screen for genes that could rescue the benomyl hypersensitivity phenotype. From about 60,000 transformants representing ninefold coverage of the *S. cerevisiae* genome, we obtained 20 independent clones. Sequencing results revealed five nonoverlapping genomic DNA inserts (data not shown). Histone H3 was one of the clones, thus validating the screening. Two multifunctional transcriptional activators, *YAP1* and *CAD1*, were found multiple times in the screen. However, these two proteins have been shown to confer resistance to a variety of stresses, including benomyl (40, 59), and hence were considered unlikely to be relevant to the tension-sensing defects. Another candidate contained the intragenic region between the *BIO1* and *YGR287C* genes without a discernible gene in this fragment. No further work was conducted on this clone. The last and most likely candidate contained the *SGO1* gene missing the first 34 amino acids and the 5' promoter element (data

not shown). Sgo1p plays a key role in mitotic tension sensing (15, 21). The identification of this gene, albeit slightly shorter, as a suppressor agreed well with the observed mitotic phenotypes of the G44S mutant. We posited that a cryptic promoter in the vector activated the expression of a slightly truncated but functional Sgo1p that was responsible for the observed suppression.

To verify that Sgo1p was a bona fide suppressor for G44S, we cloned the *SGO1* ORF, with or without the first 34 amino acids, downstream of the constitutive *ADH1* promoter in a 2μm plasmid. G44S mutant cells transformed with different *SGO1*-overexpressing plasmids were tested for responses to benomyl, cold, HU, and UV light. Overexpressing Sgo1p alone rescued hypersensitivities to benomyl and cold but not to HU or UV light (Fig. 5A), indicating that the suppression was specific to mitotic defects caused by this mutation. Deleting the first 34 amino acids did not affect the suppression (data not shown), consistent with the notion that the original 34-amino acid truncation did not alter the normal function of Sgo1p. Critically, overproducing Sgo1p alleviated the phenotypes of benomyl-induced lethality, chromosome missegregation (Fig. 5B), and the inability to stabilize Pds1p under a tensionless condition (Fig. 5C). The expression of endogenous *SGO1* was normal at both transcription and translation levels (Fig. 5D), arguing against the possibility that the G44S mutation downregulated the abundance of Sgo1p. Together, these genetic data strongly suggested that Sgo1p acted downstream of H3 and that the G44S mutation undermined the function of Sgo1p in mitosis.

G44S mutation attenuates Sgo1p interaction and localization

Based on the genetic interaction between *SGO1* and H3 revealed by the high-copy suppressor screening, we suspected that the G44S mutation might affect a function of Sgo1p. Sgo1p is enriched at centromeres and pericentric regions, where tension is most likely monitored by the hitherto unspecified machinery (22). Mutations that eliminate the Sgo1p recruitment to these loci also cause tension sensing defects (5). We thus used ChIP to examine whether the recruitment of Sgo1p was impaired by the G44S mutation. To this end, we tagged the chromosomal *SGO1* with HA at the 3' end. The HA tag did not alter the benomyl (hyper)sensitivity of either WT or G44S cells (data not shown). Mitotic cells were harvested for ChIP, and immunoprecipitation efficiency compared by semiquantitative PCR. The ChIP results showed that Sgo1p was present at both centromeres and pericentromeres in WT cells (Fig. 6). However, pericentric Sgo1p was significantly reduced in G44S mutant cells, while the centromeric localization of Sgo1p was normal. The pericentric Sgo1p domain was narrow, for PCR fragments 9.1 kb from *CEN16* and 8.3 kb from *CEN1* were so weak that it did not show a significant difference between the two strains (Fig. 6B). At the *SPT15* locus 313.3 kb from *CEN5,* there was essentially no Sgo1p detected in either background. The differential effects on centromeric and pericentric recruitment of Sgo1p were consistent with the fact that the canonical H3 is replaced by Cse4p at centromeres (35). Mutating H3 thus had no effect on Sgo1p-centromere association. In conclusion, the ChIP data demonstrated that

the G44S mutation specifically diminished the pericentric localization of Sgo1p during mitosis.

The genetic and ChIP data shown above predicted that histone H3 and Sgo1p interacted for mitotic tension surveillance, and that this association was attenuated by the G44S mutation. To test these predictions biochemically, we expressed GST and HA double-tagged Sgo1p in *E. coli* and subjected it to *in vitro* binding assays using core histones or oligonucleosomes purified from WT and G44S mutant yeast cells. In pulldown assays, histone H3 was incubated with Sgo1p and trapped by glutathione beads. Anti-H3 Western blotting then was used to compare the relative abundance of WT and G44S mutant H3 trapped by recombinant Sgo1p. In a parallel far-Western approach, the purified yeast histones were first resolved by SDS-PAGE and then blotted onto membrane. After incubating the blot with HA-tagged recombinant Sgo1p, anti-HA antibodies were used to probe the trapped Sgo1p by each histones. Figure 7A (pulldown) shows that WT free and nucleosomal H3 bound Sgo1p efficiently, whereas G44S mutant H3 bound to Sgo1p with a diminished affinity. In the far-Western assay (Fig. 7B), HA-Sgo1p also bound more effectively to WT H3. Importantly, the H3-Sgo1p interaction was independent of other histones, and Sgo1p only interacted with H3 (Fig. 7B). Furthermore, chicken H3, recombinant yeast H3, and reconstituted nucleosomal core particles all bound Sgo1p (Fig. S2). It is noteworthy that the G44S mutation did not completely eliminate Sgo1p binding (compare the 0.6x and 1x histone doses in the left panel of Fig. 7A). The remnant

affinity for Sgo1p provided a molecular explanation for the dosage-dependent suppression seen *in vivo*.

Together, these results demonstrated that the molecular basis for the G44S mitotic defects was an attenuated interaction between histone H3 and Sgo1p, resulting in the loss of Sgo1p from pericentromeres. While the centromeric enrichment of Sgo1p was not affected by the H3 mutation, the downregulation of pericentric Sgo1p enrichment was likely sufficient to cause the tension sensing phenotypes associated with the G44S mutation.

Reinstating pericentric Sgo1p partially rescues G44S mitotic defects

If the only purpose of the observed H3-Sgo1p interaction was to bring the latter to pericentromeres for tension surveillance, artificially tethering Sgo1p back to the pericentric loci should effectively eliminate the mitotic phenotypes of G44S mutant cells. On the other hand, if the interaction between H3 and Sgo1p was also important for mitotic control, forcing Sgo1p to pericentromeres by an approach other than the natural H3-Sgo1p association may, at best, only partially suppress the mitotic defects caused by the G44S mutation. The challenge of artificial tethering a protein to the pericentric regions in the budding yeast is that the pericentromeres do not form heterochromatin like other eukaryotic systems and that there is no known epigenetic mark specific to this region. Nonetheless, the ChIP data in Fig. 7A suggested that the establishment of an Sgo1p domain was likely nucleated from the H3-independent recruitment at the centromere,

where the canonical histone H3 was absent. The physical association of H3 and Sgo1p then allowed the latter to spread outward to generate a pericentric domain (see Discussion for details). If this is so, fusing Sgo1p to a general chromatin-binding motif may reestablish the pericentric retention of Sgo1p and would allow us to assess the effect of pericentric recruitment of Sgo1p in the G44S mutant background.

To regenerate the pericentric enrichment of Sgo1p in the G44S mutant background, we fused a bromodomain (BD) from Bdf1p to the carboxyl end of Sgo1p and a trimeric HA tag to the amino terminus. Bdf1p binds both histones H3 and H4 (41), and the bromodomain in different proteins has been shown to interact with acetyllysine (5, 17). Genome-wide ChIP analyses detected comparable histone acetylation between pericentromeres and the bulk of the yeast genome (29), suggesting that a general (acetylated) histone-binding module such as the bromodomain may complement the weakened affinity of Sgo1p for G44S mutant H3. As shown in Fig. 8A, this indeed was the case. When Sgo1p and Sgo1p fused to the bromodomain domain (Sgo1p-BD) were introduced to *sgo1*Δ mutant cells expressing the WT or G44S mutant allele of H3, Sgo1p-BD exhibited efficient pericentric enrichment (Fig. 8A and C), whereas Sgo1p without the BD remained underrepresented at pericentromeres. These two alleles of Sgo1p were expressed at comparable levels (Fig. 8B), indicating that the bromodomain fusion increased the affinity for a histone at the pericentromeres. Importantly, the reinstatement of pericentric Sgo1p was

accompanied by partial suppression of benomyl hypersensitivity, loss of viability following benomyl shock, and stabilization of Pds1p during *MCD1* shutdown (Fig. 9A to C). Together, these results strongly suggested that dislodging Sgo1p from pericentromeres was the major underlying cause of the G44S mutant mitotic defects.

In summary, histone H3 plays a critical role in Sgo1p recruitment to the mitotic pericentromeres, where the tension between sister chromatids is likely monitored. Genetic data strongly suggest an intimate association between H3 and Sgo1p, a notion supported by ChIP and biochemical assays. We thus conclude that the mitotic tension sensing function depends critically on the appropriate association between histone H3 and Sgo1p in the pericentric regions.

DISCUSSION

Establishment of a pericentric Sgo1p domain

This work uncovers a novel function of histone H3 in mitotic checkpoint control. By recruiting Sgo1p specifically to the pericentric region, histone H3 was shown for the first time to play a role key in segregation fidelity. As the G44S mutation selectively compromises the pericentric enrichment of Sgo1p but apparently leaves centromeric Sgo1p unaltered (Fig. 6), we suspect that Sgo1p localization is nucleated by an H3-independent mechanism at the centromere/kinetochore, followed by spreading toward the pericentric regions via direct association with histone H3. This scenario is analogous to the mechanism of establishing the telomeric heterochromatin in yeast (12), in which Rap1p nucleates the heterochromatin formation by binding to the telomeric $C_{1\text{-}3}A$ repeats. Silent Information regulator, or Sir, proteins are recruited by Rap1p. Via the direct association between Sir3p/Sir4p and the amino terminal tails of histones H3 and H4 (6), Sir proteins spread from the nucleation site to the neighboring region (45). Inserting the telomeric $C_{1\text{-}3}A$ repeats into an ectopic location is sufficient to create a new transcription silent domain, conclusively ruling out the need for a specific *cis*-acting element for Sir protein spread or retention (52). Similarly, relocating the centromere to an ectopic site establishes a new Sgo1p domain (22).

The notion that the H3-Sgo1p association is critical for mitotic regulation is also supported by the observation that the G44S allele caused mild benomyl sensitivity in the presence of the WT counterpart (Fig. S3). It is conceivable that the concomitant incorporation of wild type and G44S mutant H3 into nucleosomes in the pericentric region results in intermediate affinity for Sgo1p, thus resulting in visible but not as severe defects in coping with benomyl toxicity.

The protein directly responsible for bringing Sgo1p to the centromere remains unidentified. Among the 30-plus kinetochore proteins and the SAC components, one of the likely Sgo1p recruiters is Bub1p. Although deleting *BUB1* causes loss of Sgo1p in centromeres and pericentromeres (7, 22), the physical evidence for Bub1p-Sgo1p association is lacking to date. Moreover, Bub1p is a kinase that is essential for SAC assembly at the kinetochore (33). It is thus also possible that Bub1p regulates the protein that physically brings Sgo1p to the centromere.

Given the diverse posttranslational modifications of histones, it is tempting to speculate about an alternative model in which a novel epigenetic mark at the pericentromeres facilitates Sgo1p retention. For example, Gcn5p and Hda1p have been linked genetically to mitotic segregation (19, 57), and Ser31 phosphorylation of the human H3.3 variant is enriched at the pericentric heterochromatin (13). However, we do not believe this notion is very likely because Sgo1p interacts with bulk H3 from yeast and chicken, as well as recombinant H3 synthesized in *E. coli* (Fig. S2), arguing against an H3

modification essential for Sgo1p binding. Nonetheless, we do not rule out the possibility of an auxiliary function of an unidentified, pericentromere-specific modification. Nor do we disregard a notion that a chromosome arm-specific epigenetic mark prevents the H3-Sgo1p interaction outside the pericentric region. Due to the absence of functionally and structurally distinct pericentromeres in the budding yeast, the identification of this epigenetic mark presents a major technical challenge.

Tension sensing-specific relationship between H3 and Sgo1p

While the G44S mutation causes pleiotropic phenotypes (Fig. 1A), the genetic and physical interactions between H3 and Sgo1p are specific for tension sensing based on multiple lines of evidence. First, overexpressing Sgo1p does not have an effect on a histone H4 allele, *hhf1-20*, that impairs centromere/kinetochore functions (50) (Fig. S4). The *hta1-300* allele of histone H2A, which causes defects in ploidy control, is also insensitive to *SGO1* overexpression (I. Pinto, personal communication). Second, we have yet another H4 mutant allele, R35S, that also causes benomyl hypersensitivity (J. Luo, X. Xu, and M.-H.Kuo, unpublished data). 2μm *SGO1* constructs fail to suppress this mutant. In contrast, other candidates fished out of the original suppressor screens, such as *CAD1* and *YAP1,* which have been linked to multidrug resistance, rescued the benomyl hypersensitivity associated with either H3 G44S or the H4 R35S mutations (data not shown). Third, although G44S mutant cells are sensitive to UV light and HU, neither defects is responsive to Sgo1p overproduction (Fig. 5A),

indicating that, whereas the G44S mutation may also impair the control of DNA metabolism or damage repair, this is an *SGO1*-independent function. Indeed, deleting *SGO1* does not render cells sensitive to UV light or HU (data not shown). Lastly, the G44S mutation does not affect the pericentric recruitment of the cohesin component Mcd1p (Fig. S7), indicating that pericentric H3 is a specific interaction target for Sgo1p, whereas Mcd1p (i.e., the cohesin complex) is recruited to the pericentric region via a different pathway (8). The last notion is consistent with the fact that cohesin also forms clusters in the chromosome arms whereas Sgo1p is absent therein (19).

One might argue that the G44 mutation causes a general transcriptional defect that indirectly impairs Sgo1p recruitment or acts in a different pathway that leads to the tension sensing defects observed in this work. We do not think this notion likely because when we examined the transcription of a variety of genes representing functions in mitosis, checkpoint control, nutrient responses, mating, and transcriptional silencing, we did not detect any discernible differences between WT and G44S mutant cells (Fig. S6). The only transcription defect that we found associated with G44 mutations is the deregulation of transcription driven by cryptic promoter elements within certain ORF (20) (EMH, and JB, submitted). However, this phenotype was not affected by *SGO1* overexpression (data not shown), further strengthening the mitosis-specific relationship between H3 and Sgo1p.

While the current work focuses on the G44 allele of H3, which was obtained fortuitously in an attempt to create other mutants with mitotic phenotypes, our preliminary data indicated that residues surrounding Gly44 of H3 perform similar mitotic functions and that targeted mutations thereof lead to tension sensing defects similar to those of the G44S mutant (J. Luo and M.-H. Kuo, unpublished data). We suspect that G44 is part of a "tension-sensing motif" that makes physical contact with Sgo1p. Biochemical and molecular studies are in progress to test this hypothesis.

Other factors related to Sgo1p and tension sensing

Sgo1p belongs to the Shugoshin family proteins found in many eukaryotes. Several conserved proteins, including Bub1p, PP2A, and microtubules, are linked to Shugoshin functions. For example, Bub1 homologues are critical for centromeric and pericentric localization of Shugoshin in different organisms (7, 22, 24, 55). Human and yeast Shugoshin proteins collaborate with a specific form of protein phosphatase 2A (PP2A) to protect meiotic cohesin (26, 46, 54). The Sgo1p-PP2A cooperation appears to be independent of the Sgo1p-H3 interaction, for deleting *CDC55* or *RTS1*, the key B and B' regulatory subunits of PP2A complexes, does not affect the ability of the 2μm *SGO1* to suppress the benomyl hypersensitivity phenotype of G44S mutant (Fig. S7). The human and *Xenopus* Shugoshin bind and stabilize mitotic kinetochore microtubules (48). It is unclear whether budding yeast Sgo1p does so. However, this microtubule stabilization function is clearly a postbiorientation activity preceded by the tension

surveillance function. Therefore, we believe that histone H3 is the first protein shown to act directly upstream of Sgo1p in mitotic tension sensing.

A key player in correcting tension defects is the Aurora B kinase encoded by *IPL1* in budding yeast. Ipl1p destabilizes spindle-kinetochore attachment before anaphase nucleation, hence permitting correction of attachment errors (2). We observed synthetic phenotypes when Ipl1p or one of its partners, Sli15p, was overexpressed in an *sgo1*Δ or H3 G44S background (Fig. S8). These genetic interactions suggest that increasing the detachment activity of Ipl1p/Sli15p brings about a molecular defect (i.e. spindle detachment) similar to that caused by benomyl treatment. Lacking of functional Sgo1p or intact H3 causes growth defects.

It is critical that the BD-Sgo1p fusion protein can be recruited to the pericentromeres. However, close examination of the efficacy of suppression revealed that Sgo1p-BD only partially corrected the mitotic defects (Fig. 8). The enrichment of recombinant Sgo1p is consistent with the "nucleation-and-spread model" depicted above for establishing the Sgo1p domain. However, the inability of the Sgo1p-BD chimeric protein to completely restore benomyl tolerance suggests two possibilities. First, the bromodomain may somehow interfere with the tension sensing function of Sgo1p but not the ability to interact with the nucleating protein for recruitment. Alternatively, the physical interaction between Sgo1p and H3 at G44 might be critical for the tension sensing function. For

example, if Sgo1p docks directly to G44 and nearby residues, the bromodomain may place Sgo1p toward the far end of the amino terminal tail domain of H3 or even at a different spot on the nucleosomal particle where the H4 tail resides. If this is so, the activity of Sgo1p in tension sensing may be attenuated even though it has been directed back to the pericentromeres. Structural and biochemical experiments are required to examine these questions.

ACKNOWLEDGMENTS

We are grateful for C. David Allis, Angelika Amon, Sue Biggins, Jennifer Gerton, Phil Hieter, Karolin Luger, Mitchell Smith, and Fred Winston for generous supply of materials; Sue Biggins for advice; and Inés Pinto for sharing unpublished results. We thank Sue Biggins, Sharon Dent, and John Wang for critical reading of the manuscript, Yang Liu for creating the original G44S allele, and David Almy, No-Ya Hung, and Andy Lin for technical assistance.

This work was partly supported by a grant (CMB 0315542) from the National Science Foundation to M.-H.K.

J.L. contributed to all of the experimental data, except the following. X.X. conducted suppressor screening and initial characterization of 2μm *SGO1*. Genetic interactions among *IPL1*, H3 and *SGO1* were contributed by H.H. and T.H. Work related to cryptic promoter regulation was contributed by E.M.D. and J.D.B. M.-H.K. coordinated the project.

There is no conflict of interest for this work.

TABLE 2-1. Yeast strains used in this study

Strain	Relevant genotype	Source or reference
A10652	W303 *MATa SGO1-6HA*	(22)
JHY200	*MATa ade2-1 can1–100 his3–11,15 leu2–3,112 trp1–1 ura3-1 hht1-hhf1::KAN hht2-hhf2::KAN hta1-htb1::Nat hta2-htb2::HPH* pJH33 [*ARS CEN URA3 HTA1-HTB1 HHT2-HHF2*]	(1)
SBY214	*MATa ade2-1 bar1Δ can1-100 his3-11::pCUP1-GFP12-lacI12::HIS3 leu2,3-112 lys2Δ trp1-1::lacO::TRP1 ura3-1*	(2)
yJL118	*MATa ade2-1 bar1Δ can1-100 his3-11::pCUP1-GFP12-lacI12::HIS3 leu2,3-112 lys2Δ trp1-1::lacO::TRP1 ura3-1 hht1-hhf1::KAN*	This study
yJL145	*MATa ade2-1 can1–100 his3–11,15 leu2–3,112 trp1–1 ura3-1 hht1-hhf1::KAN hht2-hhf2::KAN hta1-htb1::Nat hta2-htb2::HPH* pMK439G44S [*ARS CEN LEU2 HTA1-HTB1 hht2-G44S-HHF2*]	This study
yJL171	*MATa ade2-1 bar1Δ can1–100 his3–11,15::pGAL-MCD1::HIS3 leu2–3,112 trp1–1::PDS1-Myc13::TRP1 ura3-1 hht1-hhf1::KAN hht2-hhf2::KAN hta1-htb1::Nat hta2-htb2::HPH* pQQ18 [*ARS CEN LEU2 HTA1-HTB1 HHT2-HHF2*]	This study
yJL172	*MATa ade2-1 bar1Δ can1–100 his3–11,15::pGAL-MCD1::HIS3 leu2–3,112 trp1–1::PDS1-Myc13::TRP1 ura3-1 hht1-hhf1::KAN hht2-hhf2::KAN hta1-htb1::Nat hta2-htb2::HPH* pMK439G44S [*ARS CEN LEU2 HTA1-HTB1 hht2-G44S-HHF2*]	This study
yJL292	*MATa ade2-1 bar1Δ can1-100 his3-11::pCUP1-GFP12-lacI12::HIS3 leu2,3-112 lys2Δ trp1-1::lacO::TRP1 ura3-1::hht2-hhf2::HHT2-HHF2::URA3 hht1-hhf1::KAN*	This study
yJL293	*MATa ade2-1 bar1Δ can1-100 his3-11::pCUP1-GFP12-lacI12::HIS3 leu2,3-112 lys2Δ trp1-1::lacO::TRP1 ura3-1::hht2-hhf2::hht2-G44S-HHF2::URA3 hht1-hhf1::KAN*	This study
yJL343	*MATa ade2-1 can1–100 his3–11,15 leu2–3,112 trp1–1::SGO1-6HA::TRP1 ura3-1 hht1-hhf1::KAN hht2-hhf2::KAN hta1-htb1::Nat hta2-htb2::HPH* pQQ18 [*ARS CEN LEU2 HTA1-HTB1 HHT2-HHF2*]	This study
yJL344	*MATa ade2-1 can1–100 his3–11,15 leu2–3,112 trp1–1::SGO1-6HA::TRP1 ura3-1 hht1-hhf1::KAN hht2-hhf2::KAN hta1-htb1::Nat hta2-htb2::HPH* pMK439G44S [*ARS CEN LEU2 HTA1-HTB1 hht2-G44S-HHF2*]	This study
yMK1243	*MATa ade2-1 can1–100 his3–11,15 leu2–3,112 trp1–1 ura3-1 hht1-hhf1::KAN hht2-hhf2::KAN hta1-htb1::Nat hta2-htb2::HPH* pQQ18 [*ARS CEN LEU2 HTA1-HTB1 HHT2-HHF2*]	This study
yMK1329	*MATa ade2-1 can1–100 his3–11,15 leu2–3,112 trp1–1::PDS1-Myc13::TRP1 ura3-1 hht1-hhf1::KAN hht2-hhf2::KAN hta1-htb1::Nat hta2-htb2::HPH* pJH33 [*ARS CEN URA3 HTA1-HTB1 HHT2-HHF2*]	This study
yMK839	*MATa leu2-3 trp1 ura3-52*	(32)

TABLE 2-2. Plasmid constructs used in this study

Plasmid	Main features	Source or reference
pJH33	pRS316-*HTA1-HTB1 HHT2-HHF2*	(1)
pJL51	2micron 3xHA-SGO1	This study
pJL53	ARS1 CEN4 URA3 p*ADH*1-3x*HA-SGO*1-t*ADH*1	This study
pJL55	pGEX-4T-1 3xHA-SGO1	This study
pJL76	ARS1 CEN4 URA3 p*ADH*1-3x*HA-SGO*1-Bromodomain-t*ADH*1	This study
pMK439G44S	pRS315-*HTA1-HTB1 hht2 G44S-HHF2*	This study
pMK572	2micron URA3 vector with ADH1 promtoer and terminator	This study
pMK573	2micron URA3 SGO1 with ADH1 promtoer and terminator	This study
pMK621	pJJ244 *URA3-HHF2-KTR5* insert	This study
pMK622G44S	pJJ244 *hht2 G44S-HHF2-URA3-HHF2-KTR5*	This study
pMK622WT	pJJ244 *HHT2-HHF2-URA3-HHF2-KTR5*	This study
pQQ18	pRS315-*HTA1-HTB1 HHT2-HHF2*	(1)
pYCF1/CEN3.L	YRp14/TEL cassette (pYCF1) with a CEN3 insert	(51)

FIG. 2-1. The G44S mutation confers pleiotropic phenotypes. (A) Yeast cells bearing the G44S allele as the sole copy of H3 were tested on YPD medium under the indicated conditions. Sixfold serially diluted log-phase cells were spotted for growth tests. All drug tests were conducted at 30°C. (B) Position of G44 of H3 within a nucleosomal core particle. Left panels: Two views of the crystal structure (Protein Data Bank entry: 1ID3) based on White et al. (58). Right panels: closeup view of the ^{42}Lys-Pro-Gly-Thr β turn (top) and the secondary structural domains (bottom) of histone H3. Numbers below the secondary structure are amino acid residues at the junctions of the indicated domains. The green dotted lines in the closeup represent possible hydrogen bonds between the carbonyl oxygen of K42 and the amide groups of G44 and Thr45. Hydrogen is not included. DNA is omitted for clarity.

Fig. 2-1

A

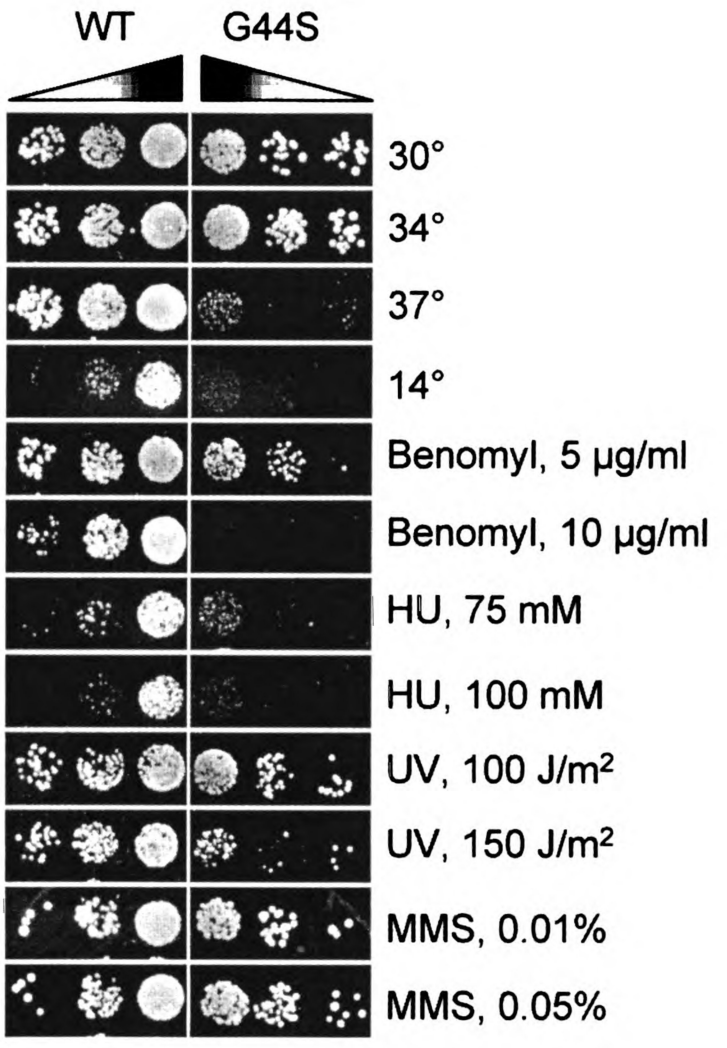
WT
G44S
30°
34°
37°
14°
Benomyl, 5 μg/ml
Benomyl, 10 μg/ml
HU, 75 mM
HU, 100 mM
UV, 100 J/m2
UV, 150 J/m2
MMS, 0.01%
MMS, 0.05%

Fig. 2-1 continued

B

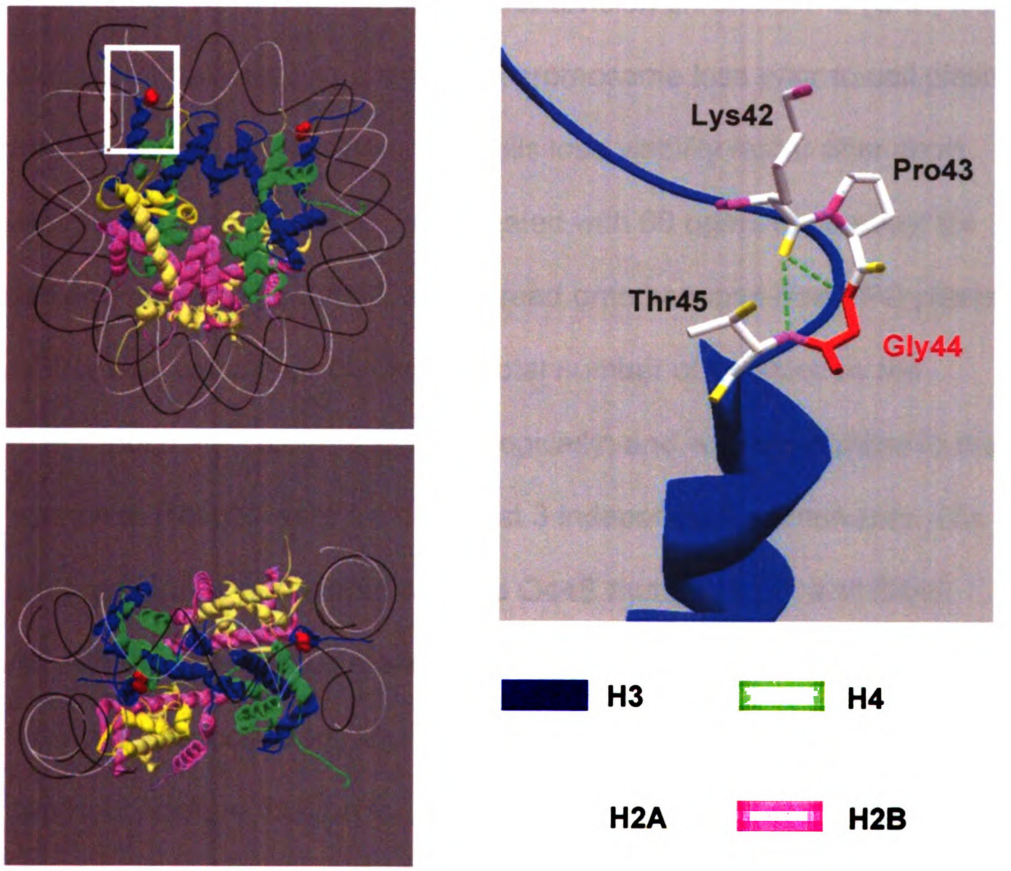

FIG. 2-2. The G44S mutation causes chromosome instability. (A) Mitotic chromosome stability tests. Representative pictures of colonies on YPD plates are shown at the top. The bar graph was prepared from three independent experiments with standard error of the mean. Colonies with at least 50% continuous red sector were counted as the first-division chromosome (Chr.) loss. Colonies that were totally red, as a result of chromosome loss prior to cell plating on YPD, were excluded. (B) G44S mutant cells lose viability faster after short benomyl exposure. Log-phase cells were treated with 60 μg/ml of benomyl for the indicated time, washed, counted, and spread onto benomyl-free YPD plates. Percent viability was calculated by dividing total number of colonies by the number of cells inoculated (counted microscopically) and was normalized to that of the *T0'* samples. Results were from at least 3 independent experiments. (C). Higher missegregation is associated with the G44S mutation. WT and G44S mutant cells with the *TRP1* locus marked by GFP were treated with 30 μg/ml benomyl for two hours, collected, and regrown in YPD medium containing α factor for two hours before fixation for microscopy. At least 200 unbudded cells with GFP dots were scored in four independent cell cultures of each strain. Green and red bars represent WT and G44S mutant cells, respectively. Error bars show standard deviations. Randomly selected images of two-dotted wild type and G44S cells (marked by white triangles) are shown on the right. w/o, without.

Fig. 2-2

A

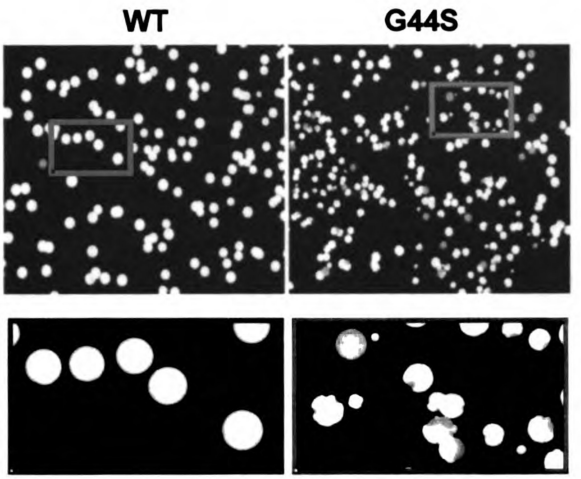

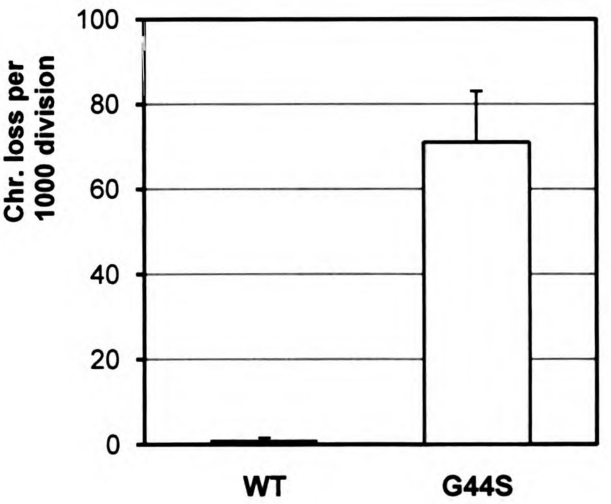

Fig. 2-2 continued

B

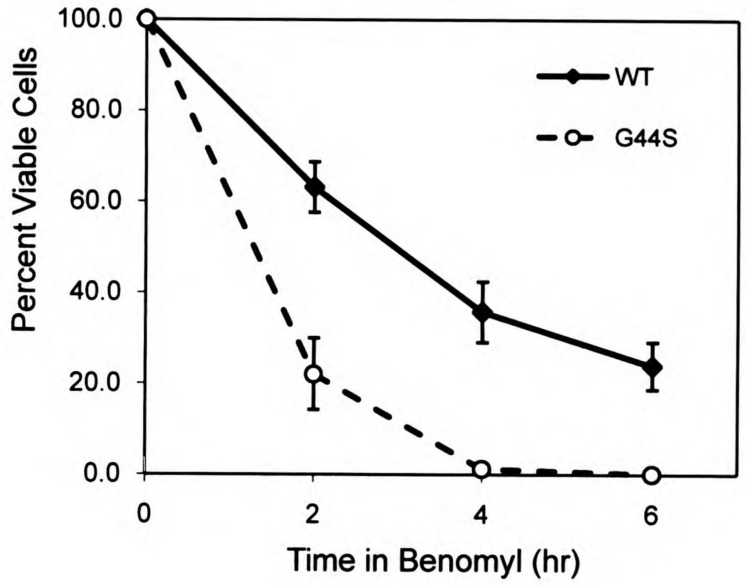

C

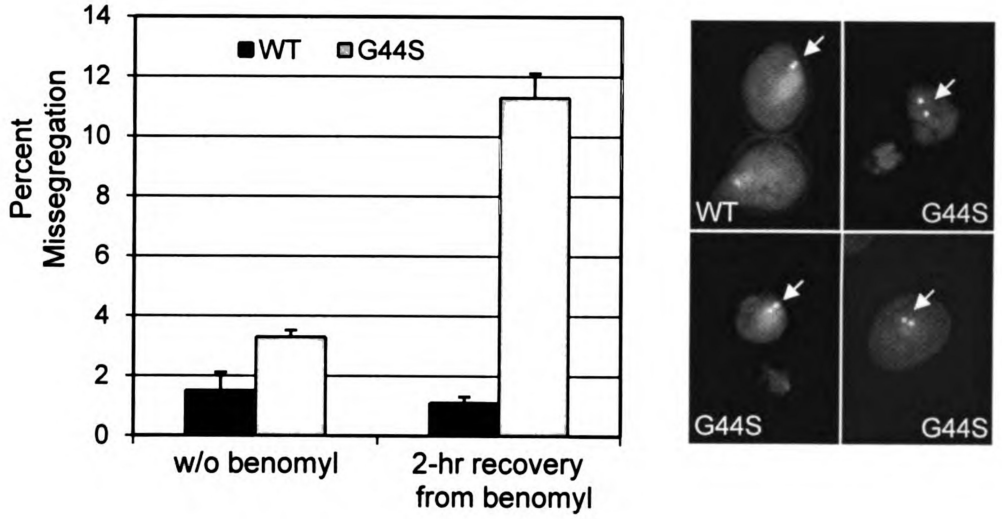

FIG. 2-3. G44S mutant cells activate the spindle checkpoint in response to benomyl toxicity. (A) Comparable budding indices were obtained from WT and mutant cells. Benomyl (60 μg/ml) was added to log-phase cells. The percentage of large-budded cells (with daughter cells at least half the diameter of their mothers) was determined microscopically. (B) Pds1p was activated and stabilized in both normal and G44S mutant cells in the presence of benomyl. Comparable numbers of α-factor arrested G_1 cells were released at T_0' into YPD medium containing 0 or 30 μg/ml of benomyl. The same volume of cell suspension was taken at the indicated times for boiling and whole-cell extract preparation, followed by anti-Myc Western blotting to quantify the abundance of Pds1p.

Fig. 2-3

A

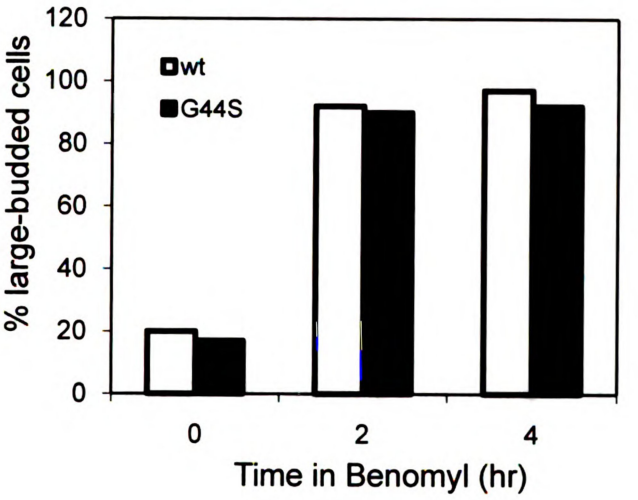
% large-budded cells
120
100
80
60
40
20
0
wt
G44S
0
2
4
Time in Benomyl (hr)

B

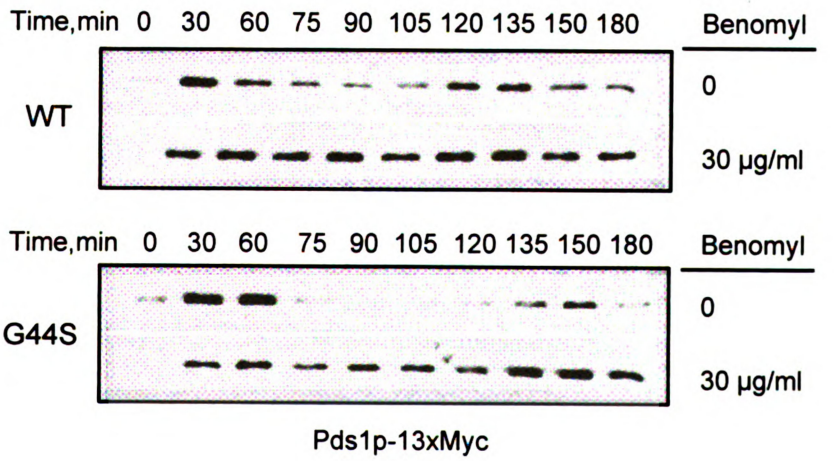
Time,min 0 30 60 75 90 105 120 135 150 180
Benomyl
WT
0
30 µg/ml
Time,min 0 30 60 75 90 105 120 135 150 180
Benomyl
G44S
0
30 µg/ml
Pds1p-13xMyc

Fig. 2-4

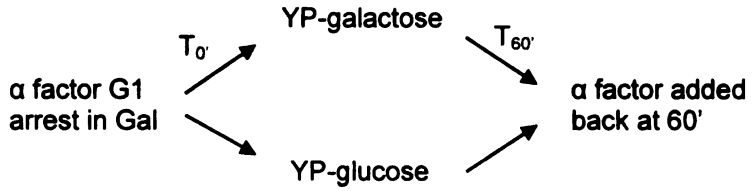

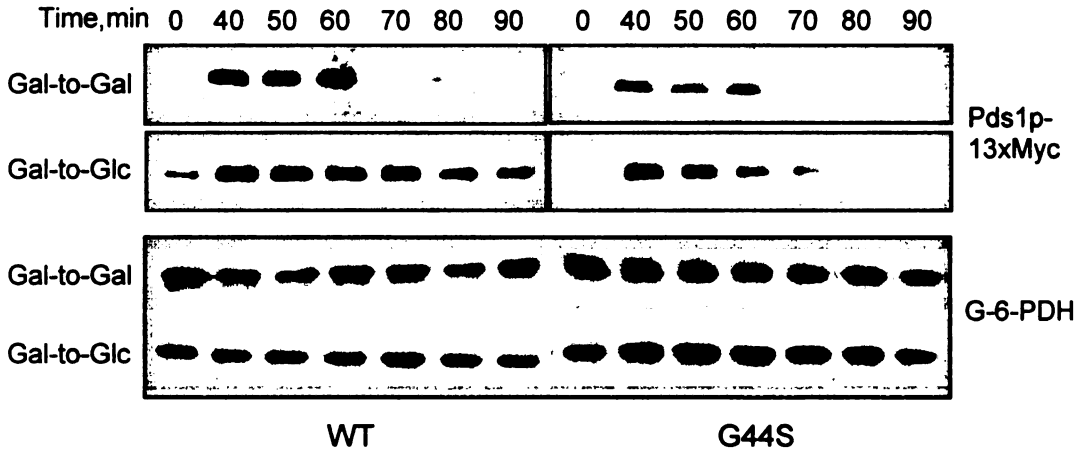

FIG. 2-4. The G44S mutation impairs the tension sensing function. *MCD1* was placed under the control of the *GAL1* promoter for glucose repression. The abundance of Myc-tagged Pds1p was analyzed by Western blotting in the presence (Gal-to-Gal) or absence (Gal-to-Glc) of Mcd1p. Experimental schemes are shown above the Western blot assay results. G-6-PDH: glucose-6-phosphate dehydrogenase.

FIG. 2-5. G44S mutant mitotic phenotypes are suppressed by overexpressing Sgo1p. (A) Sgo1p overproduction specifically rescues the mitotic phenotypes of G44S mutant cells. The *SGO1* ORF was cloned into a 2μm plasmid bearing the promoter and terminator sequences of *ADH1*. WT and G44S mutant cells transformed with *SGO1* or the corresponding vector were tested under the indicated conditions. (B) Left panel, cell viability test after benomyl treatment. This plot was generated from three independent experiments, and the error bars depict the standard deviations. Right panel, chromosome missegregation assay. Shown are percentages of two-GFP-dotted G_1 phase cells. Data were collected from three or four independent cultures, and error bars represent standard deviations. See the legend to Fig. 2B and C for details. (C) Tension sensing defects conferred by the G44S mutation are alleviated by *SGO1* overexpression. G44S mutant cells receiving a 2μm plasmid with or without the *ADH1*-driven *SGO1* gene were tested for the molecular response following *MCD1* shutdown. Experiments were done exactly as those shown in Fig. 4. (D) Neither *SGO1* transcription nor protein abundance is affected by the G44S mutation. Left, reverse transcription (RT)-PCR shows normal expression of *SGO1* in WT and G44S mutant strains. Right, Western blotting of a C'-6xHA-tagged Sgo1p demonstrates the equal abundance of Sgo1p in these two strains. The Loading control is a cross-reacting band from both yeast lysates.

Fig. 2-5

A

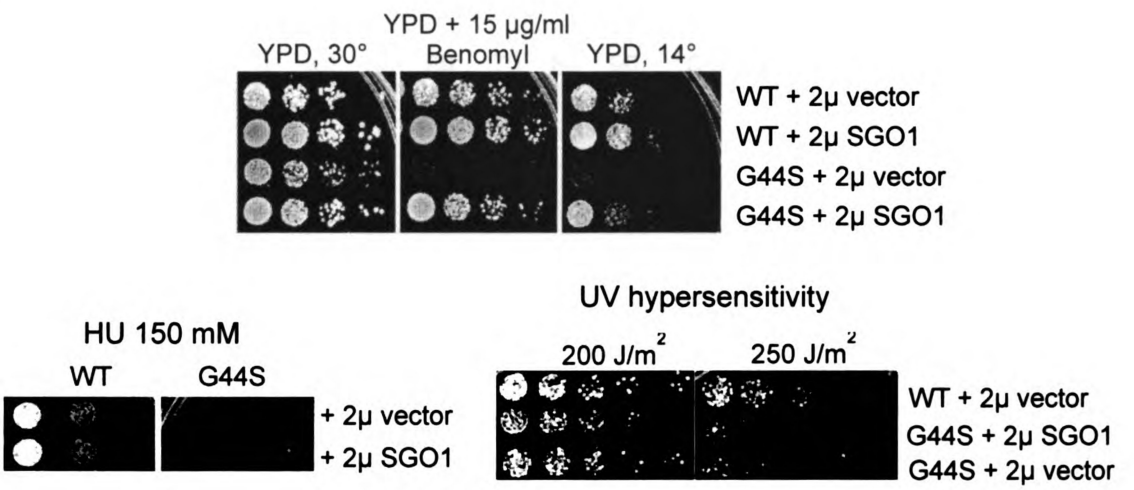
YPD + 15 µg/ml
YPD, 30°
Benomyl
YPD, 14°
WT + 2µ vector
WT + 2µ SGO1
G44S + 2µ vector
G44S + 2µ SGO1
HU 150 mM
WT
G44S
+ 2µ vector
+ 2µ SGO1
UV hypersensitivity
200 J/m2
250 J/m2
WT + 2µ vector
G44S + 2µ SGO1
G44S + 2µ vector

B

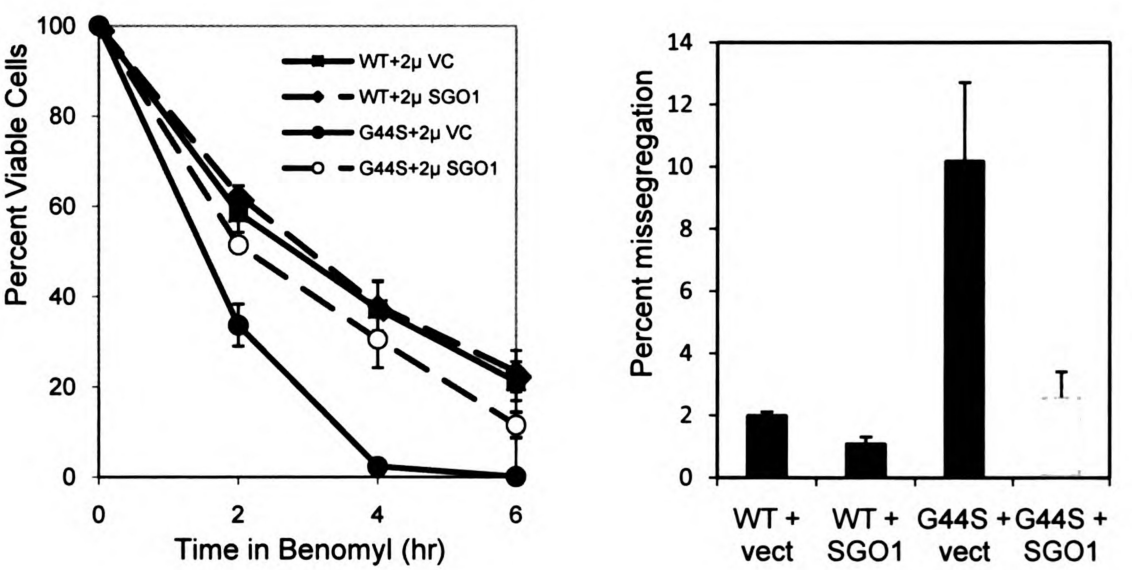
Percent Viable Cells
100
80
60
40
20
0
0
2
4
6
Time in Benomyl (hr)
WT+2µ VC
WT+2µ SGO1
G44S+2µ VC
G44S+2µ SGO1
Percent missegregation
14
12
10
8
6
4
2
0
WT + vect
WT + SGO1
G44S + vect
G44S + SGO1

Fig. 2-5 continued

C

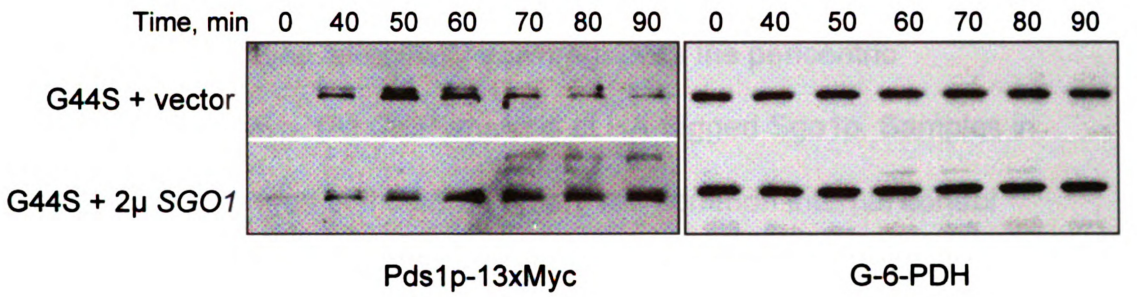

D

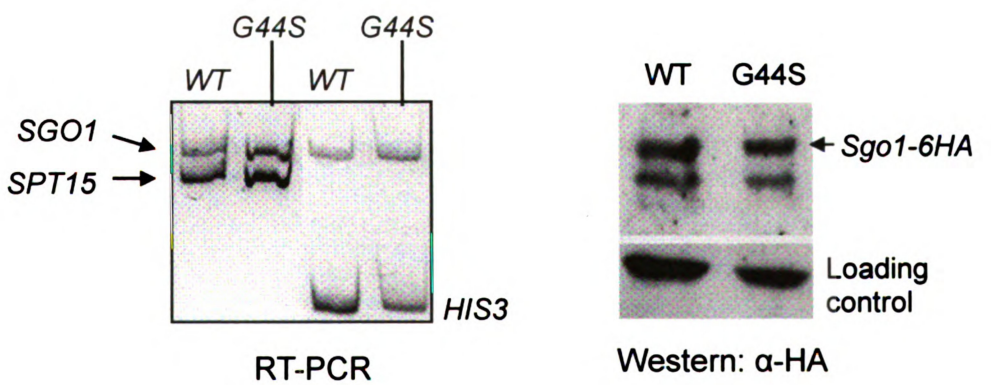

FIG. 2-6. The G44S mutation selectively downregulates the pericentric recruitment of Sgo1p *in vivo*. (A) ChIP analysis of HA-tagged Sgo1p. Samples in all of the panels are arranged in the same order. The common internal control (marked by the star on the right) for multiplex PCRs is from within the ORF of the *DED1* gene 386.2 kb to the right of *CEN15*. Targets of the PCR fragments and their distance to the cognate centromeres are listed at the top of each gel image. R: right; L: left. *SPT15* is 313.3 kb to the right of *CEN5*. (B) Quantification of ChIP results. Ethidium bromide-stained DNA gel images were quantified by NIH Image. The intensities of each *CEN* or pericentric fragment was compared to that of the *DED1* internal control (star). The ratio was then normalized to 0.1% input (*INP*) DNA (set at 1.0). Error bars represent standard deviations from at least three independent cell cultures for ChIP. Ab, antibody.

Fig. 2-6

A

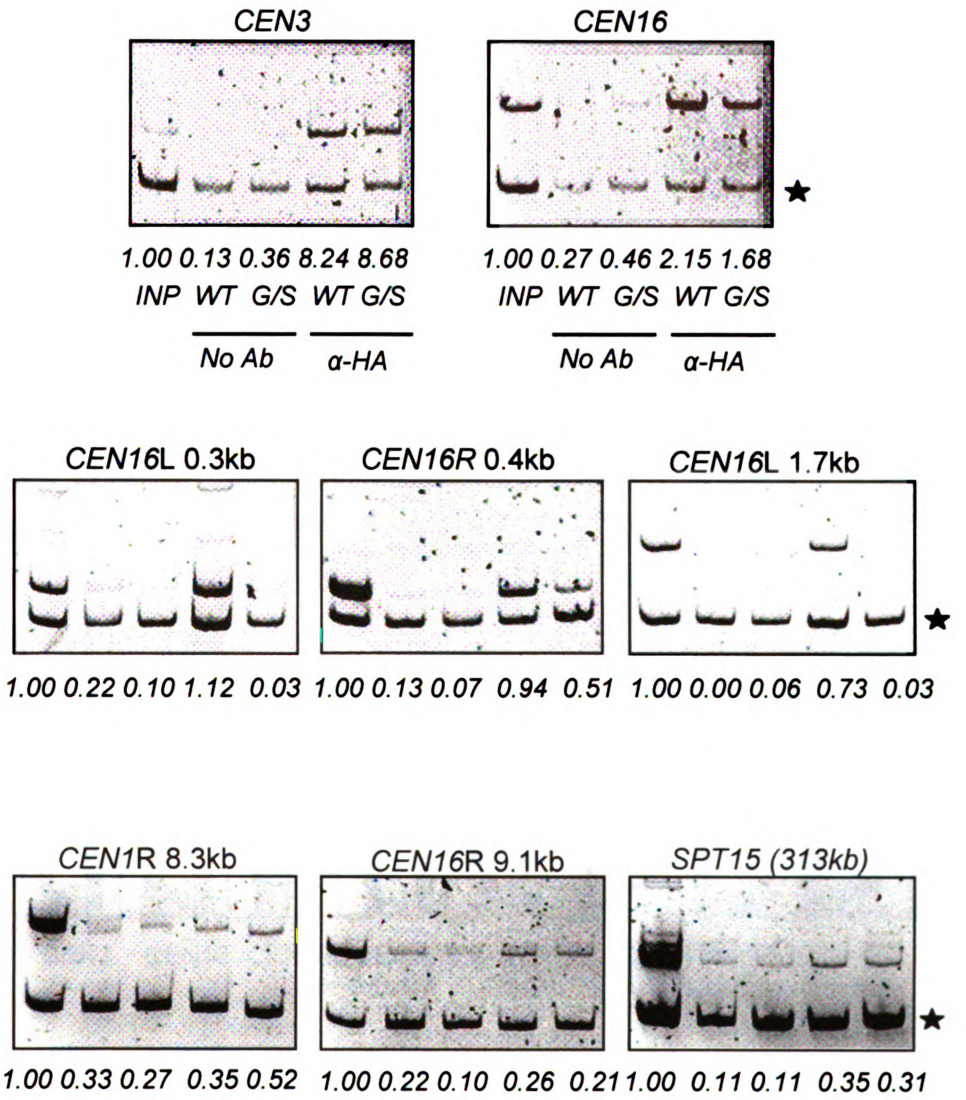
CEN3
CEN16
1.00 0.13 0.36 8.24 8.68
INP WT G/S WT G/S
No Ab
α-HA
1.00 0.27 0.46 2.15 1.68
INP WT G/S WT G/S
No Ab
α-HA
CEN16L 0.3kb
CEN16R 0.4kb
CEN16L 1.7kb
1.00 0.22 0.10 1.12 0.03
1.00 0.13 0.07 0.94 0.51
1.00 0.00 0.06 0.73 0.03
CEN1R 8.3kb
CEN16R 9.1kb
SPT15 (313kb)
1.00 0.33 0.27 0.35 0.52
1.00 0.22 0.10 0.26 0.21
1.00 0.11 0.11 0.35 0.31

Fig. 2-6 continued

B

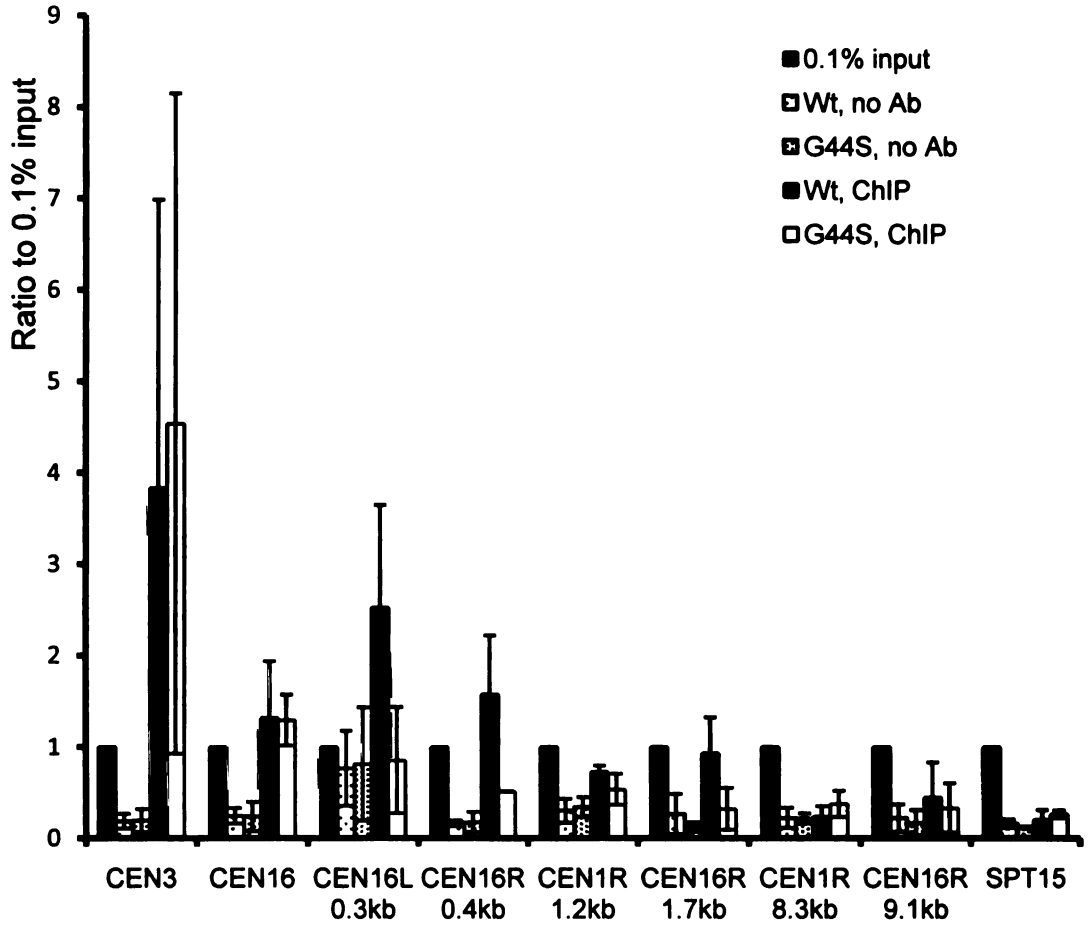

FIG. 2-7. Physical interaction between H3 and Sgo1p is attenuated by the G44S mutation. (A) Pulldown assays assessing the interactions between bacterially expressed GST-3xHA-Sgo1p and histones and oligonucleosomes purified from WT or G44S mutant yeast cells. Trapped H3 was quantified by anti-H3 antibodies. (B) Far-Western assays detecting direct binding between H3 and Sgo1p. Yeast core histones were resolved and blotted onto a PVDF membrane, and incubated with GST-3xHA-Sgo1p. Sgo1p, trapped via association with H3, was probed by anti-HA antibodies. A parallel gel was stained with Coomassie blue R250 (CBR) to reveal the relative mobility of yeast histones.

Fig. 2-7

A

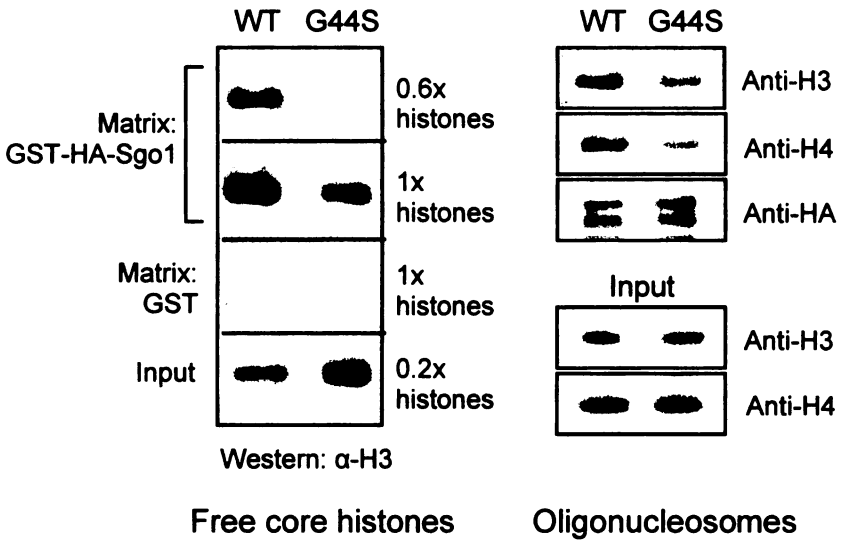
WT G44S
WT G44S
Matrix:
GST-HA-Sgo1
0.6x
histones
1x
histones
Anti-H3
Anti-H4
Anti-HA
Matrix:
GST
1x
histones
Input
Input
0.2x
histones
Anti-H3
Anti-H4
Western: α-H3
Free core histones
Oligonucleosomes

B

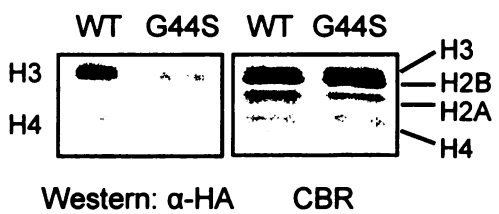
WT G44S WT G44S
H3
H4
H3
H2B
H2A
H4
Western: α-HA
CBR

FIG. 2-8. Reestablishing pericentric Sgo1p recruitment by BD fusion. (A) ChIP assays assessing the distribution of Sgo1p and Sgo1p-BD at selective loci. G44S *sgo1*Δ mutant cells were transformed with an *ARS CEN* plasmid containing 3xHA-Sgo1p or 3xHA-Sgo1p-BD genes and analyzed by anti-HA ChIP. The assay conditions were identical to those described in the legend to Fig. 6. A non-specific PCR fragment ("N") amplified along with the CEN16L 0.3 kb is marked with an arrow. (B) Comparable expression of 3xHA-Sgo1p and 3xHA-Sgo1p-BD. G44S *sgo1*Δ mutant cells bearing the indicated recombinant *SGO1* construct were examined by anti-HA Western blotting. Even loading was evidenced by Coomassie blue R250 staining (not shown) and by proteins that cross-reacted with the anti-HA antibodies. (C) Quantification of the ChIP results was done as detailed in the legend to Fig. 6B.

Fig. 2-8

A

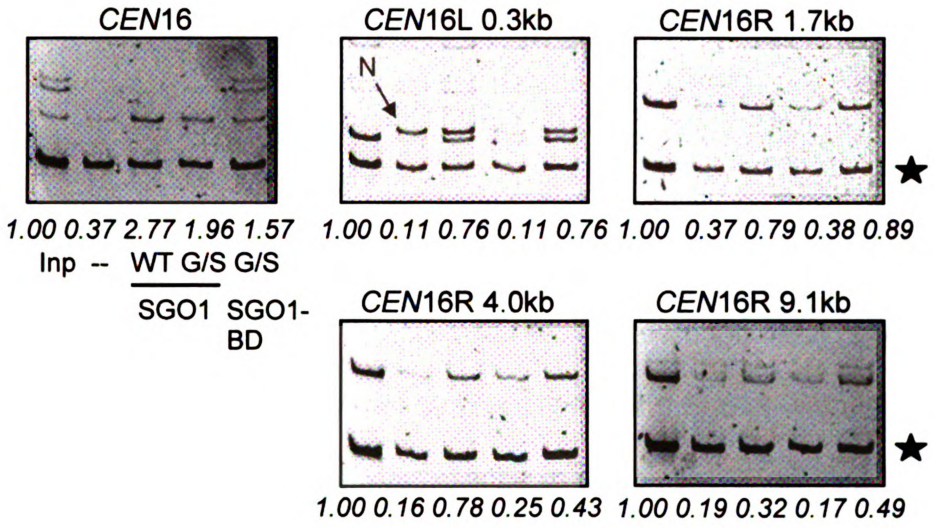
CEN16
CEN16L 0.3kb
CEN16R 1.7kb
N
1.00 0.37 2.77 1.96 1.57
1.00 0.11 0.76 0.11 0.76
1.00 0.37 0.79 0.38 0.89
Inp -- WT G/S G/S
SGO1 SGO1-BD
CEN16R 4.0kb
CEN16R 9.1kb
1.00 0.16 0.78 0.25 0.43
1.00 0.19 0.32 0.17 0.49

B

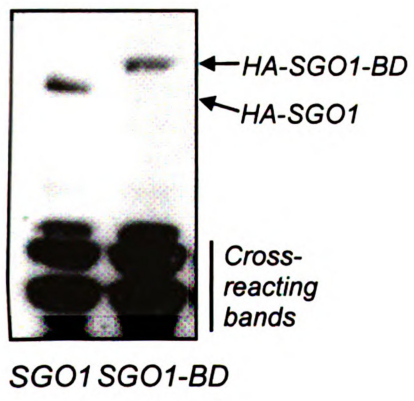
HA-SGO1-BD
HA-SGO1
Cross-reacting bands
SGO1 SGO1-BD

C

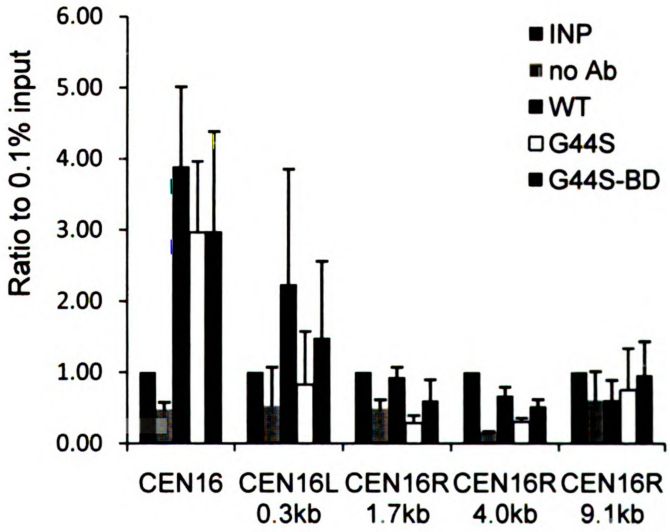
Ratio to 0.1% input
6.00
5.00
4.00
3.00
2.00
1.00
0.00
INP
no Ab
WT
G44S
G44S-BD
CEN16
CEN16L 0.3kb
CEN16R 1.7kb
CEN16R 4.0kb
CEN16R 9.1kb

FIG. 2-9. Bromodomain fusion partially rescues the tension sensing defects of G44S mutant cells. (A) The indicated yeast strains expressing Sgo1p with or without the bromodomain were tested for resistance to benomyl (A), for viability after benomyl exposure (B), and for the Pds1p level after *MCD1* shutdown. See the legends to Fig. 2 and 4 for details. In panels B and C, only data from G44S mutant cells are shown.

Fig. 2-9

A

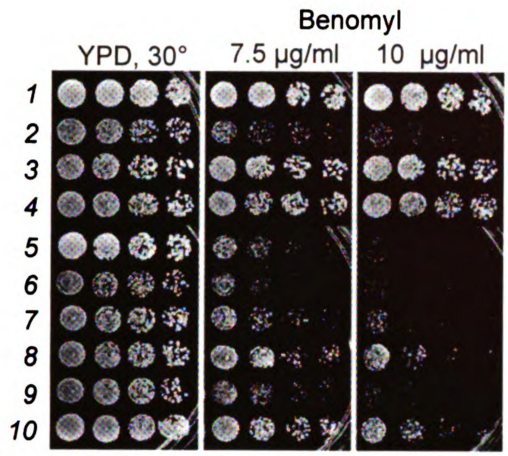

	H3	SGO1	Plasmid
1	*WT*	*WT*	*none*
2	*WT*	Δ	*Vector*
3	*WT*	Δ	*SGO1*
4	*WT*	Δ	*SGO1-BD*
5	*G/S*	*WT*	*none*
6	*G/S*	Δ	*Vector*
7	*G/S*	Δ	*SGO1*
8	*G/S*	Δ	*SGO1-BD*
9	*G/S*	Δ	*SGO1*
10	*G/S*	Δ	*SGO1-BD*

B

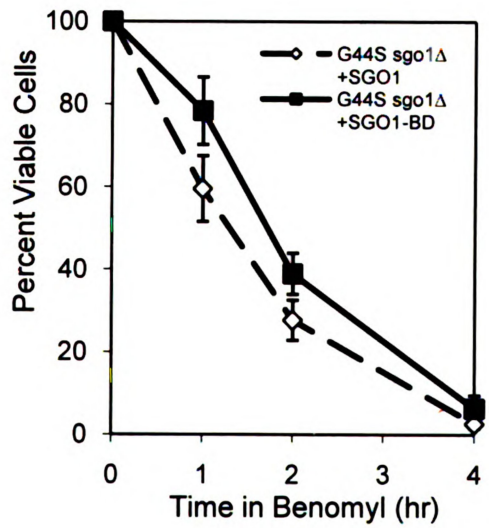

C

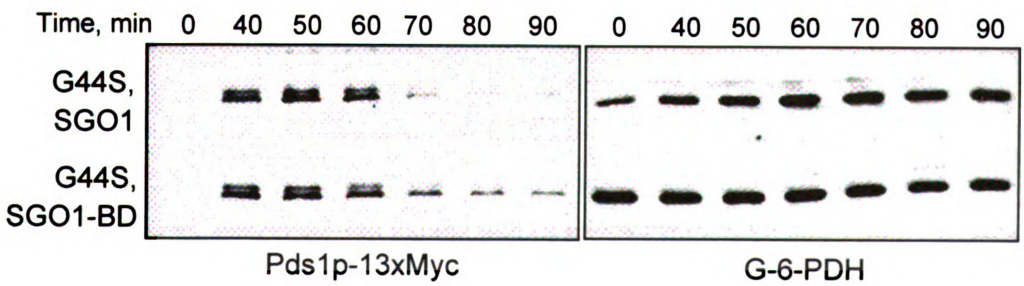

ADDITIONAL EXPERIMENTAL PROCEDURES

EMSA. Interactions between Sgo1p and reconstituted nucleosomal core particles (NCP) were examined by electrophoretic mobility shift assays (EMSA). 1.4 µg of NCP was mixed with 0.24 µg of GST-HAx3-Sgo1p (see above) or 0.3 µg of GST in HEGT buffer without MgCl2. For supershift of NCP mobility, 2 or 4 µg of 12CA5 (Roche) anti-HA monoclonal antibodies were included. After mixing all reactants on ice, reactions were loaded to 4% polyacrylamide gel (0.5 X TBE). The gel was run at constant 25 V for 6 hours. Free DNA and NCP complexes were visualized by EtBr staining.

Supplemental Data

Fig. S1

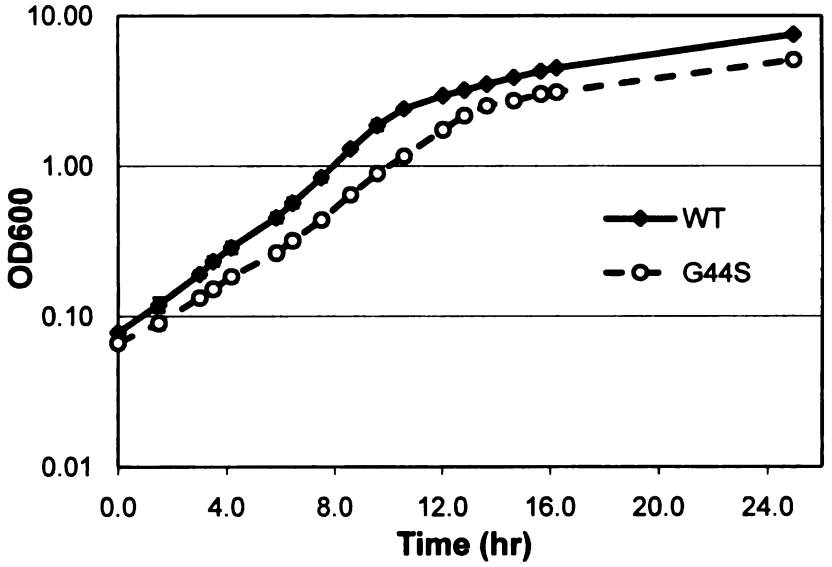

FIG. S1. G44S cells exhibited slower growth rate. Optical density at 600 nm (OD_{600}) was assessed at the indicated times after making appropriate dilution of starting log-phase WT and G44S mutant cultures. Three independent growth tests were conducted. This plot shows typical results with error bars representing standard deviations measured at each time point.

FIG. S2. Sgo1p interacts histone H3 in different contexts. (A) Bacterially expressed yeast H3 and acid-extracted chicken H3 interact with Sgo1p. Pull-down assays using GST-HA-Sgo1p (left panel) or GST alone (middle panel) were carried out by incubating acid extracted yeast (lanes 1 and 2) or chicken (lane 3) core histones, or recombinant H3 expressed in *E. coli* (lane 4). Histone bound to the matrix were resolved and probed by anti-H3 antibodies. 12% input of each histone samples is shown in the right panel. Note that lanes 1 and 2 are identical to Figure 7A (see main text). (B) Sgo1p interacts with reconstituted nucleosomal core particles (NCP). Interactions between GST-HAx3-Sgo1p and NCP were examined by EMSA assays. Moderate retardation was observed in different batches of recombinant Sgo1p with NCP (compare lane 4 with lane 2). Adding the anti-HA monoclonal antibodies to reactions containing the HA-tagged Sgo1p resulted in further NCP mobility retardation (lanes 6 and 7). Neither GST nor anti-HA antibodies (lanes 3 and 5, respectively) changed the mobility of NCP.

Fig. S2

A

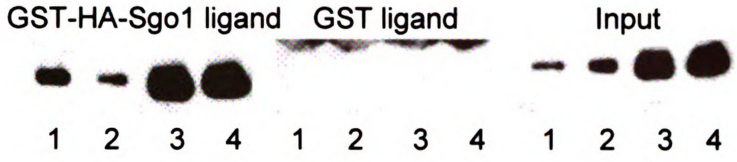

1. WT yeast histones
2. G44S yeast histones
3. Chicken histones
4. Recombinant H3

B

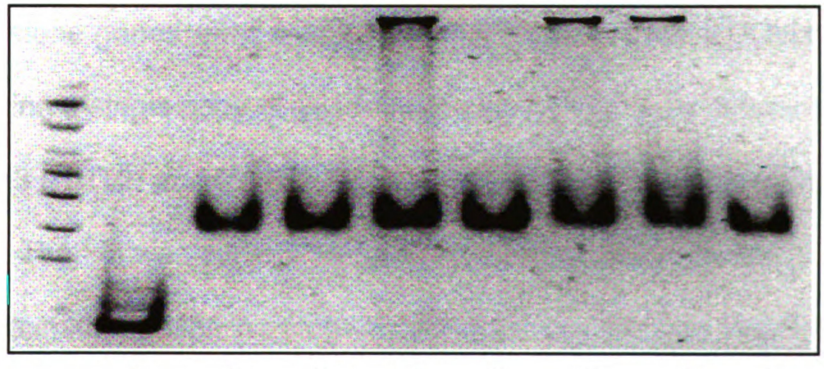

	1	2	3	4	5	6	7	8
GST	–	–	+	–	–	–	–	–
GST-HAx3-SGO1	–	–	–	+	–	+	+	–
Anti-HA Ab	–	–	–	–	+ (2μg)	+ (2μg)	+ (4μg)	–

Fig. S3

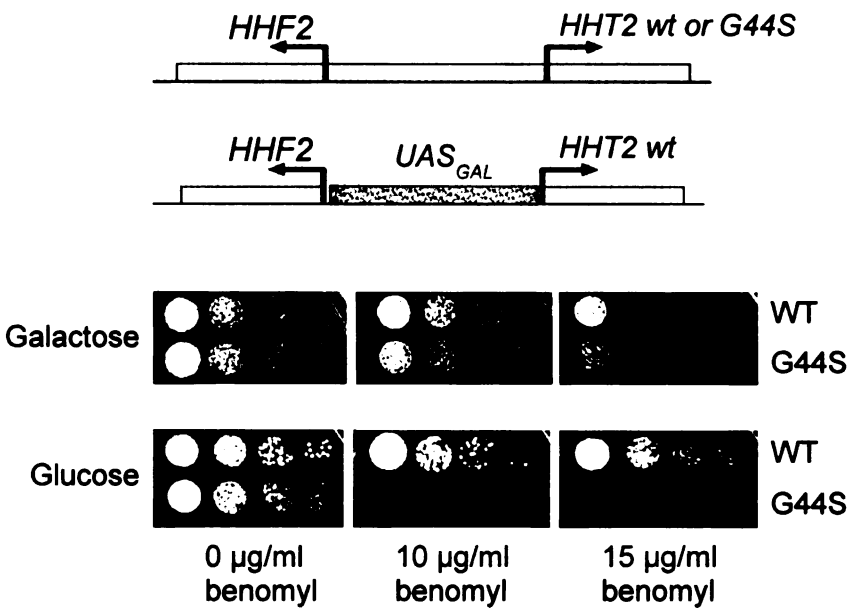

FIG. S3. G44S mutation is semi-dominant. Yeast cells with the chromosomal copies of all core histone genes were deleted and were transformed with two plasmids each bearing a single copy of genes encoding all four core histones. In the "top" plasmid, H3 (HHT2) and H4 (HHF2) were expressed from the native, divergent promoter. The H3 was either wild type or the G44S allele. In the "bottom", second plasmid, the H3/H4 promoter was replaced with the *GAL1,10* promoter, rendering the expression of these two genes repressible by glucose. Log phase YPGal cultures were spotted to the indicated plates containing either glucose or galactose. Cellular growth was then compared two to three days later.

Fig. S4

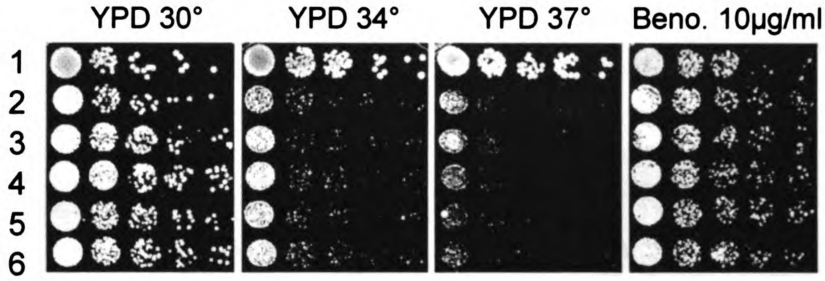

1. yMK1243 WT
2. MSYP726 *hhf*1-20

3 & 4. MSYP726 *hhf*1-20 + 2µ VC

5 & 6. MSYP726 *hhf*1-20 + 2µ SGO1

FIG. S4. 2µm *SGO1* does not rescue a histone H4 allele, *hhf1-20*, that causes temperature sensitivity and centromeric function defects (16). The *hhf1-20* strain (MSYP726) was a kind gift from M. Smith.

Fig. S5

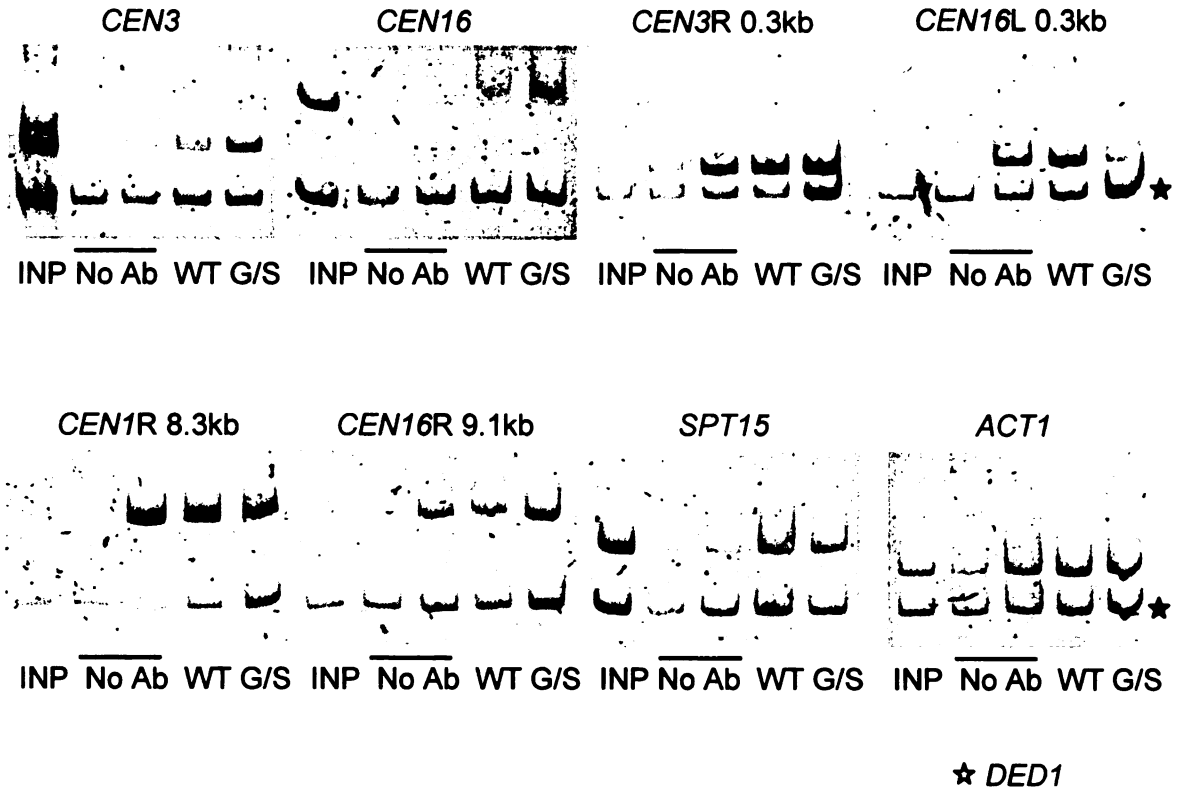

FIG. S5. Mcd1p recruitment to selective centromeres, pericentric regions, and chromosome arms is not affected by G44S mutation. ChIP assays were conducted in the wildtype and G44S strains bearing C'-Myc-tagged Mcd1p. Logarithmically growing cultures were used. All PCR reactions contained two pairs of primers with *DED1* as the common internal control for PCR reactions. Specific PCR targets and their distance from the centromere are indicated on top of each gel image. *SPT15* is 313.3 kb on the right of *CEN5*, and *ACT1* is 93.8 kb on the left of *CEN6*.

FIG. S6. No discernable transcriptional defects were observed in the G44S cells. Transcripts of different classes of yeast genes were analyzed by quantitative RT-PCR. (A) Mitosis-related genes. Each panel is clustered based on the major functions of the assayed genes. Loading control, *SPT15*, is shown in panel (B). (C) Representative inducible genes were analyzed by RT-PCR. *SUC2* and *GAL1* are induced by shifting carbon source from glucose to sucrose and from raffinose to galactose, respectively, whereas *ARG1*, *HIS1*, *HIS7*, and *TRP3* are amino acid biosynthesis genes that are induced by amino acid starvation. *SPT15* was used as the common internal control for each quantitative PCR reaction. (D) Mating type-specific genes are expressed and repressed normally in the G44S cells. Both the wildtype and the G44S cells were of the a mating type (*MATa*). Thus, a-specific genes (e.g. *a1* and the α pheromone receptor *STE2*) are expressed in *MATa* cells. In contrast, α-specific genes, such as *α1* and the a pheromone receptor *STE3*, are repressed in *MAT α* cells. Genomic DNA was also used in separate PCR reactions to demonstrate that the lack of signal in *α1* and *STE3* RT-PCR was due to the lack of the corresponding transcripts but not to a systemic failure in PCR amplification.

Fig. S6

A

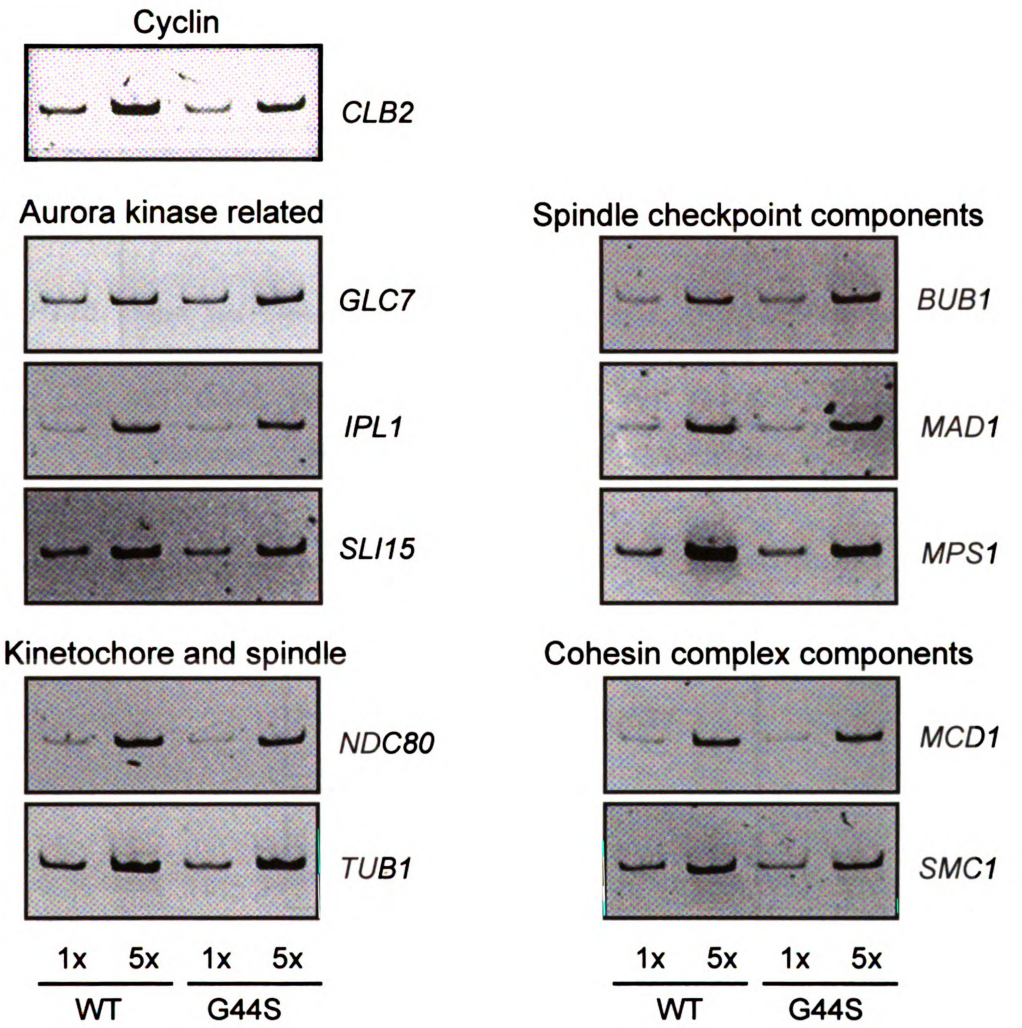
Cyclin
CLB2
Aurora kinase related
GLC7
IPL1
SLI15
Spindle checkpoint components
BUB1
MAD1
MPS1
Kinetochore and spindle
NDC80
TUB1
Cohesin complex components
MCD1
SMC1
1x 5x 1x 5x
WT G44S
1x 5x 1x 5x
WT G44S

B

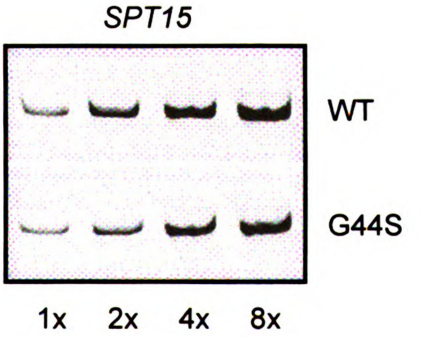
SPT15
WT
G44S
1x 2x 4x 8x

Fig. S6 continued

C

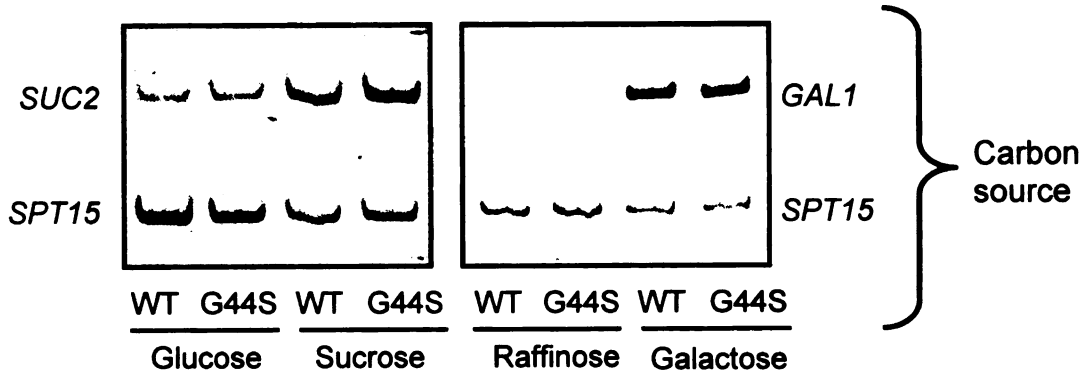

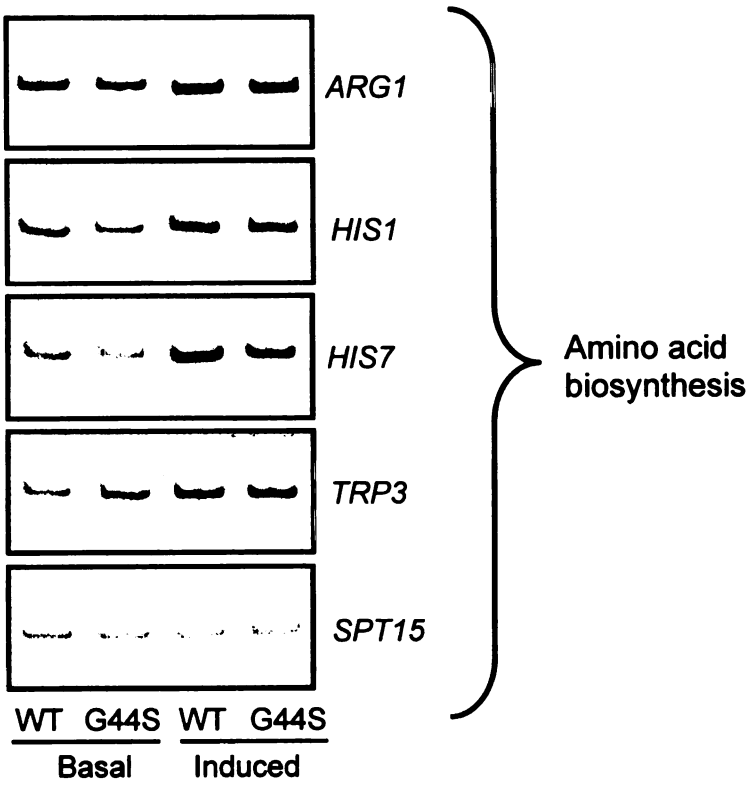

Fig. S6 continued

D

RT- PCR

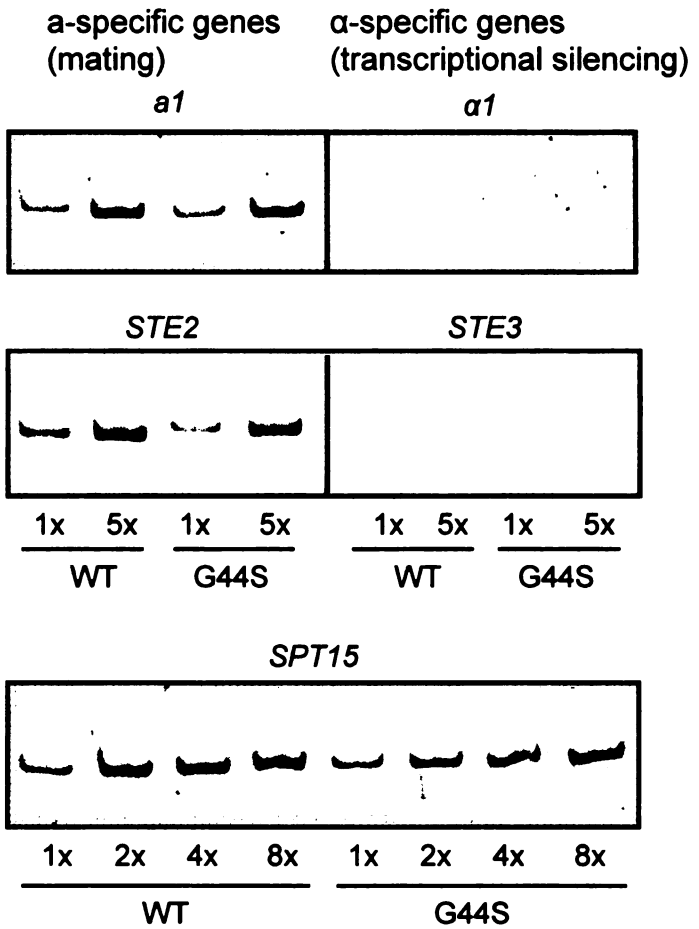

Genomic DNA PCR

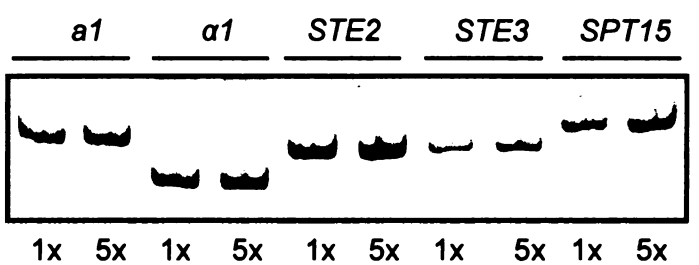

Fig. S7

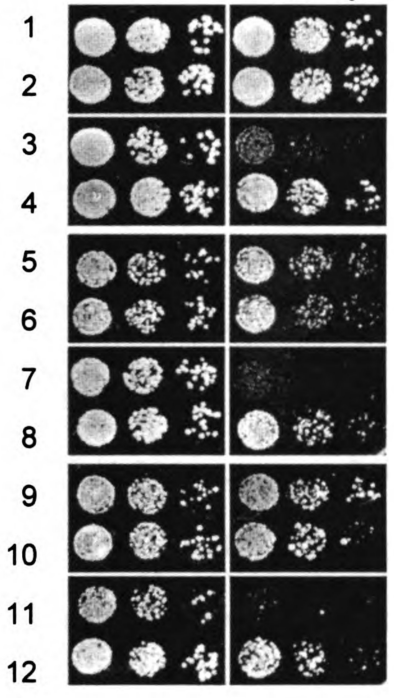

	H3	2µ DNA	*RTS1*	*CDC55*
1	WT	vector	+	+
2	WT	*SGO1*	+	+
3	*G44S*	vector	+	+
4	*G44S*	*SGO1*	+	+
5	WT	vector	Δ	+
6	WT	*SGO1*	Δ	+
7	*G44S*	vector	Δ	+
8	*G44S*	*SGO1*	Δ	+
9	WT	vector	+	Δ
10	WT	*SGO1*	+	Δ
11	*G44S*	vector	+	Δ
12	*G44S*	*SGO1*	+	Δ

FIG. S7. 2µm *SGO1* suppression is independent of the PP2A activity. Shown are benomyl resistance of WT and G44S cells in the presence or absence of two PP2A components, *RTS1* and *CDC55*, after transforming with 2µm vector or *SGO1*. Deleting either PP2A subunit does not affect the suppression by *SGO1* overexpression.

FIG. S8. Genetic interactions between the Aurora kinase, histone H3, and *SGO1*. (A) *IPL1* and *SLI15* are overexpressed in wildtype, G44S, or *sgo1*Δ cells. Cellular growth was compared at 30°. Severe synthetic growth phenotypes are seen in both G44S and *sgo1*Δ cells when *SLI15* is overexpressed, while less pronounced sickness is caused by *IPL1* induction. (B) No obvious synthetic phenotype results from G44S and *ipl1-321* mutations. The temperature sensitive *ipl1-321* strains bearing wild type or G44S H3 allele (with the other copy of H3 previously deleted) were tested for synthetic phenotypes at 30°, 32°, 34°, and 37°C.

Fig. S8

A

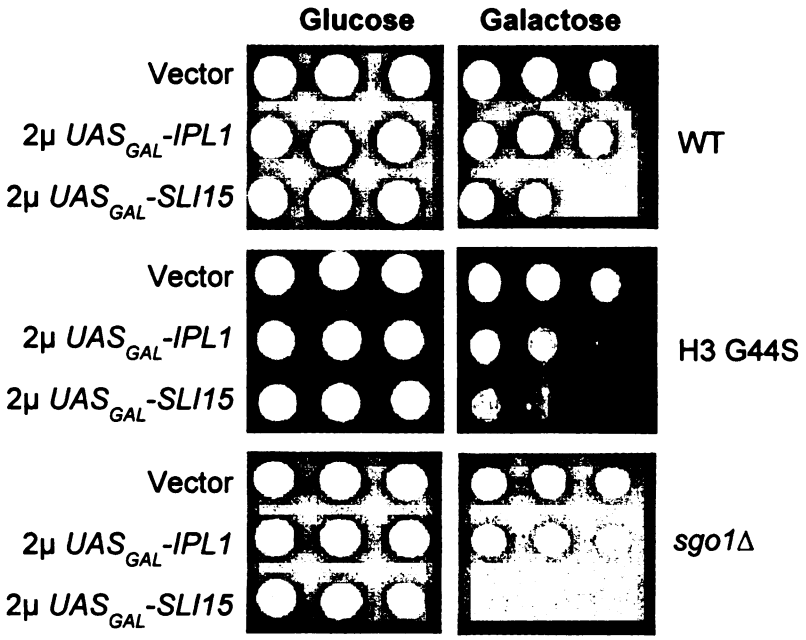
Glucose
Galactose
Vector
2μ UAS_{GAL}-*IPL1*
2μ UAS_{GAL}-*SLI15*
WT
Vector
2μ UAS_{GAL}-*IPL1*
2μ UAS_{GAL}-*SLI15*
H3 G44S
Vector
2μ UAS_{GAL}-*IPL1*
2μ UAS_{GAL}-*SLI15*
*sgo1*Δ

B

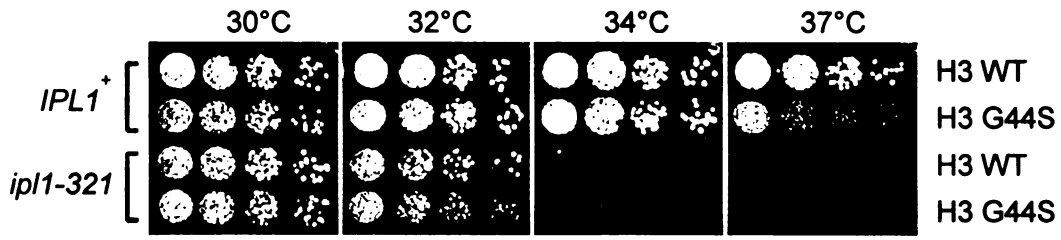
30°C
32°C
34°C
37°C
IPL1$^+$
ipl1-321
H3 WT
H3 G44S
H3 WT
H3 G44S

REFERENCES

1. **Ahn, S. H., W. L. Cheung, J. Y. Hsu, R. L. Diaz, M. M. Smith, and C. D. Allis.** 2005. Sterile 20 kinase phosphorylates histone H2B at serine 10 during hydrogen peroxide-induced apoptosis in S. cerevisiae. Cell **120:**25-36.

2. **Biggins, S., and A. W. Murray.** 2001. The budding yeast protein kinase Ipl1/Aurora allows the absence of tension to activate the spindle checkpoint. Genes Dev **15:**3118-3129.

3. **Bloom, K., S. Sharma, and N. V. Dokholyan.** 2006. The path of DNA in the kinetochore. Curr Biol **16:**R276-278.

4. **Broder, Y. C., S. Katz, and A. Aronheim.** 1998. The ras recruitment system, a novel approach to the study of protein-protein interactions. Curr Biol **8:**1121-1124.

5. **Dhalluin, C., J. E. Carlson, L. Zeng, C. He, A. K. Aggarwal, and M. M. Zhou.** 1999. Structure and ligand of a histone acetyltransferase bromodomain. Nature **399:**491-496.

6. **Edmondson, D. G., M. M. Smith, and S. Y. Roth.** 1996. Repression domain of the yeast global repressor Tup1 interacts directly with histones H3 and H4. Genes Dev **10:**1247-1259.

7. **Fernius, J., and K. G. Hardwick.** 2007. Bub1 kinase targets Sgo1 to ensure efficient chromosome biorientation in budding yeast mitosis. PLoS Genet **3:**e213.

8. **Gartenberg, M.** 2009. Heterochromatin and the cohesion of sister chromatids. Chromosome Res **17:**229-238.

9. **Gietz, D., A. St Jean, R. A. Woods, and R. H. Schiestl.** 1992. Improved method for high efficiency transformation of intact yeast cells. Nucleic Acids Res **20:**1425.

10. **Gietz, R. D., and A. Sugino.** 1988. New yeast-Escherichia coli shuttle vectors constructed with in vitro mutagenized yeast genes lacking six-base pair restriction sites. Gene **74:**527-534.

11. **Goshima, G., and M. Yanagida.** 2000. Establishing biorientation occurs with precocious separation of the sister kinetochores, but not the arms, in the early spindle of budding yeast. Cell **100:**619-633.

12. **Grunstein, M.** 1997. Molecular model for telomeric heterochromatin in yeast. Curr Opin Cell Biol **9**:383-387.

13. **Hake, S. B., B. A. Garcia, M. Kauer, S. P. Baker, J. Shabanowitz, D. F. Hunt, and C. D. Allis.** 2005. Serine 31 phosphorylation of histone variant H3.3 is specific to regions bordering centromeres in metaphase chromosomes. Proc Natl Acad Sci U S A **102**:6344-6349.

14. **He, X., S. Asthana, and P. K. Sorger.** 2000. Transient sister chromatid separation and elastic deformation of chromosomes during mitosis in budding yeast. Cell **101**:763-775.

15. **Indjeian, V. B., B. M. Stern, and A. W. Murray.** 2005. The centromeric protein Sgo1 is required to sense lack of tension on mitotic chromosomes. Science **307**:130-133.

16. **Iwaizumi, M., K. Shinmura, H. Mori, H. Yamada, M. Suzuki, Y. Kitayama, H. Igarashi, T. Nakamura, H. Suzuki, Y. Watanabe, A. Hishida, M. Ikuma, and H. Sugimura.** 2009. Human Sgo1 downregulation leads to chromosomal instability in colorectal cancer. Gut **58**:249-260.

17. **Jacobson, R. H., A. G. Ladurner, D. S. King, and R. Tjian.** 2000. Structure and function of a human TAFII250 double bromodomain module. Science **288**:1422-1425.

18. **Jones, J. S., and L. Prakash.** 1990. Yeast Saccharomyces cerevisiae selectable markers in pUC18 polylinkers. Yeast **6**:363-366.

19. **Kanta, H., L. Laprade, A. Almutairi, and I. Pinto.** 2006. Suppressor analysis of a histone defect identifies a new function for the hda1 complex in chromosome segregation. Genetics **173**:435-450.

20. **Kaplan, C. D., L. Laprade, and F. Winston.** 2003. Transcription elongation factors repress transcription initiation from cryptic sites. Science **301**:1096-1099.

21. **Kawashima, S. A., T. Tsukahara, M. Langegger, S. Hauf, T. S. Kitajima, and Y. Watanabe.** 2007. Shugoshin enables tension-generating attachment of kinetochores by loading Aurora to centromeres. Genes Dev **21**:420-435.

22. **Kiburz, B. M., D. B. Reynolds, P. C. Megee, A. L. Marston, B. H. Lee, T. I. Lee, S. S. Levine, R. A. Young, and A. Amon.** 2005. The core centromere and Sgo1 establish a 50-kb cohesin-protected domain around centromeres during meiosis I. Genes Dev **19**:3017-3030.

23. **King, R. W., J. M. Peters, S. Tugendreich, M. Rolfe, P. Hieter, and M. W. Kirschner.** 1995. A 20S complex containing CDC27 and CDC16 catalyzes the mitosis-specific conjugation of ubiquitin to cyclin B. Cell **81:**279-288.

24. **Kitajima, T. S., S. Hauf, M. Ohsugi, T. Yamamoto, and Y. Watanabe.** 2005. Human Bub1 defines the persistent cohesion site along the mitotic chromosome by affecting Shugoshin localization. Curr Biol **15:**353-359.

25. **Kitajima, T. S., S. A. Kawashima, and Y. Watanabe.** 2004. The conserved kinetochore protein shugoshin protects centromeric cohesion during meiosis. Nature **427:**510-517.

26. **Kitajima, T. S., T. Sakuno, K. Ishiguro, S. Iemura, T. Natsume, S. A. Kawashima, and Y. Watanabe.** 2006. Shugoshin collaborates with protein phosphatase 2A to protect cohesin. Nature **441:**46-52.

27. **Koshland, D. E., and V. Guacci.** 2000. Sister chromatid cohesion: the beginning of a long and beautiful relationship. Curr Opin Cell Biol **12:**297-301.

28. **Kuo, M. H., and C. D. Allis.** 1999. In vivo cross-linking and immunoprecipitation for studying dynamic Protein:DNA associations in a chromatin environment. Methods **19:**425-433.

29. **Kurdistani, S. K., S. Tavazoie, and M. Grunstein.** 2004. Mapping global histone acetylation patterns to gene expression. Cell **117:**721-733.

30. **Latham, J. A., and S. Y. Dent.** 2007. Cross-regulation of histone modifications. Nat Struct Mol Biol **14:**1017-1024.

31. **Lew, D. J., and D. J. Burke.** 2003. The spindle assembly and spindle position checkpoints. Annu Rev Genet **37:**251-282.

32. **Liu, Y., X. Xu, S. Singh-Rodriguez, Y. Zhao, and M. H. Kuo.** 2005. Histone H3 Ser10 phosphorylation-independent function of Snf1 and Reg1 proteins rescues a gcn5- mutant in HIS3 expression. Mol Cell Biol **25:**10566-10579.

33. **Logarinho, E., and H. Bousbaa.** 2008. Kinetochore-microtubule interactions "in check" by Bub1, Bub3 and BubR1: The dual task of attaching and signalling. Cell Cycle **7:**1763-1768.

34. **Luger, K., A. W. Mader, R. K. Richmond, D. F. Sargent, and T. J. Richmond.** 1997. Crystal structure of the nucleosome core particle at 2.8 A resolution. Nature **389:**251-260.

35. **Meluh, P. B., P. Yang, L. Glowczewski, D. Koshland, and M. M. Smith.** 1998. Cse4p is a component of the core centromere of Saccharomyces cerevisiae. Cell **94:**607-613.

36. **Morgan, B. A., B. A. Mittman, and M. M. Smith.** 1991. The highly conserved N-terminal domains of histones H3 and H4 are required for normal cell cycle progression. Mol Cell Biol **11:**4111-4120.

37. **Nasmyth, K.** 2005. How do so few control so many? Cell **120:**739-746.

38. **Nasmyth, K.** 2002. Segregating sister genomes: the molecular biology of chromosome separation. Science **297:**559-565.

39. **Nasmyth, K., J. M. Peters, and F. Uhlmann.** 2000. Splitting the chromosome: cutting the ties that bind sister chromatids. Science **288:**1379-1385.

40. **Nguyen, D. T., A. M. Alarco, and M. Raymond.** 2001. Multiple Yap1p-binding sites mediate induction of the yeast major facilitator FLR1 gene in response to drugs, oxidants, and alkylating agents. J Biol Chem **276:**1138-1145.

41. **Pamblanco, M., A. Poveda, R. Sendra, S. Rodriguez-Navarro, J. E. Perez-Ortin, and V. Tordera.** 2001. Bromodomain factor 1 (Bdf1) protein interacts with histones. FEBS Lett **496:**31-35.

42. **Petracek, M. E., and M. S. Longtine.** 2002. PCR-based engineering of yeast genome. Methods Enzymol **350:**445-469.

43. **Pinsky, B. A., and S. Biggins.** 2005. The spindle checkpoint: tension versus attachment. Trends Cell Biol **15:**486-493.

44. **Pinto, I., and F. Winston.** 2000. Histone H2A is required for normal centromere function in Saccharomyces cerevisiae. Embo J **19:**1598-1612.

45. **Renauld, H., O. M. Aparicio, P. D. Zierath, B. L. Billington, S. K. Chhablani, and D. E. Gottschling.** 1993. Silent domains are assembled continuously from the telomere and are defined by promoter distance and strength, and by SIR3 dosage. Genes Dev **7:**1133-1145.

46. **Riedel, C. G., V. L. Katis, Y. Katou, S. Mori, T. Itoh, W. Helmhart, M. Galova, M. Petronczki, J. Gregan, B. Cetin, I. Mudrak, E. Ogris, K. Mechtler, L. Pelletier, F. Buchholz, K. Shirahige, and K. Nasmyth.** 2006. Protein phosphatase 2A protects centromeric sister chromatid cohesion during meiosis I. Nature.

47. **Rigaut, G., A. Shevchenko, B. Rutz, M. Wilm, M. Mann, and B. Seraphin.** 1999. A generic protein purification method for protein complex characterization and proteome exploration. Nat Biotechnol **17:**1030-1032.

48. **Salic, A., J. C. Waters, and T. J. Mitchison.** 2004. Vertebrate shugoshin links sister centromere cohesion and kinetochore microtubule stability in mitosis. Cell **118:**567-578.

49. **Sherman, F.** 1991. Getting started with yeast. Methods Enzymol **194:**3-21.

50. **Smith, M. M., P. Yang, M. S. Santisteban, P. W. Boone, A. T. Goldstein, and P. C. Megee.** 1996. A novel histone H4 mutant defective in nuclear division and mitotic chromosome transmission. Mol Cell Biol **16:**1017-1026.

51. **Spencer, F., S. L. Gerring, C. Connelly, and P. Hieter.** 1990. Mitotic chromosome transmission fidelity mutants in Saccharomyces cerevisiae. Genetics **124:**237-249.

52. **Stavenhagen, J. B., and V. A. Zakian.** 1994. Internal tracts of telomeric DNA act as silencers in Saccharomyces cerevisiae. Genes Dev **8:**1411-1422.

53. **Straight, A. F., A. S. Belmont, C. C. Robinett, and A. W. Murray.** 1996. GFP tagging of budding yeast chromosomes reveals that protein-protein interactions can mediate sister chromatid cohesion. Curr Biol **6:**1599-1608.

54. **Tang, Z., H. Shu, W. Qi, N. A. Mahmood, M. C. Mumby, and H. Yu.** 2006. PP2A is required for centromeric localization of Sgo1 and proper chromosome segregation. Dev Cell **10:**575-585.

55. **Tang, Z., Y. Sun, S. E. Harley, H. Zou, and H. Yu.** 2004. Human Bub1 protects centromeric sister-chromatid cohesion through Shugoshin during mitosis. Proc Natl Acad Sci U S A **101:**18012-18017.

56. **Trautmann, S., S. Rajagopalan, and D. McCollum.** 2004. The S. pombe Cdc14-like phosphatase Clp1p regulates chromosome biorientation and interacts with Aurora kinase. Dev Cell **7:**755-762.

57. **Vernarecci, S., P. Ornaghi, A. Bagu, E. Cundari, P. Ballario, and P. Filetici.** 2008. Gcn5p plays an important role in centromere kinetochore function in budding yeast. Mol Cell Biol **28:**988-996.

58. **White, C. L., R. K. Suto, and K. Luger.** 2001. Structure of the yeast nucleosome core particle reveals fundamental changes in internucleosome interactions. Embo J **20:**5207-5218.

59. **Wu, A., J. A. Wemmie, N. P. Edgington, M. Goebl, J. L. Guevara, and W. S. Moye-Rowley.** 1993. Yeast bZip proteins mediate pleiotropic drug and metal resistance. J Biol Chem **268:**18850-18858.

60. **Yu, H.** 2002. Regulation of APC-Cdc20 by the spindle checkpoint. Curr Opin Cell Biol **14:**706-714.

61. **Zhou, J., J. Yao, and H. C. Joshi.** 2002. Attachment and tension in the spindle assembly checkpoint. J Cell Sci **115:**3547-3555.

CHAPTER III

Characterization of a Tension Sensing Motif of Histone H3 in *Saccharomyces cerevisiae*

(Manuscript in preparation)

Characterization of a Tension Sensing Motif of Histone H3 in *Saccharomyces cerevisiae*

Jianjun Luo, Xinjing Xu, and Min-Hao Kuo[1]*

Department of Biochemistry and Molecular Biology, and [1]Programs in Genetics and in Cell and Molecular Biology, Michigan State University, East Lansing, MI 48824

Running title: chromatin role in mitosis

Key words: histone H3, chromatin, mitosis, Shugoshin, *Saccharomyces cerevisiae*

*Corresponding author. 401 BCH Building, Department of Biochemistry and Molecular Biology, Michigan State University, East Lansing, MI 48824. E-mail: kuom@msu.edu; Phone: 517-355-0163; FAX: 517-353-9334

ABSTRACT

To ensure genomic stability during cell division, all chromosomes must attach to spindles emanating from the opposite spindle pole bodies before segregation. The tension between sister chromatids generated by the poleward pulling force is an integral part of chromosome biorientation. Our previous studies indicated that Gly44 of H3 is critical for recruiting/retaining Sgo1p at the pericentromeres for monitoring the tension status of sister chromatids during mitosis. Studies carried out in this work showed that Lys42, Gly44, and Thr45 of H3 form a core executing a mitotic function that is pivotal for cell survival under benomyl stress. Consistent with the G44S mutant phenotypes, K42A and T45A mutant cells failed to respond to the lack of tension between sister chromatids. The benomyl hypersensitivities of these mutants can be suppressed by the overexpression of *SGO1*. Lys42, Gly44, and Thr45 thus form a tension sensing motif (TSM). This motif functions by physically recruiting or retaining Sgo1p at the pericentromeres. Intriguingly, the histone acetyltransferase activity of Gcn5p likely plays a negative role in H3 TSM-Sgo1p function. These results reveal that a TSM of histone H3 is a key player in faithful segregation of mitotic chromosome, and that interaction with a chromatin modifying enzyme may be an important part of the mitotic quality control process.

INTRO

Histor

chrom

cycle

roles

recor

chron

contr

To e

chec

attac

cohe

whic

Cell

The

atta

Shu

34).

peric

moni

INTRODUCTION

Histones are basal structural and functional components of eukaryotic chromosome. The flexible N-terminal tail of H3 and H4 is required for normal cell cycle progression (24, 25). Although emerging data have shown the important roles of chromatin structure and histone modification in controlling transcription, recombination, DNA replication, DNA repair and establishment of sister-chromatid cohesion (2, 21), it is less clear as to how individual histones contribute mechanistically to mitotic progression and regulation.

To ensure faithful segregation of sister-chromatids, the spindle assembly checkpoint (SAC) ensures the establishment of bipolar kinetochore-spindle attachment, which results in tension between sister-chromatids that are held by cohesin complexes (11, 28). Lack of attachment or tension activates the SAC, which then arrests cell cycle by inhibiting the anaphase-promoting complex (28). Cells resume mitosis after the error is corrected.

The tension sensing function ensures that the two sister kinetochores are attached to spindles emanating from opposite spindle pole bodies. The Shugoshin proteins in different organisms are critical for this function (15, 18, 33, 34). Sgo1p in yeast and mammals is enriched at the centromeres and pericentromeres (17, 29, 30), where tension is believed to be generated and monitored (4). The recruitment of *S. pombe* Sgo1p is achieved by the

phosphorylation of Ser121 of H2A by the Bub1p kinase, and heterochromatin markers at the pericentromeres (16, 33). In *S. cerevisiae*, the Bub1p kinase and the H2A Ser121 phosphorylation also are essential for localizing Sgo1p to the centromeric region (9, 16, 17). We recently reported that histone H3 is an essential player in mitotic tension surveillance and that the pericentric, but not the centromeric, enrichment of Sgo1p is critically dependent on H3. Yeast cells harboring a unique Gly44-to-Ser (G44S) mutant allele of H3 exhibit phenotypes typical of those resulting from tension sensing defects, including chromosome instability, missegregation, and inability to activate the SAC when tension buildup is artificially prevented. Overexpressing Sgo1p or artificially tethering Sgo1p to the pericentromeres can restore the tension sensing function of H3 mutant cells (23).

Histone acetyltransferases such as Gcn5p are best known for their roles in facilitating transcription (12, 20). Other chromatin functions of Gcn5p are beginning to emerge. For example, deleting *GCN5* causes cell cycle defect and accumulation of G_2/M cells (13, 35). The notion that Gcn5p plays a mitotic function is supported by the observations that *GCN5* genetically interacts with genes encoding several inner kinetochore components, and that Gcn5p is present at the centromeric regions (32). These results suggest that Gcn5p may regulate the kinetochore function or structure that is critical for mitotic control and progression.

In this work, we defined the Tension Sensing Motif of histone H3 that is strategically positioned at the junction between the flexible tail and the structured histone core domain. Importantly, genetic data suggested that this novel tension sensing function is regulated by the histone acetyltransferase Gcn5p.

MATERIALS AND METHODS

Yeast strains and plasmid constructs. The yeast strains and plasmids used in this work are listed in Tables 3-1 and 3-2.

To assess the effects of histone H3 mutations from lysine 36 to lysine 56 (Fig. 1A) in our strain background (yMK1243 and equivalents), plasmids (*TRP1*$^+$) harboring only H3 and H4 genes with histone mutations created by the Boeke group were co-transformed with pJL74 (a *LEU2*$^+$ plasmid bearing only histones H2A and H2B) into yMK1141 (contains pMK440, a *URA3*$^+$ plasmid bearing all four core histone genes) (5). 5-FOA selection was conducted to select for yeast cells that had lost the plasmid pMK440. pJL74 was a self-ligated product of the linearized pMK439 cutted by *Sal* I (blunted) and *Pst* I (blunted), which removed H3 and H4 genes from pMK439. All other studies were carried out with histone mutations generated in pMK439 by two-step PCR site-directed mutagenesis (23).

Yeast methods. Yeast growth media, conditions, and transformation were based on standard procedures (31). When appropriate, 5% casamino acids (CAA) were used to substitute for synthetic amino acid mixtures as selective medium for uracil, tryptophan, or adenine prototroph. Yeast transformation was done with the lithium acetate method (10).

Chromosome stability assays were conducted by measuring the mating behavior

of diploid strains bearing wild-type or selective tension sensing mutants. Diploid strains with histone mutations were constructed via plasmid shuffling, yMK1174 (*MATa/α*, contains pMK440 *URA3*$^+$) were used for transformation to harbor histone mutations generated on pMK439 (*LEU2*$^+$), 5-FOA selection was followed to select for yeast cells that had lost the plasmid pMK440. To assess the chromosome stability, cells were first patched onto YPD plates and incubated at 30° for 2 to 3 days till saturation. Cell patches were again replica plated to another fresh YPD plates pre-spreaded with a or α tester cells and were allowed to mate at 30° for 10 hours, followed by further replica plating to minimum medium plates to select for cells that had mated successfully. Mating between the tester and the subject strains resulted in complete complementation of nutrient requirement, that is, cells were able to survive in the minimal medium without any amino acid or nucleoside addition.

Tension sensing tests using the P_{GAL1}-*MCD1* strains were according precisely to reference (15) using strains yJL171, yJL487 and yJL492.

For Fluorescence Activated Cell Sorting (FACS) analyses, logarithmically growing cells ($0.5OD_{600}$) were collected, washed once with 1ml water, and fixed overnight at 4°C with 1ml 70% ethanol. Cell pellets were washed with 1ml 10mM Tris (pH 7.4), 15mM NaCl, and resuspended into 300μl Tris/NaCl buffer containing 0.1mg/ml RNase A. After the incubation at 37°C for 2 hours, cell pellets were resuspended into PBS (pH7.4) at $1X10^8$ cells/ml. For propidium

iodide staining, 10µl of cell suspension was mixed with 490µl of PBS containing 40µg/ml propidium iodide. 20,000 cells were subjected to FACS analysis on a BD Vantage SE in Flow Cytometry Facility (Biochemistry, MSU).

Western analyses of yeast proteins were conducted as mentioned in reference (23). Home-made H3 antibody H3-1B2 was used at 1:20,000 dilution at 4°C for overnight.

Chromatin immunoprecipitation (ChIP). ChIP was conducted as previously described (19, 23). To quantify the ChIP results, the semi-quantitative PCR products were purified, resolved in 9% polyacrylamide gel electrophoresis, and stained by ethidium bromide. The captured gel images were then quantified by NIH Image. Intensities of each *CEN*/pericentric fragment were compared to a common internal control (*DED1* or *PGK1*). The ratio was further normalized to 0.1% input DNA (set at 1.0) for PCR amplification of all reactions carried out in parallel. The ChIP data were obtained from at least three independent yeast cultures.

Sgo1p interaction with H3. Histones were prepared according to reference (7). Recombinant Sgo1p was prepared as previously described (23). For pull-down assays, approximately 5 µg of soluble recombinant Sgo1p were incubated with about 3 µg of yeast histones in 150 µl of HEMGT buffer at 4°C for 1 hour. 6 µl of glutathione beads (1:1 slurry) along with 150 µl of the HEMGT buffer were added

to the reactions and rocked gently at 4°C for another hour. Beads were washed with 500 µl of the HEMGT buffer for 3 times, 5 min each, followed by boiling in 2x SDS-PAGE loading buffer for 5 minutes. Eluate was resolved by 15% SDS-PAGE and blotted for anti-H3 Western analyses (23).

To study the functions of *GCN5* on the H3-Sgo1p tension sensing function, H3 mutations (on pMK439 *LEU2*$^+$) were introduced into yJL486 (*gcn5*Δ, pMK440 *URA*3+) via plasmid shuffling and 5-FOA selection, resulting strains yJL506 to yJL510 (see Table 3-1). yJL486 was constructed by transforming 4.6kb *gcn5::URA3* fragment, which is released from pMK147 by *Xho* I and *Xba* I, into yMK1141 (pMK440 *URA*3$^+$). Dominant negative HAT inactive mutants of *gcn5, gcn5E173H or gcn5F221A* were carried on pMK144 and were directly transformed into cells bearing H3 mutations (For *SGO1* series, parent strains were yMK1243, yJL145 etc.; for *sgo1*Δ background, parent strains were yMK1361, yJL170 and others bearing indicated H3 mutation, see Table 3-1)

RESULTS

Mutations of a cluster of amino acid residues of H3 cause mitotic chromosome instability

Our initial findings that Gly44 of H3 is important for Sgo1p interaction and tension sensing (23) suggest that this residue is part of a functional motif that acts as the loading dock for Sgo1p recruitment. Indeed, Boeke and colleagues reported in their systematic phenotypic characterization of histone mutations that K42Q and R49A of H3 render cells hypersensitive to benomyl (5), one of the diagnostic phenotypes of our tension sensing defective G44S allele (23). To test whether Gly44 is part of a Tension Sensing Motif, amino acid substitutions of residues K36 (the end of the tail domain) through K56 (the end of the αN helix of the histone core) were introduced to yeast cells, and the growth under varying concentrations of benomyl was assessed.

Figure 1A shows that K42A, G44A and T45A caused severe hypersensitivity to benomyl whereas H39A, R40A, Y41A, and R49A were moderately sensitive to this spindle poison. While both K36 and K56 are known to be acetylated and are important for several nuclear functions (6, 26), alanine substitution of these residues did not affect benomyl tolerance. Intriguingly, although P43 is flanked by K42 and G44, alanine substitution at P43 clearly is functionally neutral. This observation is consistent with the crystal structure shown in Figure 1B (right) in that the imino acid ring structure of P43 points away from the side chains of K42

and T45, and sits flat on the beta turn. It is possible that G44 plays a more prominent role than does P43 in permitting the formation of this beta turn structure. Additionally, like G44S, the benomyl hypersensitivity of these new H3 mutants also can be suppressed by the overexpression of *SGO1* (Fig. 1D and 1E). Together, these data suggest that K42, G44, and T45 form a core executing a mitotic function together with Sgo1p that is pivotal for cell survival under the benomyl stress.

That the K42A mutation phenocopies G44S (as well as G44A) suggests one possibility that acetylation at K42 controls G44-related mitotic functions. This notion appears to be supported by the observations that the K42Q mutation that mimics a constitutively acetylated state also causes benomyl hypersensitivity (row 9, Fig. 1C), whereas K42R that mimics a constitutively unacetylated state was apparently phenotypically neutral (rows 3, Fig. 1C). Two inferences can be drawn here. First, the positive charge of this position has to be maintained by either a lysine or an arginine residue. Alternatively, K42 acetylation might be a natural negative regulator of TSM. If the latter hypothesis is correct, we predict that K42R would suppress the phenotype of G44S that undermines the Sgo1p interaction and recruitment. Contrary to this prediction, the G44S benomyl hypersensitivity phenotype could not be suppressed by K42R (compare row 3 with 2, 4, 5, Fig. 1C), arguing against that the uncorroborated acetylation of K42 was functionally relevant.

Benomyl depolymerizes microtubules, which in turn activates the spindle assembly checkpoint, SAC, that arrests cells at G_2/M phase. Hypersensitivity to benomyl may be a result of the failure of activating the SAC. However, both K42A and T45A mutants can stabilize the securin protein Pds1p when treated with benomyl (Fig. 2), ruling out the possibility that the SAC itself is defective in these mutant cells.

Together, these phenotypic comparisons suggest that the short stretch of H3 from K42 to T45 is a functional or physical target of a mitotic regulator.

Chromosome instability conferred by K42, G44, and T45 mutants

Mitotic defects frequently trigger instability of chromosomes. To see if this is true for the new H3 alleles, we compared the mating behaviors of wild-type, K42A, G44S, and T45A cells. As an additional control, we included another novel histone mutant allele, H4 R35S, which is also hypersensitivity to benomyl (Luo and Kuo, unpublished data). In the budding yeast, diploid cells inherit the transcriptionally active *MATa* and *MATα* loci on chromosome III from the two haploid parents. Concomitant expression of these two loci represses genes essential for mating. Normal a/α diploid thus is considered a non-mater. If there is an increase in chromosome instability, random loss of one of the two chromosome III homologues will enable cells to mate, regardless of the ploidy for the rest of the genome. Gaining the ability to mate is thus an easy method to examine the chromosome stability. Figure 3A shows that a substantial portion of

diploid cells bearing each of these H3 mutant alleles were able to mate with either *MATa* or *MATα* haploid tester strains, while wide-type or H4 R35S mutant cells maintained their diploid non-mating character. Genomic PCR using primers differentiating *MATa* and *MATα* loci demonstrated that the ability to mate as haploid cells correlated well with the loss of either of the two copies of chromosome III (Fig. 3B). To rule out the possibility that these maters were a result of meiosis that would have generated mating-capable haploids, we did fluorescence activated cell sorting (FACS) analysis to examine the overall DNA content of cells from the patches on minimal medium plates. Figure 3C shows that prior to mating with the tester, all starting diploid cells contained 2N or slightly higher than 2N DNA. Upon mating with the haploid mater, the DNA content further increased (marked by the arrows of the G_1 peaks), thus manifesting the fusion of two sets of genome.

Consistent with the conclusion that these H3 mutant diploid cells had the aneuploidy phenotype, we observed that K42A, G44A, G44S, and T45A diploid cells either had very low sporulation efficiency, or, if tetrads were formed, low germination rate (data not shown). Finally, in contrast to the H3 mutants, the H4 R35S mutation behaved like wild-type cells, thus arguing against the possibility that all benomyl hypersensitive mutants suffer from chromosome instability. We thus surmise that K42, G44, and T45 are important for cells to maintain mitotic chromosome stability.

K42A and T45A mutations compromise tension sensing function and Sgo1p recruitment

The physical proximity of K42, G44, and T45, as well as the similar phenotypes in benomyl hypersensitivity and chromosome instability strongly suggest that the new K42A and T45A alleles also are defective in monitoring the tension between sister chromatids. To address this question, we analyzed the Pds1p securin abundance after repressing the expression of an essential cohesin complex component, Mcd1p/Scc1p. In the absence of Mcd1p, the cohesion between sister chromatids is lost, thus eliminating the tension without affecting the spindle-kinetochore attachment (3). Shifting cells from galactose to glucose medium represses the P_{GAL1}-controlled *MCD1* expression and prevents cohesin complex formation (see panel A of Fig. 4), Figure 4B shows that wild-type cells stabilized the Pds1p, whereas K42A (Fig. 4C) and T45A (Fig. 4D) mutant cells failed to do so. The inability of cells to respond to the lack of tension is in excellent agreement of the documented tension sensing defects caused by the G44S mutation (23). We conclude that K42, G44, and T45 together form a tension sensing motif.

Yeast and other eukaryotic cells monitor the tension status via the Shugoshin family proteins. Recruitment of Sgo1p, the budding yeast Shugoshin protein, to the pericentromeres is essential for the tension sensing function. Given that overexpressing *SGO1* suppresses the benomyl hypersensitivity phenotype of both K42A and T45A mutants (Fig. 1D), we suspected that these two alleles

damaged the ability of H3 to retain Sgo1p at the pericentric region, hence compromising the tension sensing activity. We first examined the steady-state Sgo1p concentration by western blotting, and found that all strains expressed Sgo1p at a comparable level (Fig. 5C). We then conducted ChIP to see if the localization of Sgo1p is affected by the new TSM mutations.

Figure 5 shows that Sgo1p was recruited successfully to *CEN16* in all strains tested. However, the pericentric Sgo1p was significantly reduced in K42A and T45A mutant cells. The abrupt drop of the Sgo1p signal at as close as 0.3 kb to *CEN16* in these two mutants strongly suggests that the recruitment of Sgo1p to the centromere, in which the canonical H3 is replaced by a centromere-specific H3 variant Cse4p, is realized by a mechanism different from that for pericentric Sgo1p enrichment. This notion is further confirmed by *in vitro* pull-down assays that examined the physical interaction between H3 and Sgo1p. Figure 6 shows that the wild-type H3 purified from yeast was able to interact with a GST-tagged Sgo1p. In stark contrast, K42A and T45A mutant H3 exhibited much weaker affinity for the recombinant Sgo1p. Consistent with genetic test, P43A mutant H3 binds Sgo1p similarly as wild-type. We thus conclude that both K42A and T45A mutations compromise severely the ability of H3 to interact with Sgo1p *in vitro* and *in vivo*, and that the tension sensing motif of H3 functions through physically recruiting or retaining Sgo1p at the pericentromeres.

Expanding the pericentric domain of Sgo1p

One of the possible mechanisms for Sgo1p enrichment at the pericentric region is that a centromeric factor nucleates the initial recruitment. Excessive Sgo1p molecules then spill over sideway to interact with histone H3 in nucleosomes adjacent to the centromere. This model does not require an obligatory pericentromere-specific epigenetic mark for Sgo1p binding. The fact that bulk H3 associates effectively with Sgo1p *in vitro* is consistent with this notion. If correct, this model predicts that overexpressing *SGO1* would lead to expansion of existing Sgo1p domain. Indeed, yeast cells receiving a 2μ plasmid harboring the *SGO1* gene exhibited a wider Sgo1p domain around *CEN16* when compared with those expressing *SGO1* from an *ARS CEN* plasmid (Fig. 7). Moderate Sgo1p signals can be seen as far as 20 kb from *CEN16* if Sgo1p was overexpressed (Fig. 7B). This increase in Sgo1p association was not seen at the *SPT15* locus, more than 300 kb from *CEN5*. Because all ChIP PCR reactions were quantified with an internal *DED1* control (see gel pictures in Fig. 7A), the effect we saw on the pericentric Sgo1p domain clearly was not due to an increase of non-discriminating genome-wide association of Sgo1p to chromatin.

The HAT activity of Gcn5p likely regulates TSM function

While it is highly likely that Sgo1p was first recruited to the centromeres and then spreads to pericentromeres, it remains enigmatic how Sgo1p is excluded from the chromosomal arms where H3 is nearly ubiquitously present. One intriguing possibility is that the H3-Sgo1p interaction is subjected to direct or indirect regulation such that only the pericentric H3 is amenable to Sgo1p association.

Because bacterially expressed Sgo1p and H3 interact well [(23) and data not shown], it seems likely that the H3-Sgo1p interface is negatively regulated by a reversible modification. The Gcn5p histone acetyltransferase, though well-known for its roles in transcriptional activation, has also been shown to exert a centromere-related function during mitosis (32, 35). Suspecting that Gcn5p may be involved in the H3 mitotic function exerted via K42, G44, and T45, we examined the effect of deleting *GCN5* from each of these H3 mutants. Figure 8A shows that deleting *GCN5* effectively suppressed the benomyl hypersensitivity of G44S, G44A and K42A strains. Surprisingly, the T45A mutant was refractory to this suppression. The latter result is critical in that it rules out the possibility that deleting *GCN5* resulted in a global change in benomyl flux or metabolism. To further delineate whether the suppression was related to the HAT activity of Gcn5p, we overexpressed two dominant negative alleles of *GCN5*, *gcn5* F221A and *gcn5* E173H (22), that were devoid of the catalytic activity. Figure 8B shows literally identical results as those in Figure 8A. That is, the hypersensitivity to benomyl of K42A and G44A (G44S) mutant cells was suppressed by the catalytically inactive alleles of *GCN5*, whereas the T45A mutant resisted this suppression. In addition to benomyl hypersensitivity, we noticed that mutations at K42, G44, and T45 also caused cellular hypersensitivity to a nucleoside analog, hydroxyurea (HU) (Fig. 8B). However, overexpression of the *GCN5* HAT inactive mutant had no effect on the HU hypersensitivity of above mentioned H3 mutant, strongly suggesting that the genetic interaction between Gcn5p and H3 is specific to the regulation during mitosis. The notion that Gcn5p is a negative

regulator for the H3 mitotic function was further supported by the observation of enhanced benomyl sensitivity when the wild-type Gcn5p was overexpressed in the K42A, G44A, and G44S mutants (Fig. 8B). Moreover, this negative regulation of H3 function by Gcn5p HAT activity requires a functional Sgo1p. Upon removing *SGO1*, we see that the suppression by *gcn5* F221A and *gcn5* E173H was completely reverted (Fig. 9), suggesting that Gcn5p regulates H3 function in the same pathway as Sgo1p and that Gcn5p controls both H3 and Sgo1p in their mitotic functions.

DISCUSSION

This work uncovered a tension sensing motif in histone H3 that is important for mitotic checkpoint control. Three core residues of this motif, Lys42, Gly44, and Thr45 are all important for interactions with Sgo1p both *in vitro* and *in vivo.* Alanine substitutions of these three residues share similar mitotic phenotypes, and are all susceptible to the overexpression of *SGO1*, suggesting that they function in the same pathway for monitoring tension between sister chromatids.

Among the three residues, Lys42 and Thr45 are known to be modified under certain conditions. Methylation of Lys42 is important for transcriptional regulation in yeast (E. M. Hyland and J. D. Boeke, personal communication). However, transcriptional defects caused by K42A cannot be rescued by *SGO1* overexpression (our unpublished observation), arguing against the notion that the mitotic function involving Lys42 is modulated by its methylation. Consistent with this notion, K42R, which prevents such modifications as acetylation and methylation, is functionally neutral for mitotic control (Fig. 1C). Thus, we do not believe that Lys42 modification is functionally linked to mitotic regulation.

On the other hand, it is intriguing that deleting *GCN5*, or simply inactivating its acetyltransferase activity, is sufficient to suppress the benomyl hypersensitivity phenotype associated with K42A, G44A, and G44S mutations, but not the T45A mutation. It is tempting to speculate that Thr45 is a downstream target of Gcn5p.

Threonine acetylation, though not yet known by Gcn5p, has been documented in at least one report (27). Another possibility is that a yeast Thr45 kinase is regulated by the HAT activity of Gcn5p. When H3 Thr45 is phosphorylated, the H3-Sgo1p interaction will be inhibited, thus compromising the H3 function for tension sensing. Thr45 phosphorylation has been documented recently by the Kouzarides group (14). They showed that phosphorylation of Thr45 is elevated in apoptotic neutrophils, and postulated that this modification somehow facilitates the nick and fragmentation of the surrounding DNA during apoptosis (14). Recently, Grant and colleagues also reported the phosphorylation of H3 Thr45 in *S. cerevisiae.* H3 Thr45 phosphorylation peaks during DNA replication, and is mediated by the S phase kinase Cdc7-Dbf4 complex (1). It will be interesting to see whether phosphorylation of Thr45 by Cdc7-Dbf4 complex depends on the functional Gcn5p, and whether that phosphorylation is linked to the H3 TSM-Sgo1p mitotic function.

Studies in fission yeast indicated that Bub1p phosphorylates histone H2A at a conserved residue Ser 121. H2A S121A mutant cells phenocopy Bub1p kinase-inactive mutant *bub1-KD* in defects of kinetochore-microtubule attachment and centromeric protection. The phosphorylation of H2A and Bub1p kinase activity function in the same pathway for the centromeric localization of Sgo1p (8, 16). It will thus be interesting to examine whether pericentic H2A also actively regulates Sgo1p localization, and whether the phosphorylation level of H2A is affected by the HAT activity of Gcn5p.

All tension sensing mutants selectively eliminate the pericentric Sgo1p but leave the centromeric Sgo1p unaltered, suggesting that Sgo1p is first recruited to the centromere/kinetochore, and then spreads to the neighboring pericentric H3 TSM for protein-protein interactions. Moreover, overexpressing Sgo1p widens the pericentric domain of Sgo1p. Therefore, we propose a Spillover model explaining the establishment of the Sgo1p domain at pericentromeres and how chromatin modulators such as Gcn5p may affect the H3-Sgo1p interaction that is central to the tension sensing function of H3. In this model, we suggest that a centromere factor, likely the Bub1p kinase and the phosphorylated H2A (16) nucleates the recruitment of Sgo1p at centromere. Excessive Sgo1p molecules then spill over to the pericentric region where they are retained by the TSM of H3, hence establishing the pericentric domain by which the tension status is monitored. The spreading or maintenance of Sgo1p at the pericentromeres is also hypothesized to be regulated by Gcn5p. Genetic data suggested that Gcn5p negatively regulates the H3 TSM-Sgo1p mitotic function. It is possible that the HAT activity of Gcn5p prevents pericentromeres from recruiting/retaining of Sgo1p.

TABLE 3-1. Yeast strains used in this study

Strain	Relevant genotype	Source or reference
yJL170	*MAT***a** *ade2-1 can1–100 his3–11,15 leu2–3,112 trp1–1::sgo1*::TRP1 *ura3-1 hht1-hhf1::KAN hht2-hhf2::KAN hta1-htb1::Nat hta2-htb2::HPH* pMK439G44S [*ARS CEN LEU2 HTA1-HTB1 hht2-G44S-HHF2*]	This study
yJL171	*MAT***a** *ade2-1 bar1Δ can1–100 his3–11,15::pGAL-MCD1::HIS3 leu2–3,112 trp1–1::PDS1-Myc13::TRP1 ura3-1 hht1-hhf1::KAN hht2-hhf2::KAN hta1-htb1::Nat hta2-htb2::HPH* pQQ18 [*ARS CEN LEU2 HTA1-HTB1 HHT2-HHF2*]	(23)
yJL339	*MAT***a**/α *his3Δ1 leu2Δ0 met15Δ0 ura3Δ0 hht1-hhf1::KAN hhf-2hht2::NAT hta1-htb1::HPH hta2-htb2::NAT pQQ18 [CEN LEU2 HTA1-HTB1 HHT2-HHF2]*	This study
yJL340	*MAT***a**/α *his3Δ1 leu2Δ0 met15Δ0 ura3Δ0 hht1-hhf1::KAN hhf-2hht2::NAT hta1-htb1::HPH hta2-htb2::NAT pMK439G44S [CEN LEU2 HTA1-HTB1 hht2-G44S-HHF2]*	This study
yJL343	*MAT***a** *ade2-1 can1–100 his3–11,15 leu2–3,112 trp1–1::SGO1-6HA::TRP1 ura3-1 hht1-hhf1::KAN hht2-hhf2::KAN hta1-htb1::Nat hta2-htb2::HPH* pQQ18 [*ARS CEN LEU2 HTA1-HTB1 HHT2-HHF2*]	(23)
yJL369	*MAT***a** *ade2-1 can1–100 his3–11,15 leu2–3,112 trp1–1 ura3-1 hht1-hhf1::KAN hht2-hhf2::KAN hta1-htb1::Nat hta2-htb2::HPH* pMK439P43A [*ARS CEN LEU2 HTA1-HTB1 hht2-P43A-HHF2*]	This study
yJL431	*MAT***a** *ade2-1 can1–100 his3–11,15 leu2–3,112 trp1–1::sgo1*::TRP1 *ura3-1 hht1-hhf1::KAN hht2-hhf2::KAN hta1-htb1::Nat hta2-htb2::HPH* pMK439G44A [*ARS CEN LEU2 HTA1-HTB1 hht2-G44A-HHF2*]	This study
yJL467	*MAT***a** *ade2-1 can1–100 his3–11,15 leu2–3,112 trp1–1 ura3-1 hht1-hhf1::KAN hht2-hhf2::KAN hta1-htb1::Nat hta2-htb2::HPH* pMK439K42A [*ARS CEN LEU2 HTA1-HTB1 hht2-K42A-HHF2*]	This study
yJL468	*MAT***a** *ade2-1 can1–100 his3–11,15 leu2–3,112 trp1–1 ura3-1 hht1-hhf1::KAN hht2-hhf2::KAN hta1-htb1::Nat hta2-htb2::HPH* pMK439K42Q [*ARS CEN LEU2 HTA1-HTB1 hht2-K42Q-HHF2*]	This study
yJL469	*MAT***a** *ade2-1 can1–100 his3–11,15 leu2–3,112 trp1–1 ura3-1 hht1-hhf1::KAN hht2-hhf2::KAN hta1-htb1::Nat hta2-htb2::HPH* pMK439K42R [*ARS CEN LEU2 HTA1-HTB1 hht2-K42R-HHF2*]	This study
yJL470	*MAT***a** *ade2-1 can1–100 his3–11,15 leu2–3,112 trp1–1 ura3-1 hht1-hhf1::KAN hht2-hhf2::KAN hta1-htb1::Nat hta2-htb2::HPH* pMK439K42R/G44S [*ARS CEN LEU2 HTA1-HTB1 hht2-K42R/G44S-HHF2*]	This study
yJL471	*MAT***a** *ade2-1 can1–100 his3–11,15 leu2–3,112 trp1–1 ura3-1 hht1-hhf1::KAN hht2-hhf2::KAN hta1-htb1::Nat hta2-htb2::HPH* pMK439T45A [*ARS CEN LEU2 HTA1-HTB1 hht2-T45A-HHF2*]	This study
yJL475	*MAT***a**/α *his3Δ1 leu2Δ0 met15Δ0 ura3Δ0 hht1-hhf1::KAN hhf-2hht2::NAT hta1-htb1::HPH hta2-htb2::NAT pMK439K42A [CEN LEU2 HTA1-HTB1 hht2-K42A-HHF2]*	This study
yJL479	*MAT***a**/α *his3Δ1 leu2Δ0 met15Δ0 ura3Δ0 hht1-hhf1::KAN hhf-2hht2::NAT hta1-htb1::HPH hta2-htb2::NAT pMK439T45A [CEN LEU2 HTA1-HTB1 hht2-T45A-HHF2]*	This study

TABLE 3-1 Cont

yJL480	*MATa ade2-1 can1–100 his3–11,15 leu2–3,112 trp1–1::sgo1*::TRP1 *ura3-1 hht1-hhf1::KAN hht2-hhf2::KAN hta1-htb1::Nat hta2-htb2::HPH* pMK439K42A [*ARS CEN LEU2 HTA1-HTB1 hht2-K42A-HHF2*]	This study
yJL481	*MATa ade2-1 can1–100 his3–11,15 leu2–3,112 trp1–1::sgo1*::TRP1 *ura3-1 hht1-hhf1::KAN hht2-hhf2::KAN hta1-htb1::Nat hta2-htb2::HPH* pMK439T45A [*ARS CEN LEU2 HTA1-HTB1 hht2-T45A-HHF2*]	This study
yJL486	*MATa ade2-1 can1–100 his3–11,15 leu2–3,112 trp1–1 ura3-1::gcn5 hht1-hhf1::KAN hht2-hhf2::KAN hta1-htb1::Nat hta2-htb2::HPH* pJH33 [*ARS CEN URA3 HTA1-HTB1 HHT2-HHF2*]	This study
yJL487	*MATa ade2-1 bar1Δ can1–100 his3–11,15::pGAL-MCD1::HIS3 leu2–3,112 trp1–1::PDS1-Myc13::TRP1 ura3-1 hht1-hhf1::KAN hht2-hhf2::KAN hta1-htb1::Nat hta2-htb2::HPH pMK439K42A [ARS CEN LEU2 HTA1-HTB1 hht2-K42A-HHF2]*	This study
yJL492	*MATa ade2-1 bar1Δ can1–100 his3–11,15::pGAL-MCD1::HIS3 leu2–3,112 trp1–1::PDS1-Myc13::TRP1 ura3-1 hht1-hhf1::KAN hht2-hhf2::KAN hta1-htb1::Nat hta2-htb2::HPH pMK439T45A [ARS CEN LEU2 HTA1-HTB1 hht2-T45A-HHF2]*	This study
yJL506	*MATa ade2-1 can1–100 his3–11,15 leu2–3,112 trp1–1 ura3-1::gcn5 hht1-hhf1::KAN hht2-hhf2::KAN hta1-htb1::Nat hta2-htb2::HPH pQQ18 [ARS CEN LEU2 HTA1-HTB1 HHT2-HHF2]*	This study
yJL507	*MATa ade2-1 can1–100 his3–11,15 leu2–3,112 trp1–1 ura3-1::gcn5 hht1-hhf1::KAN hht2-hhf2::KAN hta1-htb1::Nat hta2-htb2::HPH pMK439G44S [ARS CEN LEU2 HTA1-HTB1 htt2-G44S-HHF2]*	This study
yJL508	*MATa ade2-1 can1–100 his3–11,15 leu2–3,112 trp1–1 ura3-1::gcn5 hht1-hhf1::KAN hht2-hhf2::KAN hta1-htb1::Nat hta2-htb2::HPH pMK439G44A [ARS CEN LEU2 HTA1-HTB1 htt2-G44A-HHF2]*	This study
yJL509	*MATa ade2-1 can1–100 his3–11,15 leu2–3,112 trp1–1 ura3-1::gcn5 hht1-hhf1::KAN hht2-hhf2::KAN hta1-htb1::Nat hta2-htb2::HPH pMK439K42A [ARS CEN LEU2 HTA1-HTB1 htt2-K42A-HHF2]*	This study
yJL510	*MATa ade2-1 can1–100 his3–11,15 leu2–3,112 trp1–1 ura3-1::gcn5 hht1-hhf1::KAN hht2-hhf2::KAN hta1-htb1::Nat hta2-htb2::HPH pMK439T45A [ARS CEN LEU2 HTA1-HTB1 htt2-T45A-HHF2]*	This study
yJL540	*MATa ade2-1 can1–100 his3–11,15 leu2–3,112 trp1–1::SGO1-6HA::TRP1 ura3-1 hht1-hhf1::KAN hht2-hhf2::KAN hta1-htb1::Nat hta2-htb2::HPH pMK439K42A [ARS CEN LEU2 HTA1-HTB1 hht2-K42A-HHF2]*	This study
yJL543	*MATa ade2-1 can1–100 his3–11,15 leu2–3,112 trp1–1::SGO1-6HA::TRP1 ura3-1 hht1-hhf1::KAN hht2-hhf2::KAN hta1-htb1::Nat hta2-htb2::HPH pMK439T45A [ARS CEN LEU2 HTA1-HTB1 hht2-T45A-HHF2]*	This study
yMK1174	*MATa/α his3Δ1 leu2Δ0 met15Δ0 ura3Δ0 hht1-hhf1::KAN hhf-2hht2::NAT hta1-htb1::HPH hta2-htb2::NAT pJH33 [ARS CEN URA3 HTA1-HTB1 HHT2-HHF2]*	This study
yMK1243	*MATa ade2-1 can1–100 his3–11,15 leu2–3,112 trp1–1 ura3-1 hht1-hhf1::KAN hht2-hhf2::KAN hta1-htb1::Nat hta2-htb2::HPH* pQQ18 [*ARS CEN LEU2 HTA1-HTB1 HHT2-HHF2*]	(23)
yMK1361	*MATa ade2-1 can1–100 his3–11,15 leu2–3,112 trp1–1::sgo1*::TRP1 *ura3-1 hht1-hhf1::KAN hht2-hhf2::KAN hta1-htb1::Nat hta2-htb2::HPH* pQQ18 [*ARS CEN LEU2 HTA1-HTB1 HHT2-HHF2*]	This study

TABLE 3-2. Plasmid constructs used in this study

Plasmid	Main features	Source or reference
pJH33/pMK440	*pRS316-HTA1-HTB1 HHT2-HHF2*	(23)
pJL51	*2μm URA3 pADH1-3xHA-SGO1-tADH1*	This study
pJL52	*ARS1 CEN4 URA3 pADH1-3xHA-tADH1*	This study
pJL53	*ARS1 CEN4 URA3 pADH1-3xHA-SGO1-tADH1*	This study
pJL55	*pGEX-4T-1 3xHA-SGO1*	This study
pJL74	*pRS315-HTA1-HTB1*	This study
pMK572	*2μm URA3 vector with ADH1 promtoer and terminator*	(23)
pMK573	*2μm URA3 SGO1*	(23)
pQQ18/Pmk439	*pRS315-HTA1-HTB1 HHT2-HHF2*	(23)

FIG. 3-1. The Tension Sensing Motif (TSM) residues function through Sgo1p. Yeast cells bearing the specific allele (wide-type or mutated as noted) as the sole copy of H3 were tested on YPD medium under indicated conditions. Six-fold serially diluted log-phase cells were spotted for growth test at 30°C for two days. (A) K42, G44, T45 are key residues of a TSM of H3. Single mutations of residues from K36 through K56 were compared for growth on benomyl plates. Arbitrary scores for benomyl hypersensitivity were assigned. -1 and -2 represent mild and severe hypersensitivity, respectively. (B) Structural view of the region that contains TSM. Left panel: close-up view of the TSM (marked red from K42 to T45), showing that the β-turn and a preceding region (K37 to Y41, marked yellow) connects the flexible H3 N-terminal tail (Pink) and the rigid α N domain (Blue). Right panel: close-up view of the ^{42}Lys-Pro-Gly-Thr β-turn. (C) Detailed benomyl hypersensitivity analysis of the TSM residues with focus on mutations on K42, G44, and T45, single or in combination. (D, E) Over-expression of *SGO1* suppresses the benomyl hypersensitivity of tension sensing mutants. "–" sign indicates unaltered residues or no plasmids introduced. Yeast cells were transformed with 2μm *SGO1* (pMK573) or the corresponding empty vector (pMK575), followed by spot assays to compare the benomyl hypersensitivity. VC, vector control.

Fig. 3-1

A

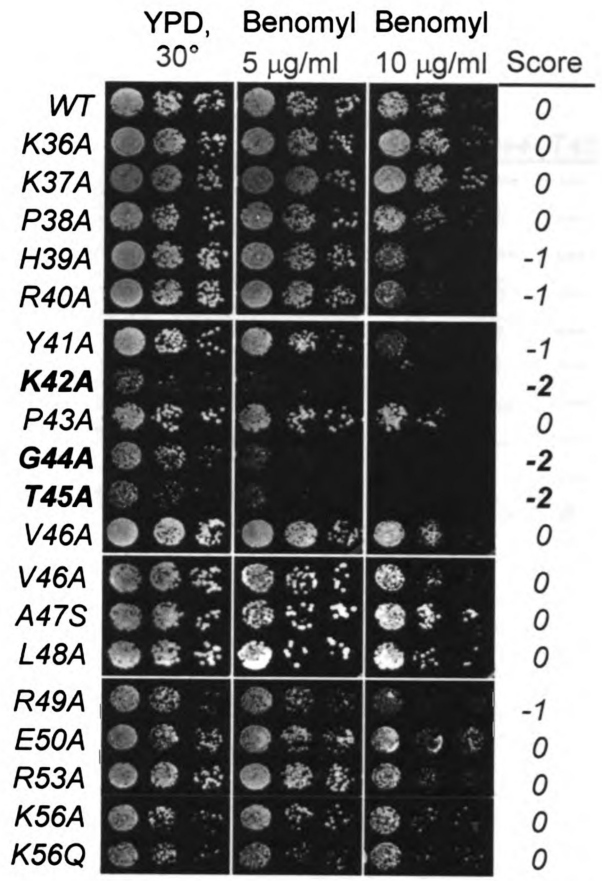

I51A, R52A, F54A, Q55A: too sick to score

B

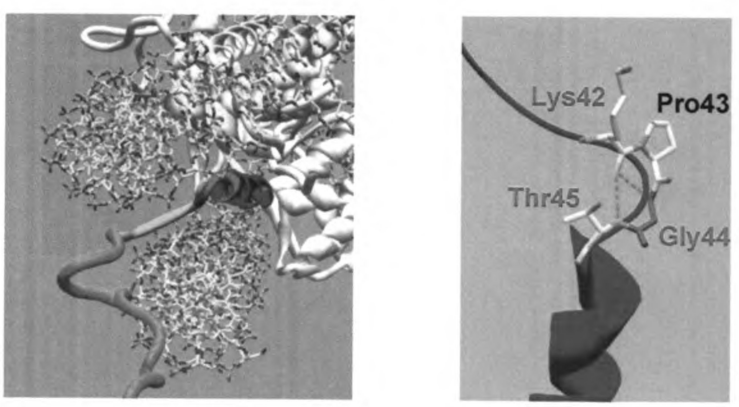

Fig. 3-1 continued

C

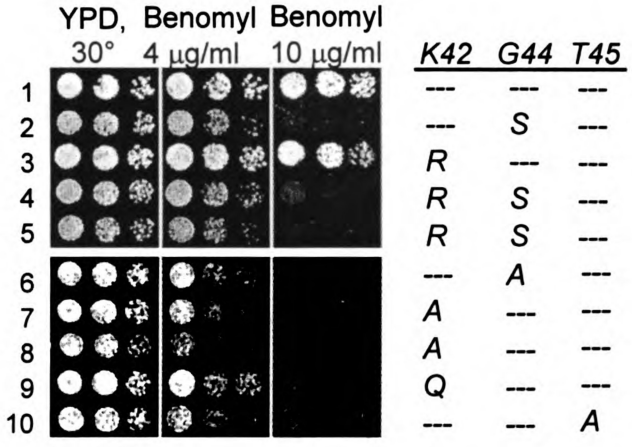

D

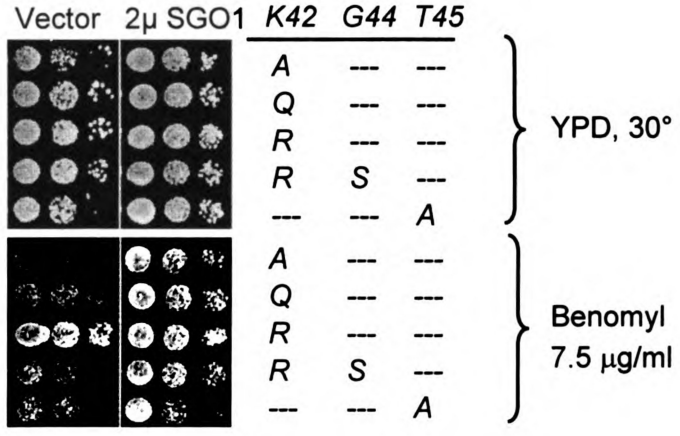

Fig. 3-1 continued

E

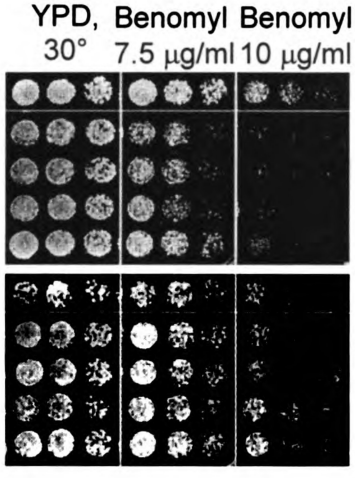

H3	2μ plasmid
WT	-----
H39A	-----
H39A	*VC*
R40A	-----
R40A	*VC*
WT	*SGO1*
H39A	*SGO1*
H39A	*SGO1*
R40A	*SGO1*
R40A	*SGO1*

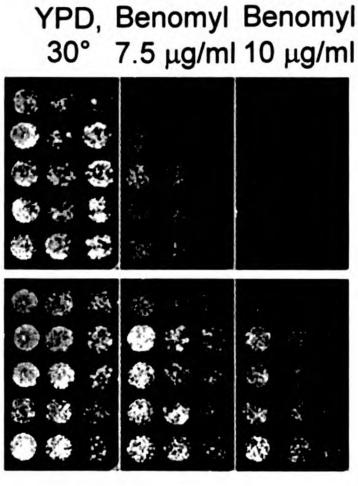

H3	2μ plasmid
G44A	-----
Y41A	-----
Y41A	*VC*
R49A	-----
R49A	*VC*
G44A	*SGO1*
Y41A	*SGO1*
Y41A	*SGO1*
R49A	*SGO1*
R49A	*SGO1*

Fig. 3-2

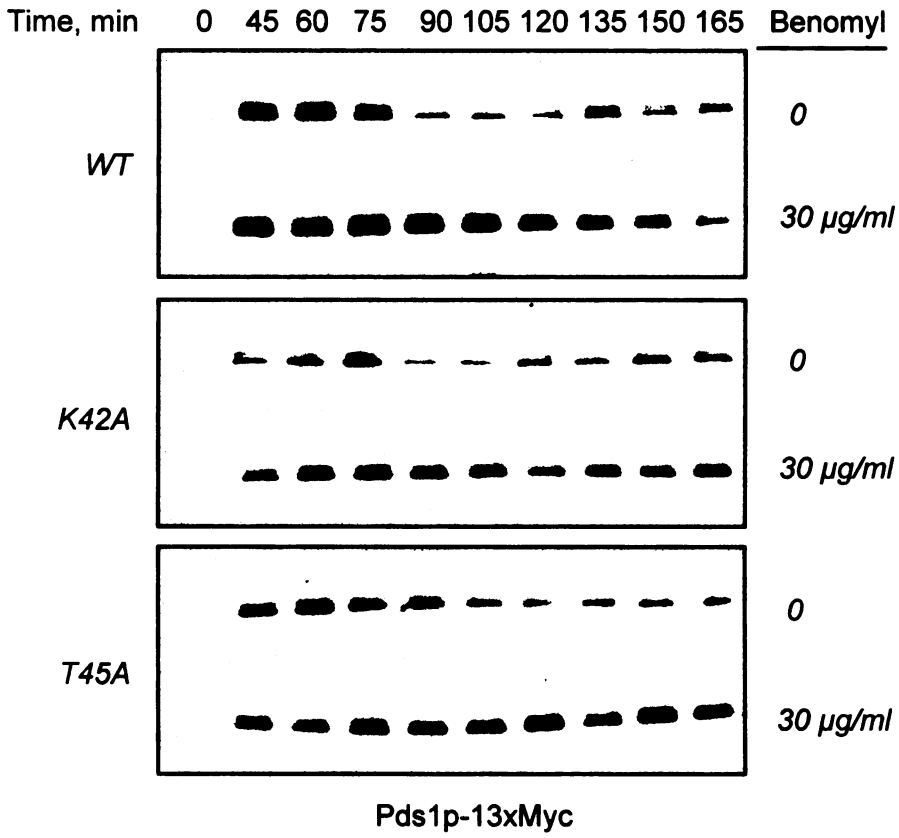

FIG. 3-2. K42A and T45A mutant cells responded normally to benomyl treatment by activating the spindle assembly checkpoint. Pds1p was activated and stabilized in wild-type, K42A and T45A mutant cells in the presence of benomyl. G_1 arrested cells were released at T0' into rich medium containing 0 or 30 µg/ml of benomyl. The same number of cells was taken at the indicated times for boiling and whole-cell extract preparation, followed by anti-Myc western blotting analysis to quantify the abundance of Pds1p.

FIG. 3-3. The K42A and T45A mutant cells exhibited chromosome instability. (A) Diploid mating assays. Yeast diploid cells (yMK1174 derivative, defective in expression of *trp, ura, his*) bearing histone (H3 or H4) mutation as listed in the left to the image were first patched into YPD (rich medium) plates, and then replica plated into SD (minimum medium) plates containing haploid mating tester cells, three control strains (in an order as, *MATa*, *MATα*, and *MATa/α*) were included for comparison in the last row. Mating with the tester cells complemented the nutrient requirement for strains bearing histone mutations, thus selectively allowed the mated cells to grow on the SD minimal medium. (B) Diploid mating ability correlated well with the loss of one of two copies of chromosome III. Shown were genomic PCR results with primers flanking the mating loci to differentiate the existence of *MATa* or *MATα*. Except haploid control cells *MATa* and *MATα*, all others used mated cells to extract genomic DNA for PCR. Listed below gel image were images from their corresponding mating assays. G/S, G44S; WT, wild-type; K/A, K42A; T/A, T45A. (C) Representative images from Fluorescence Activated Cell Sorting (FACS) analyses. Logarithmically growing cells were stained with propidium iodide and subjected to FACS analysis. Dash lines were aligned to G_1 peak of wild-type cells, and fine dot lines to G_1 peaks of their parent strains (original diploid cells before mating), arrows used to highlight the shifts of G_1 peaks.

Fig. 3-3

A

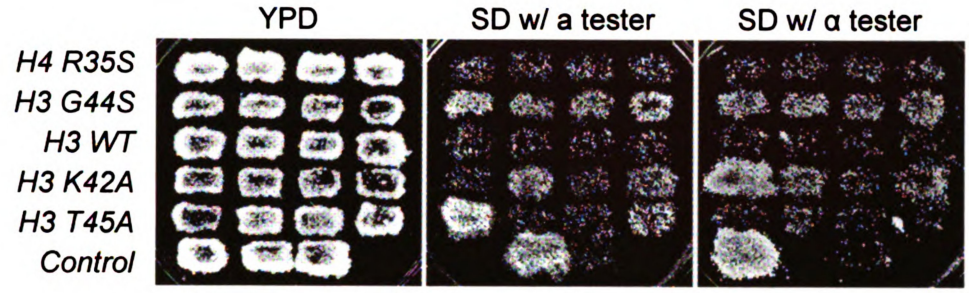
YPD
SD w/ a tester
SD w/ α tester
H4 R35S
H3 G44S
H3 WT
H3 K42A
H3 T45A
Control

B


MATα
MATa
YPD
+ a tester
+ α tester
G/S WT a α K/A K/A K/A K/A K/A K/A K/A T/A T/A T/A T/A T/A T/A T/A T/A

Fig. 3-3 continued

C

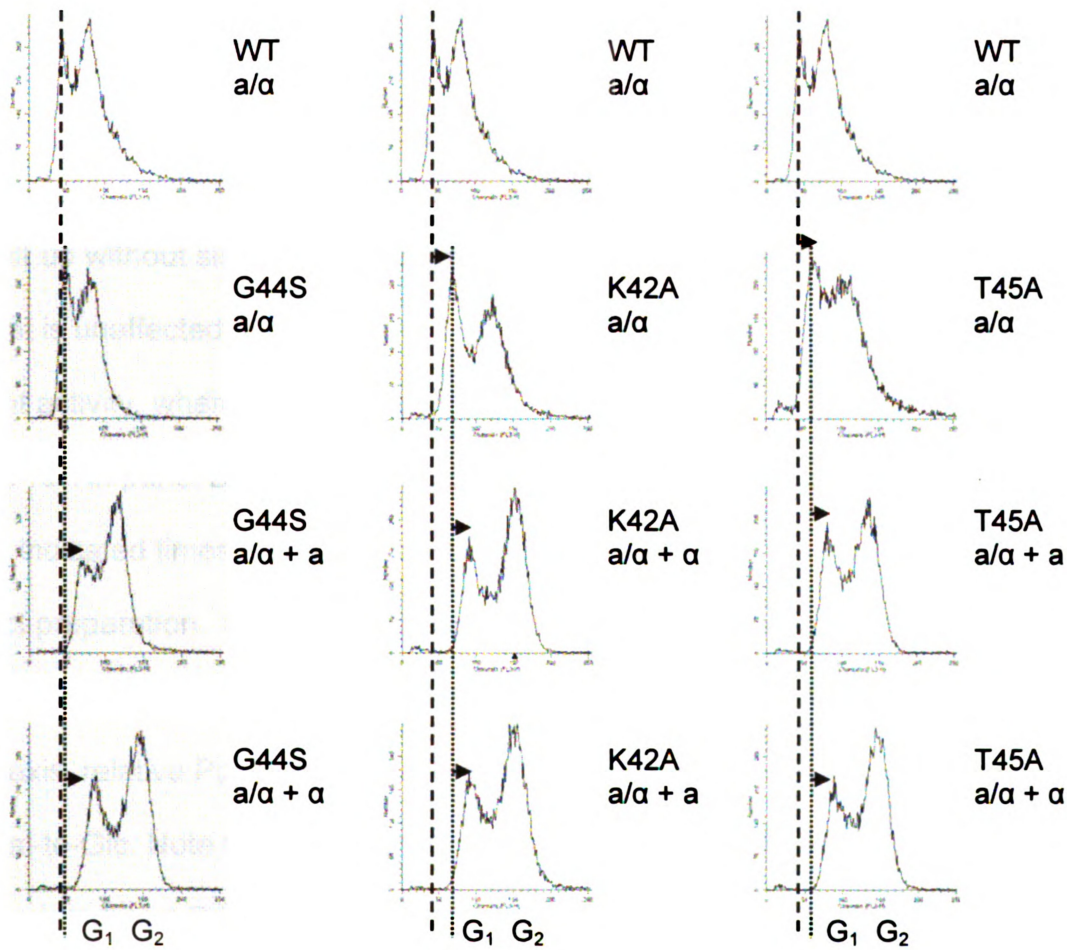

FIG. 3-4. Defects in responding to tensionless crisis in K42A and T45A mutants. (A) Schematic drawing to elucidate the experimental design. The *MCD1* gene, which encodes an essential cohesin component, was placed under the *GAL1* promoter control. Shifting G_1-arrested cells from galactose (Gal) to glucose (Glc) represses *MCD1* expression that is needed for cohesion in S phase. Tension will not be built up without sister cohesion, even though the spindle-kinetochore attachment is unaffected. Normal cells (B) stabilize Pds1p to sustain the spindle checkpoint activity, whereas tension sensing defective mutant cells (K42A in panel C, T45A in panel D) fail to do so, giving rise to Pds1p oscillation in Glc media. At indicated times same number of cells was taken for boiling and whole-cell extract preparation. The abundance of Pds1p was quantified by normalizing with the loading control (western against G-6-PDH antibody). X axis, time in Gal or Glc; Y axis, relative Pds1p band intensity. Close diamonds, Gal-to-Gal; open circles: Gal-to-Glc. Note that the T45A cells grew more slowly, wider intervals was needed to detect Pds1p fluctuation.

Fig. 3-4

A

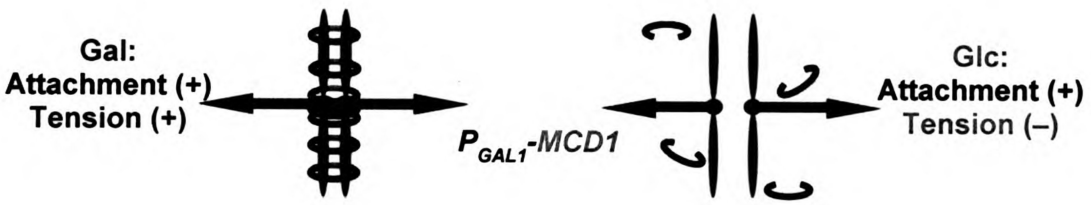
Gal:
Attachment (+)
Tension (+)
P_{GAL1}-MCD1
Glc:
Attachment (+)
Tension (–)

B

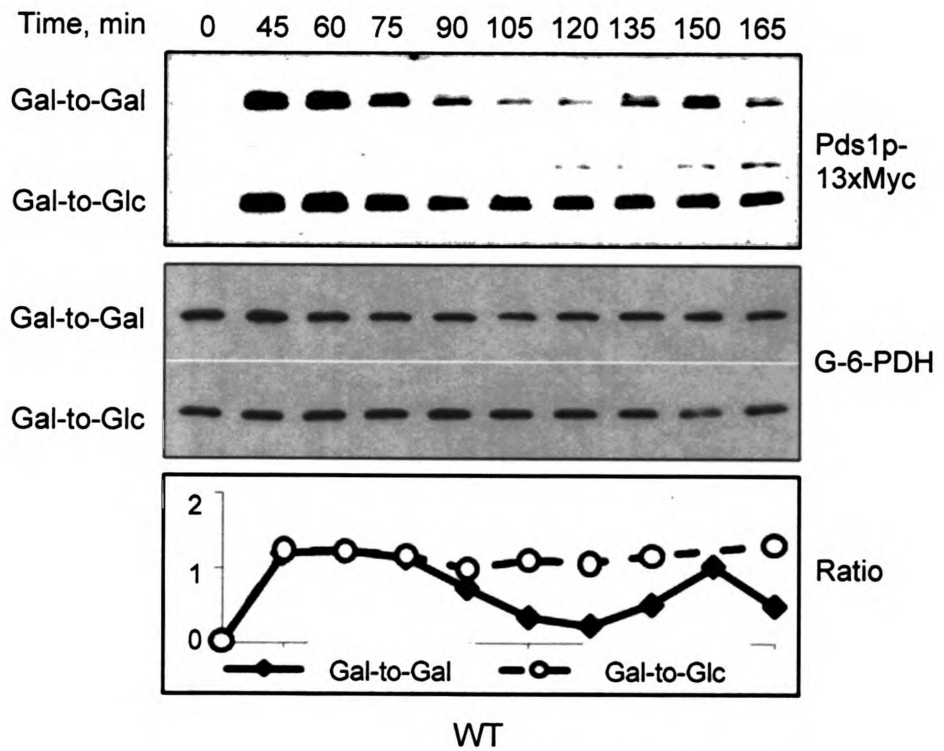
Time, min
0 45 60 75 90 105 120 135 150 165
Gal-to-Gal
Gal-to-Glc
Pds1p-13xMyc
Gal-to-Gal
Gal-to-Glc
G-6-PDH
2
1
0
Gal-to-Gal
Gal-to-Glc
Ratio
WT

Fig. 3-4 continued

C

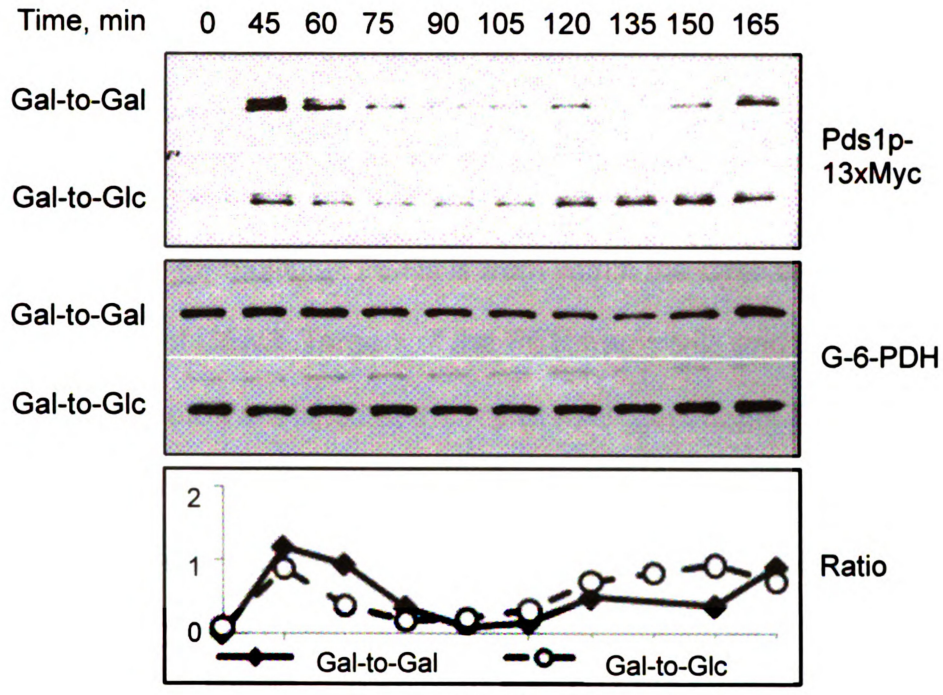

K42A

D

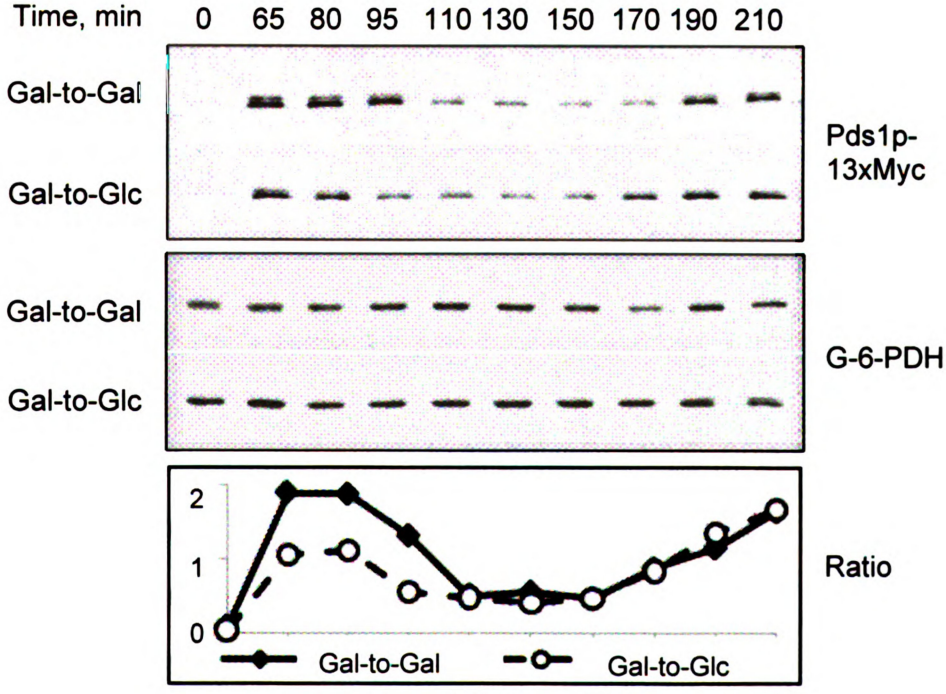

T45A

FIG. 3-5. The K42A and T45A mutation selectively downregulates the pericentric recruitment of Sgo1p *in vivo*. (A) ChIP analysis of HA-tagged Sgo1p. Samples in all of the panels are arranged in the same order. The common internal control (marked by the star on the right) for multiplex PCRs is from within the ORF of the *PGK*1 gene 24.3 kb to the right of *CEN3*. Targets of the PCR fragments and their distance to the cognate centromeres are listed at the top of each gel image. R, right; L, left. *SPT15* is 313.3 kb to the right of *CEN5*. (B) Quantification of the ChIP results. Ethidium bromide-stained DNA gel images were quantified by NIH Image J. The intensity of each *CEN* or pericentric fragment was compared to that of the *PGK*1 internal control (star). The ratio was then normalized to 0.1% input (INP) DNA (set at 1.0 and showed with a dash line). Error bars represent standard deviations from at least three independent cell cultures for ChIP. Ab, antibody. (C) Sgo1p protein abundance is not affected by the K42A and T45A mutation. Western blotting of C'-6xHA-tagged Sgo1p demonstrates the equal abundance of Sgo1p in these three strains. The loading control is cross-reacting bands from yeast lysates.

Fig. 3-5

A

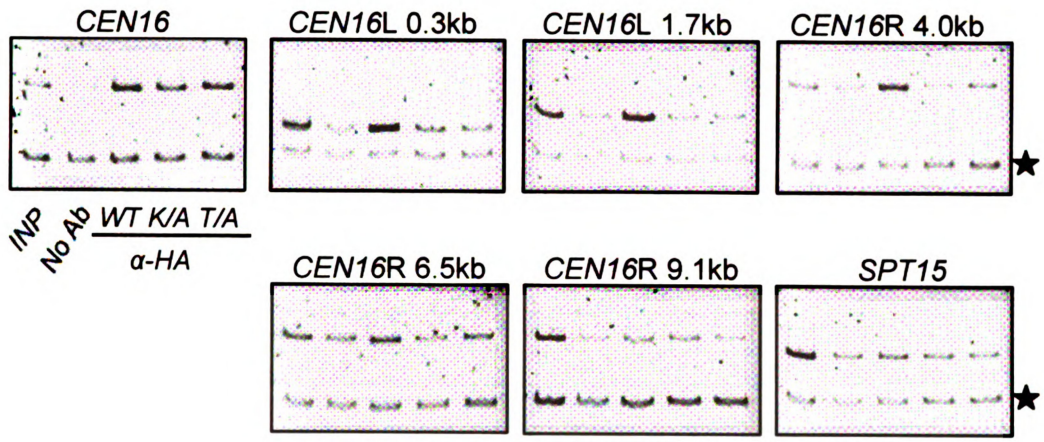
CEN16
CEN16L 0.3kb
CEN16L 1.7kb
CEN16R 4.0kb
INP
No Ab
WT K/A T/A
α-HA
CEN16R 6.5kb
CEN16R 9.1kb
SPT15

B

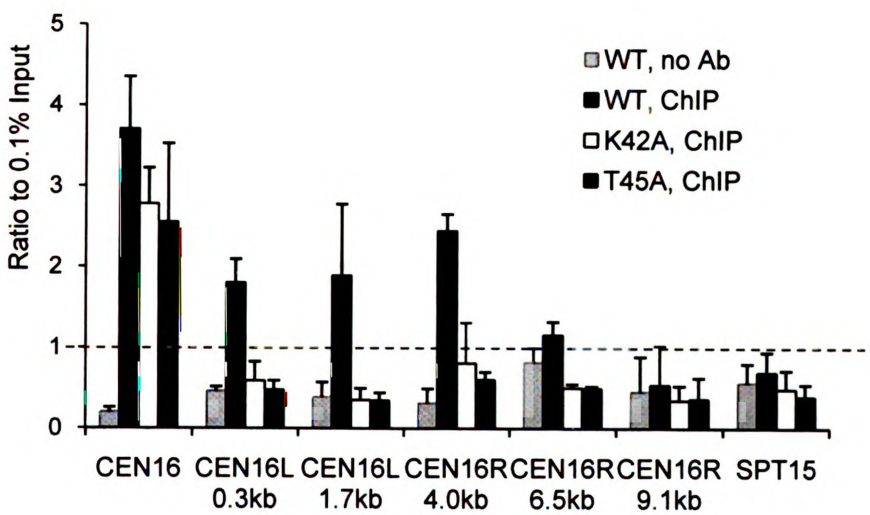
Ratio to 0.1% Input
0
1
2
3
4
5
WT, no Ab
WT, ChIP
K42A, ChIP
T45A, ChIP
CEN16
CEN16L 0.3kb
CEN16L 1.7kb
CEN16R 4.0kb
CEN16R 6.5kb
CEN16R 9.1kb
SPT15

C

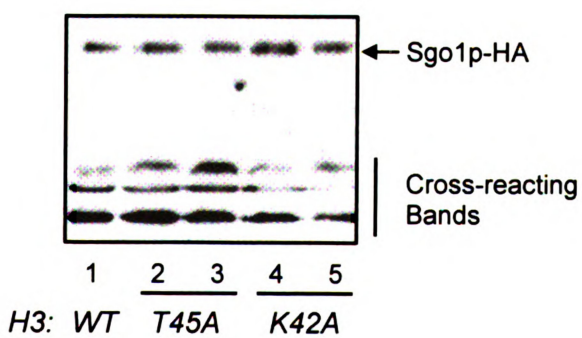
Sgo1p-HA
Cross-reacting Bands
1
2
3
4
5
H3: WT
T45A
K42A

Fig. 3-6

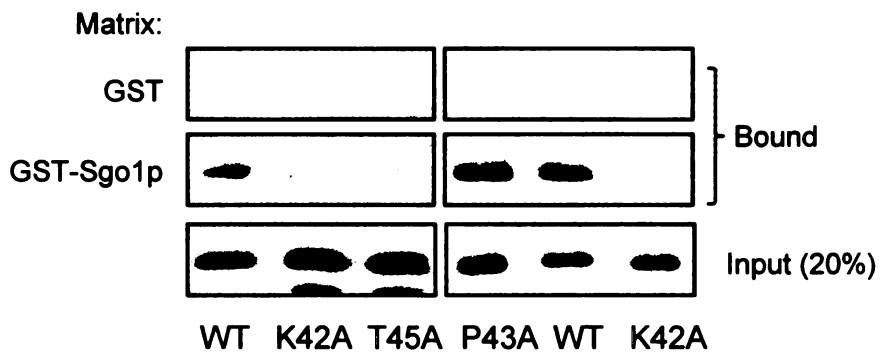

FIG. 3-6. The K42A and T45A mutation attenuates the affinity of H3 to Sgo1p *in vitro*. GST pull-down assays were conducted with bacterially expressed GST alone or GST-Sgo1p fusion proteins, as well as core histones purified from yeast cells expressing the wild-type, K42A, P43A, or T45A alleles of H3. Bound or input materials were resolved and blotted by anti-H3 antibodies.

FIG. 3-7. Over-expression of *SGO1* in wild-type cells expands the existing pericentric domain of Sgo1p. (A) Yeast cells transformed with either a high-copy 2μm plasmid (pJL51) or an *ARS CEN* low-copy plasmid (pJL53) expressing HA-Sgo1p were analyzed by anti-HA ChIP. The assay conditions were identical to those described in the legend to Fig. 5. except the common internal control (marked by the star on the right) for multiplex PCRs is from within the open reading frame of the *DED*1 gene 386.2 kb to the right of *CEN15*. The *CEN* or pericentric PCR fragments were marked by the arrow on the right. (B) Quantification of the ChIP results was done as detailed in the legend to Fig. 5B. (C) Comparable expression of 2μm 3xHA-Sgo1p (pJL51) and *ARS CEN* 3xHA-Sgo1p (pJL53). H3 wide-type cells bearing the indicated recombinant *SGO1* constructs were examined by anti-HA Western blotting. Equal loading was evidenced by Coomassie blue R250 staining (not shown) and by proteins that cross-reacted with the anti-HA antibodies.

Fig. 3-7

A

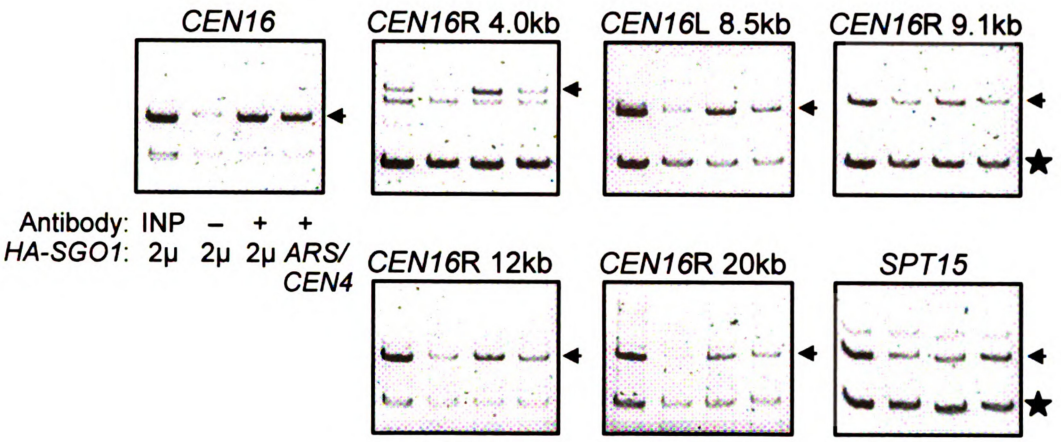
CEN16
CEN16R 4.0kb
CEN16L 8.5kb
CEN16R 9.1kb
Antibody: INP – + +
HA-SGO1: 2μ 2μ 2μ ARS/CEN4
CEN16R 12kb
CEN16R 20kb
SPT15

B

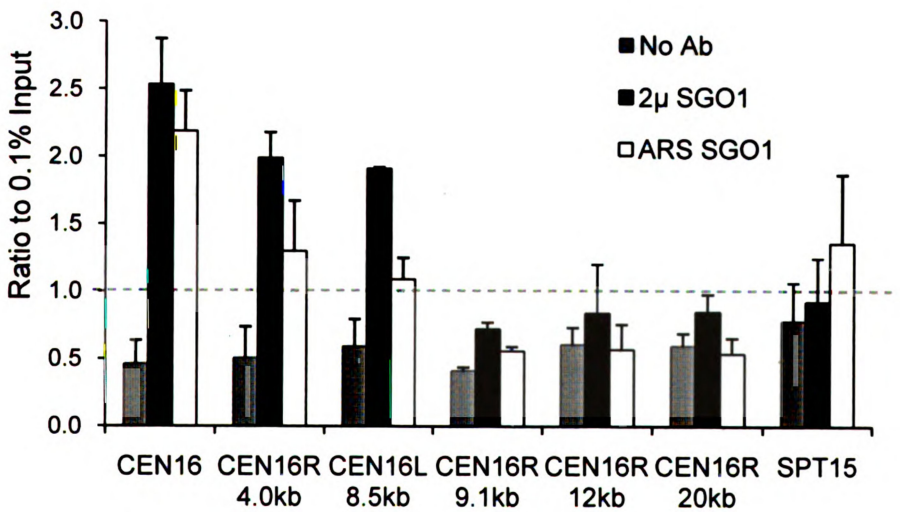
Ratio to 0.1% Input
3.0
2.5
2.0
1.5
1.0
0.5
0.0
No Ab
2μ SGO1
ARS SGO1
CEN16
CEN16R 4.0kb
CEN16L 8.5kb
CEN16R 9.1kb
CEN16R 12kb
CEN16R 20kb
SPT15

C

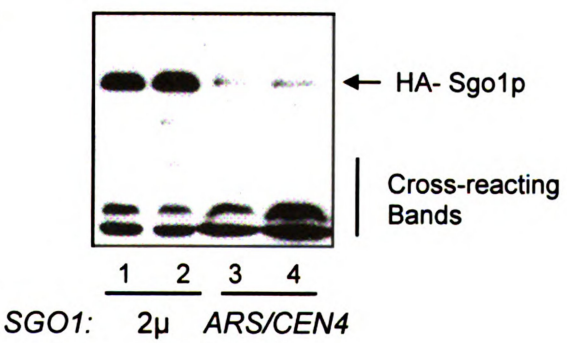
HA- Sgo1p
Cross-reacting Bands
1 2 3 4
SGO1: 2μ ARS/CEN4

FIG. 3-8. The HAT activity of Gcn5p is a negative regulator of the tension sensing function of H3. (A) *GCN5* was deleted in the indicated H3 strains, which were then tested for benomyl tolerance. Note that the T45A is refractory to the *gcn5*Δ suppression. (B) Wild-type and two catalytically inactive alleles of *GCN5*, *gcn5*F221A and *gcn5*E173H, were over-expressed in the indicated (H3 wild-type or mutants, shown at the top of images) strains, and the cellular resistance to benomyl and hydroxyurea (HU) were examined.

Fig. 3-8

A

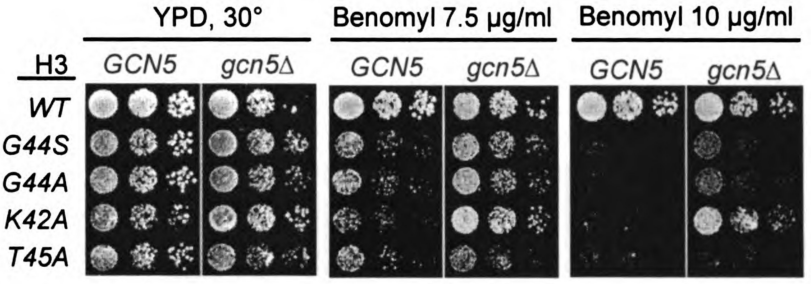
YPD, 30°
Benomyl 7.5 µg/ml
Benomyl 10 µg/ml
H3
GCN5
gcn5Δ
GCN5
gcn5Δ
GCN5
gcn5Δ
WT
G44S
G44A
K42A
T45A

B

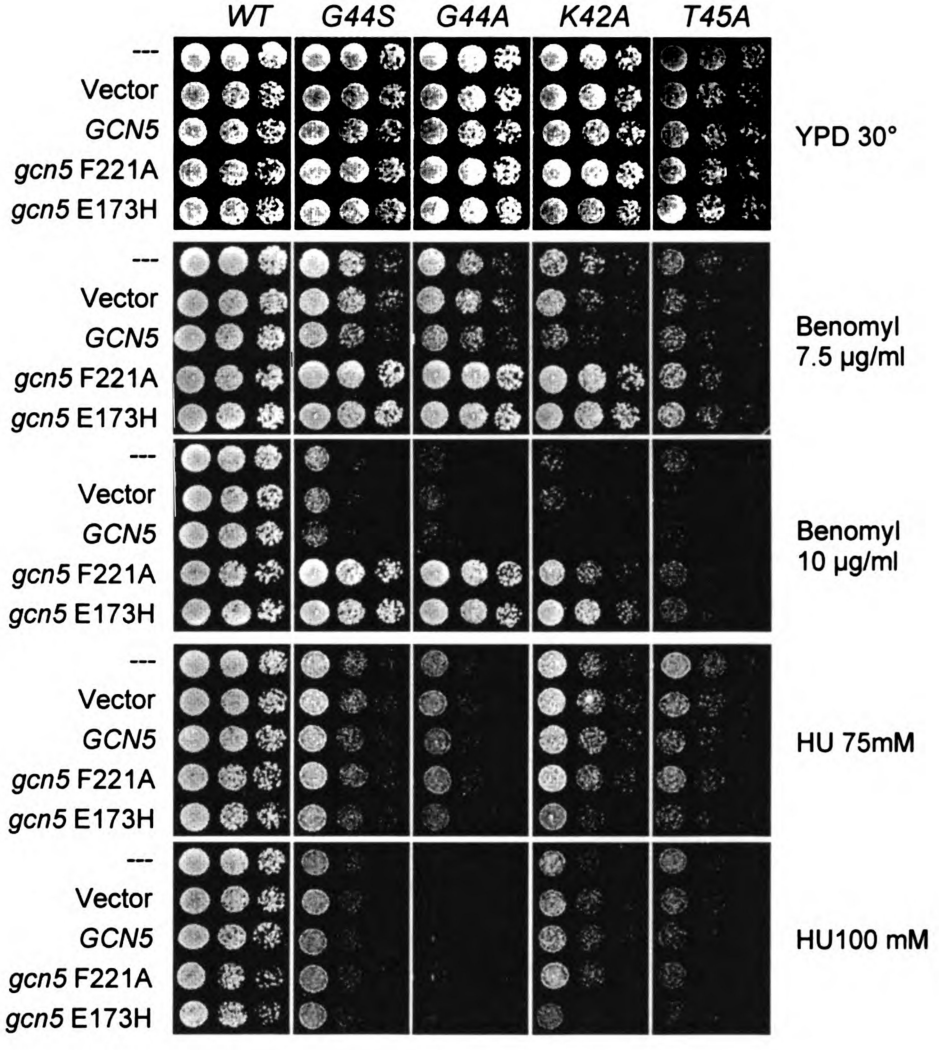
WT
G44S
G44A
K42A
T45A

Vector
GCN5
gcn5 F221A
gcn5 E173H
YPD 30°
Benomyl 7.5 µg/ml
Benomyl 10 µg/ml
HU 75mM
HU100 mM

Fig. 3-9

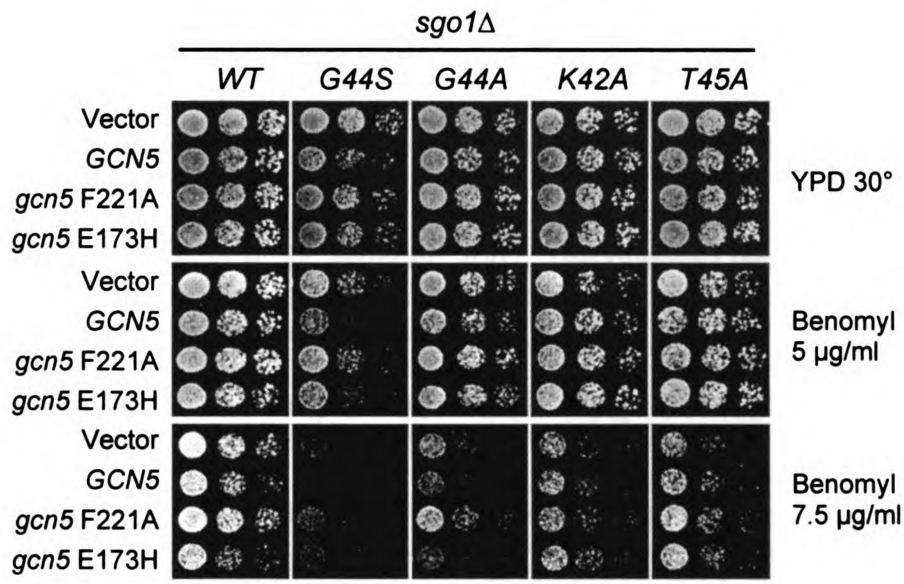

FIG. 3-9. The negative regulation of Gcn5p on H3 tension sensing function depends on functional *SGO1*. *SGO1* was deleted in the indicated strains, which were H3 wild-type or mutants (shown at the top of images) with the over-expression of wild-type or two catalytically inactive alleles of *GCN5*, *gcn5*F221A and *gcn5*E173H, the cellular resistance to benomyl was compared.

REFERENCES

1. **Baker, S. P., J. Phillips, S. Anderson, Q. Qiu, J. Shabanowitz, M. M. Smith, J. R. Yates, 3rd, D. F. Hunt, and P. A. Grant.** 2010. Histone H3 Thr 45 phosphorylation is a replication-associated post-translational modification in S. cerevisiae. Nat Cell Biol **12:**294-8.

2. **Bernard, P., J. F. Maure, J. F. Partridge, S. Genier, J. P. Javerzat, and R. C. Allshire.** 2001. Requirement of heterochromatin for cohesion at centromeres. Science **294:**2539-42.

3. **Biggins, S., and A. W. Murray.** 2001. The budding yeast protein kinase Ipl1/Aurora allows the absence of tension to activate the spindle checkpoint. Genes Dev **15:**3118-29.

4. **Bloom, K., S. Sharma, and N. V. Dokholyan.** 2006. The path of DNA in the kinetochore. Curr Biol **16:**R276-8.

5. **Dai, J., E. M. Hyland, D. S. Yuan, H. Huang, J. S. Bader, and J. D. Boeke.** 2008. Probing nucleosome function: a highly versatile library of synthetic histone H3 and H4 mutants. Cell **134:**1066-78.

6. **Downs, J. A.** 2008. Histone H3 K56 acetylation, chromatin assembly, and the DNA damage checkpoint. DNA Repair (Amst) **7:**2020-4.

7. **Edmondson, D. G., M. M. Smith, and S. Y. Roth.** 1996. Repression domain of the yeast global repressor Tup1 interacts directly with histones H3 and H4. Genes Dev **10:**1247-59.

8. **Fernius, J., and K. G. Hardwick.** 2007. Bub1 kinase targets Sgo1 to ensure efficient chromosome biorientation in budding yeast mitosis. PLoS Genet **3:**2312-2325.

9. **Fernius, J., and K. G. Hardwick.** 2007. Bub1 kinase targets Sgo1 to ensure efficient chromosome biorientation in budding yeast mitosis. PLoS Genet **3:**e213.

10. **Gietz, D., A. St Jean, R. A. Woods, and R. H. Schiestl.** 1992. Improved method for high efficiency transformation of intact yeast cells. Nucleic Acids Res **20:**1425.

11. **Goshima, G., and M. Yanagida.** 2000. Establishing biorientation occurs with precocious separation of the sister kinetochores, but not the arms, in the early spindle of budding yeast. Cell **100:**619-33.

12. **Govind, C. K., F. Zhang, H. Qiu, K. Hofmeyer, and A. G. Hinnebusch.** 2007. Gcn5 promotes acetylation, eviction, and methylation of nucleosomes in transcribed coding regions. Mol Cell **25:**31-42.

13. **Howe, L., D. Auston, P. Grant, S. John, R. G. Cook, J. L. Workman, and L. Pillus.** 2001. Histone H3 specific acetyltransferases are essential for cell cycle progression. Genes Dev **15:**3144-54.

14. **Hurd, P. J., A. J. Bannister, K. Halls, M. A. Dawson, M. Vermeulen, J. V. Olsen, H. Ismail, J. Somers, M. Mann, T. Owen-Hughes, I. Gout, and T. Kouzarides.** 2009. Phosphorylation of histone H3 Thr-45 is linked to apoptosis. J Biol Chem **284:**16575-83.

15. **Indjeian, V. B., B. M. Stern, and A. W. Murray.** 2005. The centromeric protein Sgo1 is required to sense lack of tension on mitotic chromosomes. Science **307:**130-3.

16. **Kawashima, S. A., Y. Yamagishi, T. Honda, K. I. Ishiguro, and Y. Watanabe.** 2009. Phosphorylation of H2A by Bub1 Prevents Chromosomal Instability Through Localizing Shugoshin. Science.

17. **Kiburz, B. M., D. B. Reynolds, P. C. Megee, A. L. Marston, B. H. Lee, T. I. Lee, S. S. Levine, R. A. Young, and A. Amon.** 2005. The core centromere and Sgo1 establish a 50-kb cohesin-protected domain around centromeres during meiosis I. Genes Dev **19:**3017-30.

18. **Kitajima, T. S., T. Sakuno, K. Ishiguro, S. Iemura, T. Natsume, S. A. Kawashima, and Y. Watanabe.** 2006. Shugoshin collaborates with protein phosphatase 2A to protect cohesin. Nature **441:**46-52.

19. **Kuo, M. H., and C. D. Allis.** 1999. In vivo cross-linking and immunoprecipitation for studying dynamic Protein:DNA associations in a chromatin environment. Methods **19:**425-33.

20. **Kuo, M. H., J. Zhou, P. Jambeck, M. E. Churchill, and C. D. Allis.** 1998. Histone acetyltransferase activity of yeast Gcn5p is required for the activation of target genes in vivo. Genes Dev **12:**627-39.

21. **Latham, J. A., and S. Y. Dent.** 2007. Cross-regulation of histone modifications. Nat Struct Mol Biol **14:**1017-1024.

22. **Liu, Y., X. Xu, S. Singh-Rodriguez, Y. Zhao, and M. H. Kuo.** 2005. Histone H3 Ser10 phosphorylation-independent function of Snf1 and Reg1 proteins rescues a gcn5- mutant in HIS3 expression. Mol Cell Biol **25:**10566-79.

23. **Luo, J., X. Xu, H. Hall, E. M. Hyland, J. D. Boeke, T. Hazbun, and M. H. Kuo.** 2009. Histone H3 Exerts Key Function in Mitotic Checkpoint Control. Mol Cell Biol **30**:537-549.

24. **Megee, P. C., B. A. Morgan, and M. M. Smith.** 1995. Histone H4 and the maintenance of genome integrity. Genes Dev **9**:1716-27.

25. **Morgan, B. A., B. A. Mittman, and M. M. Smith.** 1991. The highly conserved N-terminal domains of histones H3 and H4 are required for normal cell cycle progression. Mol Cell Biol **11**:4111-20.

26. **Morris, S. A., B. Rao, B. A. Garcia, S. B. Hake, R. L. Diaz, J. Shabanowitz, D. F. Hunt, C. D. Allis, J. D. Lieb, and B. D. Strahl.** 2007. Identification of histone H3 lysine 36 acetylation as a highly conserved histone modification. J Biol Chem **282**:7632-40.

27. **Mukherjee, S., Y. H. Hao, and K. Orth.** 2007. A newly discovered post-translational modification--the acetylation of serine and threonine residues. Trends Biochem Sci **32**:210-6.

28. **Pinsky, B. A., and S. Biggins.** 2005. The spindle checkpoint: tension versus attachment. Trends Cell Biol **15**:486-93.

29. **Riedel, C. G., V. L. Katis, Y. Katou, S. Mori, T. Itoh, W. Helmhart, M. Galova, M. Petronczki, J. Gregan, B. Cetin, I. Mudrak, E. Ogris, K. Mechtler, L. Pelletier, F. Buchholz, K. Shirahige, and K. Nasmyth.** 2006. Protein phosphatase 2A protects centromeric sister chromatid cohesion during meiosis I. Nature **441**:53-61.

30. **Salic, A., J. C. Waters, and T. J. Mitchison.** 2004. Vertebrate shugoshin links sister centromere cohesion and kinetochore microtubule stability in mitosis. Cell **118**:567-78.

31. **Sherman, F.** 1991. Getting started with yeast. Methods Enzymol **194**:3-21.

32. **Vernarecci, S., P. Ornaghi, A. Bagu, E. Cundari, P. Ballario, and P. Filetici.** 2008. Gcn5p plays an important role in centromere kinetochore function in budding yeast. Mol Cell Biol **28**:988-96.

33. **Yamagishi, Y., T. Sakuno, M. Shimura, and Y. Watanabe.** 2008. Heterochromatin links to centromeric protection by recruiting shugoshin. Nature **455**:251-5.

34. **Yin, S., J. S. Ai, L. H. Shi, L. Wei, J. Yuan, Y. C. Ouyang, Y. Hou, D. Y. Chen, H. Schatten, and Q. Y. Sun.** 2008. Shugoshin1 may play important

roles in separation of homologous chromosomes and sister chromatids during mouse oocyte meiosis. PLoS ONE **3**:e3516.

35. **Zhang, W., J. R. Bone, D. G. Edmondson, B. M. Turner, and S. Y. Roth.** 1998. Essential and redundant functions of histone acetylation revealed by mutation of target lysines and loss of the Gcn5p acetyltransferase. Embo J **17**:3155-67.

APPENDICES

Appendix I: Linking H3 phosphorylation to a *Saccharomyces cerevisiae* 14-3-3 protein Bmh1p

INTRODUCTION

Phosphorylation of histone H3 at serine 10 (S10) has stimulated considerable interests since the first discovery that this modification is associated with chromosome condensation and segregation during mitosis and meiosis (3, 12, 26, 27). At interphase, H3 S10 phosphorylation is linked to transcriptional activation of a subset of inducible genes (22). Mitotic phosphorylation of H3 also has been found to occur at serine 28 (S28) (9). A newly discovered mitotic phosphorylation was mapped to serine 31 (S31) of the H3 variant H3.3 (13). Interestingly, *Saccharomyces cerevisiae* contains only one type of H3, which is most similar to mammalian H3.3 and also contains S31 (1). However, the phosphorylation of H3 at S28 and S31 in *S. cerevisiae* has not been addressed yet.

Mitosis-specific phosphorylation of H3 starts in late G_2 phase on pericentric chromatin. As mitosis proceeds, phosphorylation of H3 spreads along the chromosome arms and completes its coating the entire chromosome at prophase. The dephosphorylation process starts at anaphase and finishes at telophase (10, 14). Recently, members of the Aurora serine/threonine kinase family have been shown to be important for mitotic phosphorylation of H3 at S10 (15) and S28 (10).

In *S. cerevisiae*, the sole Aurora kinase encoded by the *IPL1* gene (4), is required for the high-fidelity chromosome segregation (6). Later on, studies indicated that Ipl1p is required to activate the spindle checkpoint in response to defects in the tension between two sister chromatids (21). How the phosphorylation of H3 contributes to the mitotic progression and the proteins that interact directly with the phosphorylated H3 remain elusive.

14-3-3 proteins are a family of highly conserved, ubiquitously expressed, and abundant acidic proteins in all eukaryotes studied (2). 14-3-3s were first recognized to interact with a discrete phosphoserine or phosphothreonine motif by forming homo- or heterodimers (28). While there are seven 14-3-3 isoforms in mammals, Bmh1p and Bmh2p are the only two 14-3-3 proteins in *S. cerevisiae*. Bmh1p (267aa, Mw: 30kDa) and Bmh2p (273aa, Mw: 31kDa) share 91% overall identity and >97% identity over their first 256 residues (7, 25). Simultaneous knockouts of these two functionally redundant isoforms in *S. cerevisiae* is lethal, while single knockout cells are viable (24). Bmh1p and Bmh2p are also required for a timely G_1/S transition, DNA damage checkpoint and genome stability (16, 17). Utilizing the Tethered catalysis/Yeast two-hybrid (TC/Y2H) system that we developed for the identification of protein-protein interaction induced by a post-translational modification (11), we found that Bmh1p interacts with phosphorylated H3 (Kuo, unpublished data). Recently, Macdonald and colleagues reported that three human 14-3-3 isoforms (ε, ζ, γ) bind H3 (aa 1-20) peptides in a phosphorylation-dependent fashion (19). In their studies, 14-3-3s

are found to be recruited to the nucleosomes at inducible genes upon transcriptional activation. However, how this association contributes to the function of H3 phosphorylation in mitotic progression is still elusive. We set out to examine whether yeast 14-3-3 protein Bmh1p is involved in this regulation through interaction with the phosphorylated H3. Investigation of their interactions and other functionally related factors will further our understanding of the roles of H3 phosphorylation in mitotic progression and chromosome segregation.

MATERIALS AND METHODS

Yeast strains and plasmid constructs. The yeast strains and plasmids used in this work are listed in Tables A-1 and A-2.

Mutations introduced in histone or *BMH1* were generated by two-step PCR site-directed mutagenesis (18). Yeast two hybrid screen plasmids were constructed by N. Y. Hung and D. W. Guo as mentioned in reference (11); Biotinylated Bmh1 plasmid (pJL31) was constructed by PCR amplification of the entire *BMH1* ORF region followed by subcloning that fragment into pAN6 plasmid at restrictions sites of *BamH* I and *Kpn* I in the C-terminus of Biotin Avitag peptide sequence (Avidity), the constructs were then transformed into AVB101 (Avidity) for biotinylated Bmh1p expression; His-Bmh1p plasmids (pJL33) was constructed by subcloning from pJL1 by *Kpn* I (blunted) and *BamH* I digestion into pET-28a plasmid (Novagen) on *Hind* III (blunted) and *BamH* I restriction sites and was

transformed into BL21 (DE3) (Sigma).

Yeast methods. Yeast growth media, conditions, and transformation were based on standard procedures (23). When appropriate, 5% casamino acids (CAA) were used to substitute for synthetic amino acid mixtures as selective medium for uracil, tryptophan, or adenine prototroph. Yeast transformation was done with the lithium acetate method (8).

Histone preparation. Histones were prepared from mid-log phase cultures in the presence of protease and phosphatase inhibitors as described (5). To obtain hypophosphorylated histones, the purified histones were treated at 30°C for 1h by λ phosphatase (NEB) in the presence or absence of high concentration sodium phosphate (150mM, pH 7.4), which inhibits the activity of λ phosphatase.

Protein pull down assay. Biotinylated Bmh1p and His-Bmh1p were purified from *E. coli*. Recombinant Bmh1p and purified yeast histones were incubated in binding buffer (10mM HEPES, pH7.5; 150mM NaCl; 3.4mM EDTA; 0.05% NP-40) at 4°C for 1hr, then Soft-link avidin resin (Promega) or Ni-NTA beads were added to trap tagged Bmh1p and associated histones at 4°C for an additional hour. Resins were washed with binding buffer for three times, and bound materials were eluted by 2 x sodium dodecyl sulfate (SDS) loading buffer and resolved by 15% SDS-polyacrylamide gel electrophoresis (PAGE). Western analyses were conducted as mentioned in reference (18).

RESULTS

Bmh1p specifically interacts with phosphorylated histone H3.

To understand whether phosphorylated H3 (phos.H3) performs its biological function by recruiting specific associating proteins, we used the TC/Y2H approach (11) to screen for yeast proteins that interact specifically with phos.H3. Figure 1 shows that when H3 (aa 1-59) was fused to a wildtype *IPL1* within the context of the yeast two hybrid system, H3 S10 was constitutively phosphorylated. An H3 fusion with Ipl1p kinase inactive mutant was hypophosphorylated at S10. Due to the lack of appropriate antibody, we do not yet know whether H3 S28 can be phosphorylated by the tethered Ipl1p. Using the phos.H3-Ipl1p bait, we collaborated with S. Fields and T. Hazbun (HHMI, University of Washington, Seattle) to screen for yeast proteins that specifically interact with phos.H3. Figure 2A shows that yeast 14-3-3 protein Bmh1p was identified as a potential phos.H3 interacting protein, and that mutations at either S10 and/or S28 diminished significantly the interactions between phos.H3 and Bmh1p.

To characterize the physical interaction between Bmh1p and phos.H3 biochemically, pulldown assays using purified histones were performed. Yeast histones were prepared and further treated with λ phosphatase. Western analyses confirmed that λ phosphatase effectively dephosphorylated H3 (at least at S10), whereas 150mM sodium phosphate (pH 7.4) inhibited the λ phosphatase

activity and partially maintained the phosphorylation status of H3 (Fig. 2B). Phosphorylated and hypophosphorylated histones were then incubated with recombinant biotinylated Bmh1p expressed and purified in E. coli. Soft-link avidin resin was then used to purify the biotinylated Bmh1p and the associated proteins. Western analyses with anti-H3 antibody demonstrated that Bmh1p interacts preferentially with phos.H3 (Fig. 2C). Taken together, these data support the hypothesis that phosphorylation of H3 stimulates the Bmh1p binding to H3.

Residues important for Bmh1p-phos.H3 interaction.

To further investigate the molecular mechanism underlying Bmh1p-phos.H3 interaction, we constructed single, double, and triple alanine substitutions at S10, S28, and S31 of H3 and examined the specific involvement of these potential H3 phosphorylation sites. The Bmh1p binding capacity was compared by incubating comparable amounts of H3 wildtype or mutant histones with purified Hexahistidine tagged Bmh1p. Proteins were recovered by Ni-NTA beads and eluates were subjected to SDS-PAGE and western analyses (Fig. 3A). Compared with the wildtype, H3 S28A and S10A/S28A both failed to interact with Bmh1p, whereas S10A and S10A/S28A/S31A showed much diminished association with Bmh1p. These results suggested that S28 phosphorylation is a major determinant for Bmh1p association. Interestingly, S10A/S31A, S28A/S31A, and S10A/S28A/S31A all bound Bmh1p better than their counterparts with wildtype S31. This surprising result suggests that the S31A mutation may suppress the defect induced by S10A and S28A.

Structural studies on phosphoserine binding pocket of the human 14-3-3ζ isoform indicated that residues Lys49, Arg56, Arg60, Arg127, and Tyr128 are critical for 14-3-3s binding to the phosphate moiety (20, 28). Sequence alignment showed that these residues are completely conserved and are equivalent to Lys51, Arg58, Arg62, Arg132, and Tyr133 of Bmh1p (2). Comparable binding assays were performed to examine the binding affinity among His-Bmh1p wildtype and R58A/R62A, R132A/Y133A, R58A/R62A/R132A/Y133A mutants (Lys51 not included here). Figure 3B shows that R132A/Y133A completely and R58A/R62A/R132A/Y133A nearly completely caused the loss of their affinity for phos.H3, whereas the R58A/R62A mutation had no effect on Bmh1p binding to phos.H3. These results further supported the notion that Bmh1p-H3 association is stimulated by phosphorylation.

Functional studies of the mitotic phosphorylation on H3.

To understand how H3 S10 and S28 may contribute to the mitotic progression, I examined cellular growth in benomyl-containing media after mutations had been introduced into the sole copy of H3. Benomyl depolymerizes microtubules and triggers the spindle assembly checkpoint (SAC) which halts the cell cycle at G_2/M. Sensitivity to benomyl can be used to evaluate the spindle or kinetochore function. Mutants defective for spindle or kinetochore function frequently show benomyl hypersensitivity. Figure 4 shows that all H3 mutants (S10A, S28A, S10A/S28A, and S10A/S28A/S31A) behave similarly to wildtype. The lack of benomyl hypersensitivity of H3 S10A is consistent with the findings of others (15),

suggesting that phosphorylation at other sites or other histones substitutes for the important role of histone phosphorylation during mitosis in yeast.

DISCUSSION

TC/Y2H results revealed that Bmh1p is a likely phos.H3 binding protein. Such observation was biochemically verified in this study as recombinant Bmh1p rather weakly binds purified hypophosphorylated H3 (Fig. 2C). Slot blot assays using synthetic H3 (aa 1-20) peptides also substantiated that Bmh1p preferentially binds phos.H3 (data not shown). Given the 91% overall sequence identity between Bmh1p and Bmh2p, Bmh2p might perform similar functions as Bmh1p.

It is widely accepted that phosphorylation of H3 at S10 (S10-P) is critical for mitotic chromosome segregation in *Tetrahymena* (27), however, in *S. cerevisiae*, H3 S10A by itself imposes no discernible mitotic phenotype (Fig. 4) (15), suggesting that phosphorylation at other sites of H3 can compensate for the loss of S10-P, or that other histones may substitute for this important role during mitosis in yeast. The binding assays shown in Figure 3 indicated that H3 S28 phosphorylation is more important for Bmh1p association. The observation that binding between Bmh1p and H3 S10A and/or S28A mutants was partially restored when alanine was introduced at S31 (Fig. 3A) imposes another layer of

complexity to their interactions. One possibility is that S31A induces compensatory phosphorylation at other sites.

The observation that Bmh1 R132A/Y133A and R58A/R62A/R132A/Y133A mutants lost their affinity for phos.H3 is consistent with structural analyses from human 14-3-3ζ isoform (20, 28). The Bmh1 R58A/R62A mutant shows no defects in Bmh1p-phos.H3 interaction. However, it must be noted that Lys51 of Bmh1 might be critical and its mutation to alanine should be considered.

However, mutations in phosphorylation sites of H3 (S10, 28, 31) and H2B (S10) confer no defective phenotype tested thus far (Fig. 4), suggesting that phosphorylation at other sites of H3 (or H2B) or that other histones may substitute for this important role of H3 phosphorylation during mitosis in yeast.

To summarize, Bmh1p was identified as a phosphorylated H3 binding protein. *In vitro* binding assays demonstrated that S10, S28 of H3 and R132, Y133 of Bmh1 are critical for the Bmh1p-phos.H3 interaction.

TABLE A-1. Yeast strains used in this study

Strain	Relevant genotype	Source or reference
yJL111	*MATa ade2-1 can1–100 his3–11,15 leu2–3,112 trp1–1 ura3-1 hht1-hhf1::KAN hht2-hhf2::KAN hta1-htb1::Nat hta2-htb2::HPH* pMK439 H3S10/31A [*ARS CEN LEU2 HTA1-HTB1 hht2-S10A/S31A-HHF2*]	This study
yJL153	*MATa ade2-1 can1–100 his3–11,15 leu2–3,112 trp1–1 ura3-1 hht1-hhf1::KAN hht2-hhf2::KAN hta1-htb1::Nat hta2-htb2::HPH* pMK439 H3S28A [*ARS CEN LEU2 HTA1-HTB1 hht2-S28A-HHF2*]	This study
yJL166	*MATa ade2-1 can1–100 his3–11,15 leu2–3,112 trp1–1 ura3-1 hht1-hhf1::KAN hht2-hhf2::KAN hta1-htb1::Nat hta2-htb2::HPH* pMK439 H3S10/28A [*ARS CEN LEU2 HTA1-HTB1 hht2-S10A/S28A-HHF2*]	This study
yMK1243	*MATa ade2-1 can1–100 his3–11,15 leu2–3,112 trp1–1 ura3-1 hht1-hhf1::KAN hht2-hhf2::KAN hta1-htb1::Nat hta2-htb2::HPH* pMK439 [*ARS CEN LEU2 HTA1-HTB1 HHT2-HHF2*]	This study
yMK1244	*MATa ade2-1 can1–100 his3–11,15 leu2–3,112 trp1–1 ura3-1 hht1-hhf1::KAN hht2-hhf2::KAN hta1-htb1::Nat hta2-htb2::HPH* pMK439 H3S10A [*ARS CEN LEU2 HTA1-HTB1 hht2-S10A-HHF2*]	This study
yMK1246	*MATa ade2-1 can1–100 his3–11,15 leu2–3,112 trp1–1 ura3-1 hht1-hhf1::KAN hht2-hhf2::KAN hta1-htb1::Nat hta2-htb2::HPH* pMK439 H3S31A [*ARS CEN LEU2 HTA1-HTB1 hht2-S31A-HHF2*]	This study
yMK1249	*MATa ade2-1 can1–100 his3–11,15 leu2–3,112 trp1–1 ura3-1 hht1-hhf1::KAN hht2-hhf2::KAN hta1-htb1::Nat hta2-htb2::HPH* pMK439 H3S28/31A [*ARS CEN LEU2 HTA1-HTB1 hht2-S28A/S31A-HHF2*]	This study
yMK1250	*MATa ade2-1 can1–100 his3–11,15 leu2–3,112 trp1–1 ura3-1 hht1-hhf1::KAN hht2-hhf2::KAN hta1-htb1::Nat hta2-htb2::HPH* pMK439 H3S10/28/31A [*ARS CEN LEU2 HTA1-HTB1 hht2-S10A/S28A/S31A-HHF2*]	This study

TABLE A-2. Plasmid constructs used in this study

Plasmid	Main features	Source or reference
pAN6	Plasmid expresses N-terminal AviTag-protein fusions	Avidity
pJL31	pAN6-*BMH1*	This study
pJL32	pAN6-*BMH2*	This study
pJL33	pET28a-*BMH1*	This study
pJL34	pET28a-*BMH2*	This study

Fig. A-1

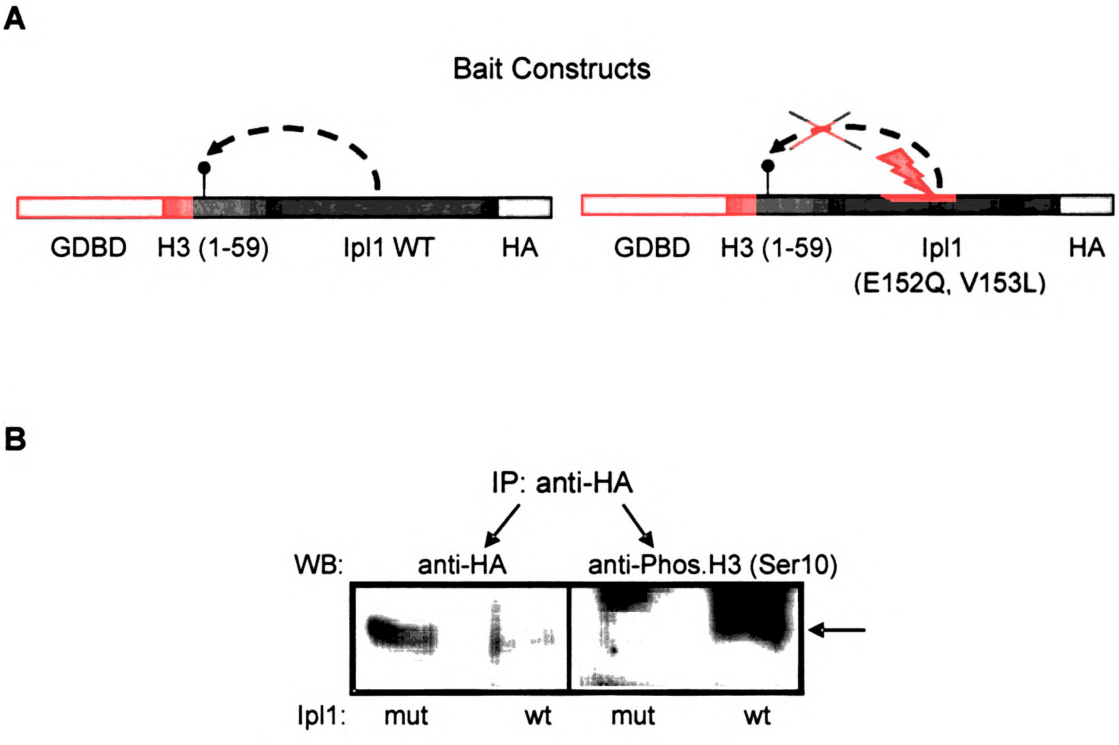

FIG. A-1. Tethered catalysis approach to phosphorylate N-terminal tail of histone H3. (A) Schematic drawing of the tethered catalysis histone H3 baits. GDBD: Gal4 DNA-binding domain; wt: wildtype. A trimeric hemagglutinin (HA) epitope tag was fused at the C-terminus of the chimeras. Point mutation of Ipl1 at E152 and V153 results in a catalytically inactive form of Ipl1 and is used as a control in the screen. (B) Auto-phosphorylation of the H3 N-terminal domain shown by western analyses. Yeast whole cell extracts from strains expressing wt and mut (mutant) Ipl1 fusion were used in western analyses using anti-HA and anti-phosphorylated H3 antibodies. Unpublished data of D. W. Guo and M. H. Kuo.

FIG. A-2. Bmh1p specifically interacts with phosphorylated histone H3. (A) TC/Y2H analyses indicated that Bmh1p preferentially interacts with phosphorylated H3. Bait constructs that contain H3-Ipl1 fusion or with mutations introduced at H3 serine 10, serine 28 or the Ipl1 catalytic domain were used for two-hybrid test. Prey construct contains Bmh1 fused to an activation domain. S10G and/or S28A depleted the potential phosphorylation site(s) of H3. Yeast cells transformed with the indicated bait and prey constructs were grew to log phase and streaked into SC-Ade plate to detect the gene expression of *ADE2* reporter. Unpublished data of X.J.Xu and M.H.Kuo. (B, C) Association of Bmh1p with phosphorylated histone H3. (B) Purified wildtype histone was treated by λ phosphatase in the presence or absence of 150mM sodium phosphate (pH 7.4). Histones were separated in parallel lanes and analyzed by western blot using anti-H3 or anti-phosphorylated H3 (serine 10 specific) antibody. (C) Western analyses of the *in vitro* pull down assays. The similar amount of biotinylated Bmh1p was incubated with untreated wildtype histone, histones treated by λ phosphatase in the absence or presence of sodium phosphate (150mM, pH 7.4) separately. Top: streptavidin-HRP western analyses showing evenly immobilized Bmh1p in the assay; middle: histones bound by immobilized Bmh1p were detected by anti-H3 antibody; bottom: 10% of input histones were separated in parallel lanes and probed by anti-H3 antibody.

Fig. A-2

A

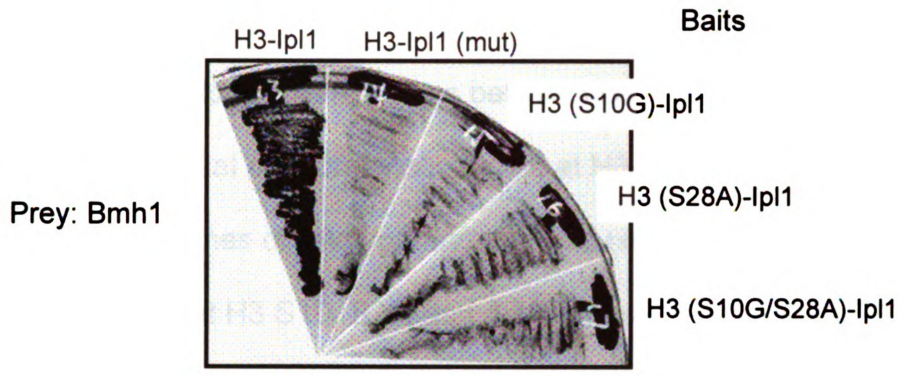
Baits
H3-Ipl1
H3-Ipl1 (mut)
H3 (S10G)-Ipl1
H3 (S28A)-Ipl1
H3 (S10G/S28A)-Ipl1
Prey: Bmh1

B

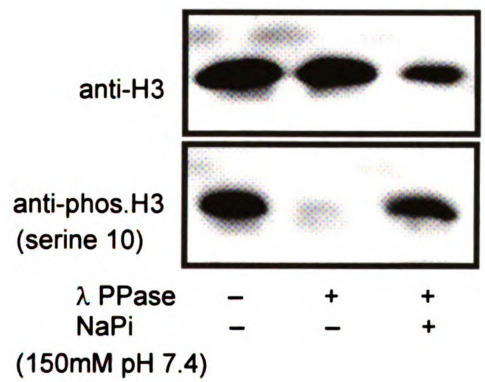
anti-H3
anti-phos.H3
(serine 10)
λ PPase – + +
NaPi – – +
(150mM pH 7.4)

C

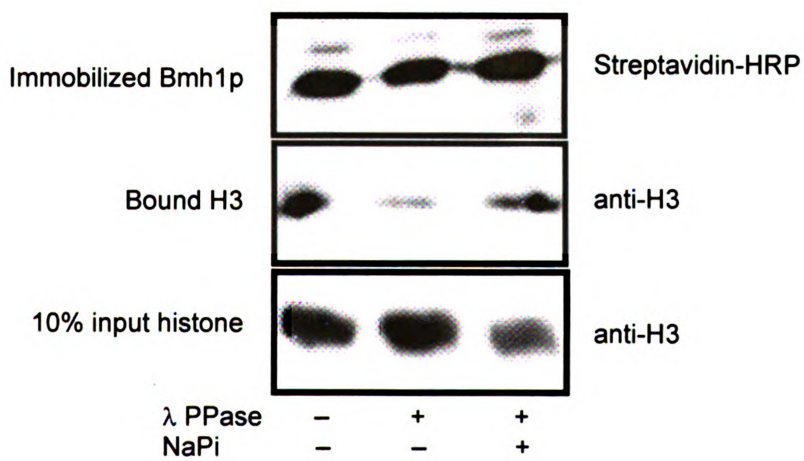
Immobilized Bmh1p
Streptavidin-HRP
Bound H3
anti-H3
10% input histone
anti-H3
λ PPase – + +
NaPi – – +

FIG. A-3. Residues important for the interactions between Bmh1p and phosphorylated H3. (A) Potential phosphorylation sites at H3 critical for association with Bmh1p. Histones of wildtype and mutants (single or multiple serine to alanine substitution at H3 S10, S28, and S31) were prepared from yeast mid-log phase cells in the presence of phosphatase inhibitors and incubated with purified recombinant N-terminal His tagged Bmh1p and were pulldown with Ni-NTA beads, the bound materials were eluted and subjected to SDS-PAGE and western analyses. Top: Ponceau S staining of immobilized Bmh1p; bound histones (middle) and 30% of the histone input (bottom, separated in parallel lanes) were probed by anti-H3 antibody. S represents Serine, A represents Alanine. (B) Residues in Bmh1p essential for its binding to phosphorylated H3. The same amount of phosphorylated histone was used for each binding assay. Top: Ponceau S staining of immobilized wildtype or mutant His-Bmh1p; bottom: bound histones were probed by anti-H3 antibody. Lane 1: Bmh1 wildtype; Lane 2: Bmh1 R58A/R62A mutant; lane 3: Bmh1 R132A/Y133A mutant; lane 4: Bmh1 R58A/R62A/R132A/Y133A quadruple mutant.

Fig. A-3

A

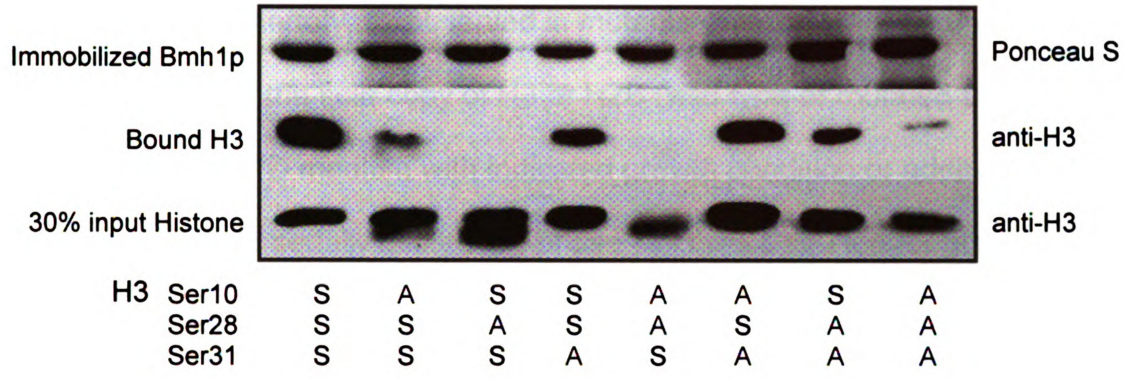
Immobilized Bmh1p
Bound H3
30% input Histone
Ponceau S
anti-H3
anti-H3
H3
Ser10 S A S S A A S A
Ser28 S S A S A S A A
Ser31 S S S A S A A A

B

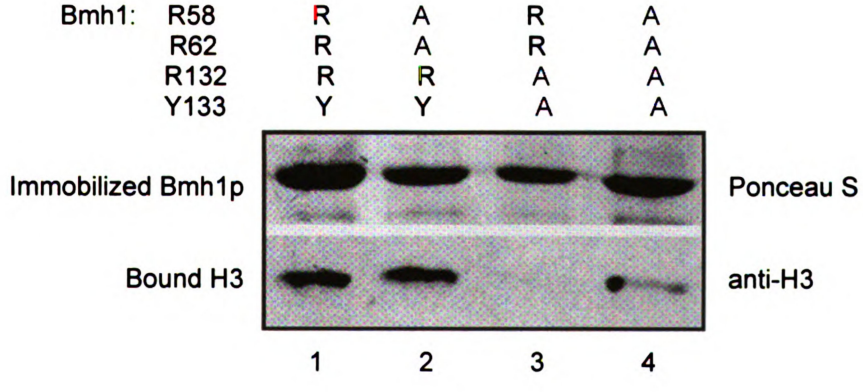
Bmh1:
R58 R A R A
R62 R A R A
R132 R R A A
Y133 Y Y A A
Immobilized Bmh1p
Bound H3
Ponceau S
anti-H3
1 2 3 4

FIG. A-4. No defective phenotypes observed in mutants of histone H3 and/or H2B. Yeast cells bearing the sole copy of H3 or H2B (wild type or mutated as noted) were tested on YPD medium with indicated growth condition or additional chemical reagent. Sixfold serially diluted log-phase cells were spotted for growth for two days at 30°, 37° or seven days at 14°. (A) Alanine substitutions at H3 serine 10 and/or serine 28 cause no additional growth defects in response to stress of high temperature (37°), low temperature (14°), or benomyl. Cells tested on top panel are derived from yDA81 (S288C) genetic background, whereas bottom panel are derived from yMK1141 (W303) background. (B) Additional test similar as panel A to compare wildtype and triple mutant, H3 S10A/S28A/S31A. (C) Combined mutations of H3 and H2B cause no defective phenotypes. Genetic features of strains used are listed below the image, as a control, a known mitotic defective H3 mutant, G44S, was included. WT: wildtype.

Fig. A-4

A

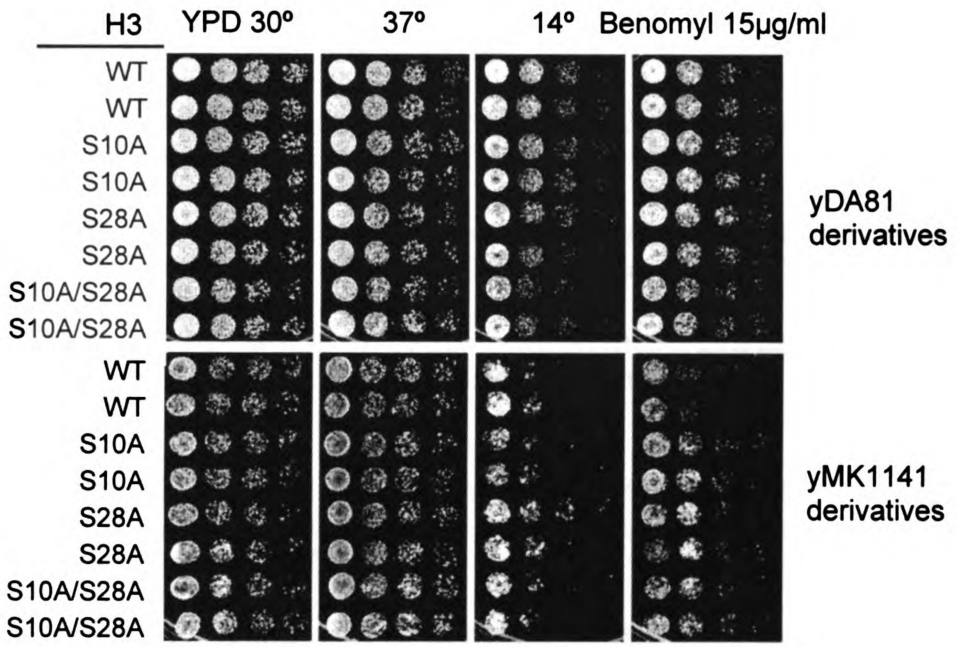
H3
YPD 30°
37°
14°
Benomyl 15µg/ml
WT
WT
S10A
S10A
S28A
S28A
S10A/S28A
S10A/S28A
WT
WT
S10A
S10A
S28A
S28A
S10A/S28A
S10A/S28A
yDA81 derivatives
yMK1141 derivatives

B

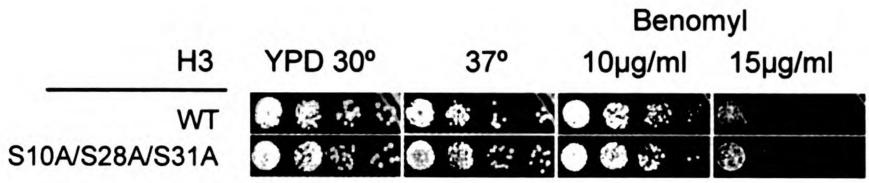
H3
YPD 30°
37°
Benomyl
10µg/ml
15µg/ml
WT
S10A/S28A/S31A

C

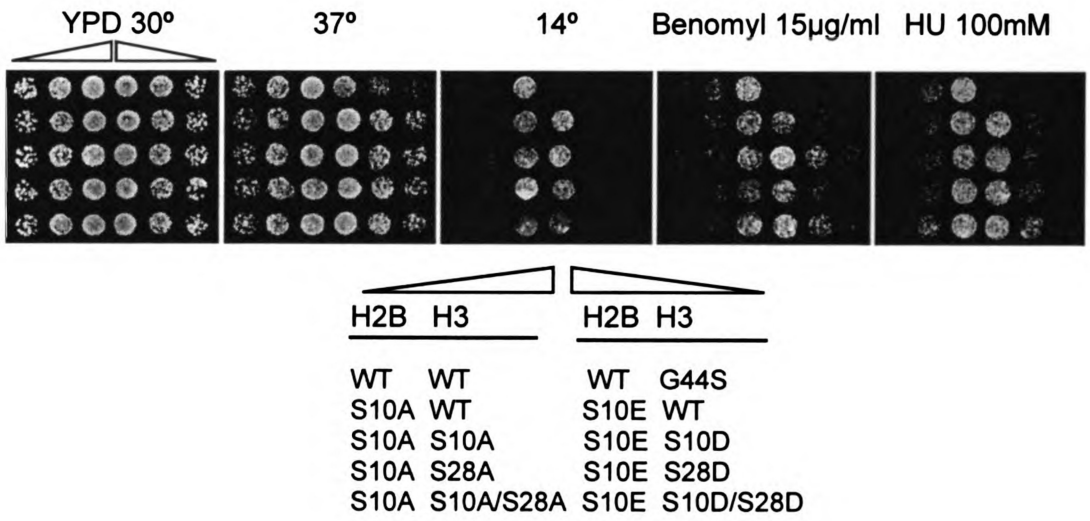
YPD 30°
37°
14°
Benomyl 15µg/ml
HU 100mM
H2B H3
H2B H3
WT WT
S10A WT
S10A S10A
S10A S28A
S10A S10A/S28A
WT G44S
S10E WT
S10E S10D
S10E S28D
S10E S10D/S28D

REFERENCES

1. **Brandt, W. F., and C. von Holt.** 1982. The primary structure of yeast histone H3. Eur J Biochem **121:**501-10.

2. **Bridges, D., and G. B. Moorhead.** 2005. 14-3-3 proteins: a number of functions for a numbered protein. Sci STKE **2005:**re10.

3. **Cerutti, H., and J. A. Casas-Mollano.** 2009. Histone H3 phosphorylation: universal code or lineage specific dialects? Epigenetics **4:**71-5.

4. **Chan, C. S., and D. Botstein.** 1993. Isolation and characterization of chromosome-gain and increase-in-ploidy mutants in yeast. Genetics **135:**677-91.

5. **Edmondson, D. G., M. M. Smith, and S. Y. Roth.** 1996. Repression domain of the yeast global repressor Tup1 interacts directly with histones H3 and H4. Genes Dev **10:**1247-59.

6. **Francisco, L., W. Wang, and C. S. Chan.** 1994. Type 1 protein phosphatase acts in opposition to IpL1 protein kinase in regulating yeast chromosome segregation. Mol Cell Biol **14:**4731-40.

7. **Gelperin, D., J. Weigle, K. Nelson, P. Roseboom, K. Irie, K. Matsumoto, and S. Lemmon.** 1995. 14-3-3 proteins: potential roles in vesicular transport and Ras signaling in Saccharomyces cerevisiae. Proc Natl Acad Sci U S A **92:**11539-43.

8. **Gietz, D., A. St Jean, R. A. Woods, and R. H. Schiestl.** 1992. Improved method for high efficiency transformation of intact yeast cells. Nucleic Acids Res **20:**1425.

9. **Goto, H., Y. Tomono, K. Ajiro, H. Kosako, M. Fujita, M. Sakurai, K. Okawa, A. Iwamatsu, T. Okigaki, T. Takahashi, and M. Inagaki.** 1999. Identification of a novel phosphorylation site on histone H3 coupled with mitotic chromosome condensation. J Biol Chem **274:**25543-9.

10. **Goto, H., Y. Yasui, E. A. Nigg, and M. Inagaki.** 2002. Aurora-B phosphorylates Histone H3 at serine28 with regard to the mitotic chromosome condensation. Genes Cells **7:**11-7.

11. **Guo, D., T. R. Hazbun, X. J. Xu, S. L. Ng, S. Fields, and M. H. Kuo.** 2004. A tethered catalysis, two-hybrid system to identify protein-protein interactions requiring post-translational modifications. Nat Biotechnol **22:**888-92.

12. **Gurley, L. R., J. A. D'Anna, S. S. Barham, L. L. Deaven, and R. A. Tobey.** 1978. Histone phosphorylation and chromatin structure during mitosis in Chinese hamster cells. Eur J Biochem **84:**1-15.

13. **Hake, S. B., B. A. Garcia, M. Kauer, S. P. Baker, J. Shabanowitz, D. F. Hunt, and C. D. Allis.** 2005. Serine 31 phosphorylation of histone variant H3.3 is specific to regions bordering centromeres in metaphase chromosomes. Proc Natl Acad Sci U S A **102:**6344-9.

14. **Hendzel, M. J., Y. Wei, M. A. Mancini, A. Van Hooser, T. Ranalli, B. R. Brinkley, D. P. Bazett-Jones, and C. D. Allis.** 1997. Mitosis-specific phosphorylation of histone H3 initiates primarily within pericentromeric heterochromatin during G2 and spreads in an ordered fashion coincident with mitotic chromosome condensation. Chromosoma **106:**348-60.

15. **Hsu, J. Y., Z. W. Sun, X. Li, M. Reuben, K. Tatchell, D. K. Bishop, J. M. Grushcow, C. J. Brame, J. A. Caldwell, D. F. Hunt, R. Lin, M. M. Smith, and C. D. Allis.** 2000. Mitotic phosphorylation of histone H3 is governed by Ipl1/aurora kinase and Glc7/PP1 phosphatase in budding yeast and nematodes. Cell **102:**279-91.

16. **Lottersberger, F., A. Panza, G. Lucchini, S. Piatti, and M. P. Longhese.** 2006. The Saccharomyces cerevisiae 14-3-3 Proteins Are Required for the G1/S Transition, Actin Cytoskeleton Organization and Cell Wall Integrity. Genetics **173:**661-75.

17. **Lottersberger, F., F. Rubert, V. Baldo, G. Lucchini, and M. P. Longhese.** 2003. Functions of Saccharomyces cerevisiae 14-3-3 proteins in response to DNA damage and to DNA replication stress. Genetics **165:**1717-32.

18. **Luo, J., X. Xu, H. Hall, E. M. Hyland, J. D. Boeke, T. Hazbun, and M. H. Kuo.** 2009. Histone H3 Exerts Key Function in Mitotic Checkpoint Control. Mol Cell Biol.

19. **Macdonald, N., J. P. Welburn, M. E. Noble, A. Nguyen, M. B. Yaffe, D. Clynes, J. G. Moggs, G. Orphanides, S. Thomson, J. W. Edmunds, A. L. Clayton, J. A. Endicott, and L. C. Mahadevan.** 2005. Molecular basis for the recognition of phosphorylated and phosphoacetylated histone h3 by 14-3-3. Mol Cell **20:**199-211.

20. **Petosa, C., S. C. Masters, L. A. Bankston, J. Pohl, B. Wang, H. Fu, and R. C. Liddington.** 1998. 14-3-3zeta binds a phosphorylated Raf peptide and an unphosphorylated peptide via its conserved amphipathic groove. J Biol Chem **273:**16305-10.

21. **Pinsky, B. A., C. Kung, K. M. Shokat, and S. Biggins.** 2006. The Ipl1-Aurora protein kinase activates the spindle checkpoint by creating unattached kinetochores. Nat Cell Biol **8:**78-83.

22. **Prigent, C., and S. Dimitrov.** 2003. Phosphorylation of serine 10 in histone H3, what for? J Cell Sci **116:**3677-85.

23. **Sherman, F.** 1991. Getting started with yeast. Methods Enzymol **194:**3-21.

24. **van Heusden, G. P., D. J. Griffiths, J. C. Ford, A. W. T. F. Chin, P. A. Schrader, A. M. Carr, and H. Y. Steensma.** 1995. The 14-3-3 proteins encoded by the BMH1 and BMH2 genes are essential in the yeast Saccharomyces cerevisiae and can be replaced by a plant homologue. Eur J Biochem **229:**45-53.

25. **van Heusden, G. P., and H. Y. Steensma.** 2006. Yeast 14-3-3 proteins. Yeast **23:**159-71.

26. **Wei, Y., C. A. Mizzen, R. G. Cook, M. A. Gorovsky, and C. D. Allis.** 1998. Phosphorylation of histone H3 at serine 10 is correlated with chromosome condensation during mitosis and meiosis in Tetrahymena. Proc Natl Acad Sci U S A **95:**7480-4.

27. **Wei, Y., L. Yu, J. Bowen, M. A. Gorovsky, and C. D. Allis.** 1999. Phosphorylation of histone H3 is required for proper chromosome condensation and segregation. Cell **97:**99-109.

28. **Yaffe, M. B., K. Rittinger, S. Volinia, P. R. Caron, A. Aitken, H. Leffers, S. J. Gamblin, S. J. Smerdon, and L. C. Cantley.** 1997. The structural basis for 14-3-3:phosphopeptide binding specificity. Cell **91:**961-71.

Appendix II: Further investigation of the interactions between H3 and Sgo1p in mitotic tension sensing

INTRODUCTION

Histones are the basic structural and functional components of eukaryotic chromosome. During mitosis, chromatin is decondensed for DNA replication, with the incorporation of newly replicated DNA, it condenses to form sister chromatids, which then will be segregated into daughter cells by pulling forces from spindles emanating from opposite spindle pore bodies. To monitor faithful segregation, spindle assembly checkpoint components function by delaying the metaphase to anaphase transition if either one of the following requirements is missing, bipolar attachment of kinetochores by spindles and tension that is generated between two sister-chromatids held by cohesin complex to remit the pulling forces of the spindles emanating from opposite spindle pole bodies.

My previous studies showed that histone H3 proactively participated in the Sgo1p-mediated tension sensing checkpoint activation, H3 binds directly with Sgo1p and that interaction was diminished largely by mutations in H3 tension sensing motif (3). It is still worthy to continue the investigation of the underlying molecular mechanisms of the interactions between H3 and Sgo1p, particularly in the side of Sgo1p. This study was thus aimed to screen for intra-genic mutations in *SGO1* that would strengthen or bypass the interactions with the mutated H3.

Genetic and biochemical analyses will be followed to characterize the obtained intra-genic suppressor.

MATERIAL AND METHODS

Yeast strains and plasmid constructs. The yeast strains and plasmids used in this work are listed in Tables B-1 and B-2.

Yeast methods. Yeast growth media, conditions, and transformation were based on standard procedures (4). When appropriate, 5% casamino acids (CAA) were used to substitute for synthetic amino acid mixtures as selective medium for uracil, tryptophan, or adenine prototroph. Yeast transformation was done with the lithium acetate method (1).

ChIP experiments were carried out as described (2), using anti-HA (12CA5, Sigma) antibody.

Intra-genic suppressor screen. To screen for Sgo1 mutations that are able to rescue H3 G44S or G44A benomyl hypersensitivity, the error-prone PCR amplification approach was utilized to introduce random mutations into *SGO1* ORF. To that end, primers MHK98 and MHK99 were used to amplify *SGO1* ORF from pJL53 in a mixture of 1X PCR reaction buffer, 7mM $MgCl_2$, 1mM dNTP mixture, 0.4μM primers, 0.4mM $MnCl_2$, and 0.05unit DNA polymerase per

microliter reaction. PCR program is 30 cycles of 1min 94°, 1min 45°, and 2min 72°. The PCR product was gel purified and co-transformed with a *Not* I linearized basal expression plasmid (pJL52) into H3 G44S or G44A mutant cells with *sgo1*Δ background (strains yJL170 and yJL431). Transformants that were able to suppress the benomyl hypersensitivity caused not only by *sgo1*Δ, but also by H3 G44S or G44A mutation were processed for further analyses. Those transformants were patched into YPD and YPD plus 20μg/ml benomyl to screen for potential suppressors. For positive suppressors, 5-FOA selection was applied to pop out the plasmid bearing mutant *sgo1* to verify the plasmid dependency. After the verification of the plasmid dependent suppression, plasmid DNA was extracted, sequenced with primer MHK98 or MHK99, and re-transformed into *sgo1*Δ H3 G44S or G44A mutant cells (strains yJL170 and yJL431), spot assays and chromatin immunoprecipitation approaches were followed to characterize these intra-genic suppressors.

RESULTS

Screen for Sgo1 intra-genic mutations that can rescue H3 G44S tension sensing defect.

My previous studies indicated that H3 plays important roles in sister chromatid tension sensing by either recruiting or retaining Sgo1p at the pericentric region. The mutation of H3 G44S impairs the H3-Sgo1p association both *in vitro* and *in vivo* (3). Considering the fact that G44A phenocopies the G44S defects and that

Gly44 is part of a β turn in H3 N-terminal tail, we suspect that mutating Gly44 to serine or alanine causes a conformational change of H3 β turn, which then diminishes the H3-Sgo1p association. To better understand the interface of H3-Sgo1p association, I carried out an intra-genic screen for mutants/suppressors that can rescue H3 G44S benomyl hypersensitivity, looking for some allele to allele specific mutations in sgo1 that can complement the low affinity of Sgo1p to H3 G44S. As shown in Figure 1, suppressors S68 and S71 can rescue H3 G44S benomyl hypersensitivity while S70 and S75 only slightly rescue that defect, although all suppressors S64, S65, S67, S68, S69, S70, S71 and S75 rescue the defective growth of H3 G44S at 14°. Suppressors S68, S71 were chosen for further studies. Similarly, other suppressors S53, A1, A5 (A1, A5 are from H3 G44A suppression screen) were identified, all characterized intra-genic mutations are mapped and listed in Figure 2.

Overproduction of Sgo1p can rescue the H3 G44S benomyl hypersensitivity. To rule out the possibility that the observed suppression of benomyl hypersensitivity resulted from a higher protein level of Sgo1p, Western blot analysis was performed (Fig. 3). The variable Sgo1p protein levels in sgo1 intra-genic suppressors A5, S53, S68, S71 did not exceed the expression level of wildtype Sgo1p (lane 3), Interestingly, suppressor S71 expresses a truncated Sgo1p and sequencing result also indicates that is the case (Fig. 2).

To examine whether these suppressors can restore Sgo1p back into the pericentric region in H3 G44S cells, chromatin immunoprecipitation was performed. Figure 4A indicated that suppressor S53 is unable to restore the pericentric association of Sgo1p in H3 G44S cells. Similar patterns were also observed in Figure 4B, where although A5, S71 (lane 6, 8 respectively) show comparable centromeric Sgo1p association when compared to wildtype Sgo1p (lane 4, 5), these suppressors did not distinguish themselves from wildtype Sgo1p in the pericentric (CEN16R 1.7kb) region. Suggesting the observed genetic suppression by these suppressors was not due to the restoration of Sgo1p to pericentric region in H3 G44S cells.

DISCUSSION

Throughout the studies of H3 G44S and its interaction with Sgo1p, we proposed a model in which the structural features of Gly44 and nearby residues allow that region to form a β turn, and a tension dependent conformational change of which regulates the binding of Sgo1p to H3. Histone H3 thus plays a structural role in tension sensing. I wished to examine this interaction in a great detail by characterizing sgo1 mutants that can restore the tension sensing function of the G44S and G44A mutants.

With little structural information of Sgo1p in hand, it is hard to even predict how or which region of Sgo1p is important for H3-Sgo1p interaction. Intra-genic

suppressor screen of Sgo1 for H3 G44S (or G44A) benomyl hypersensitivity generated five good candidates. One important finding is that the removal of C-terminal 270aa of Sgo1p (total 590aa) actually rescues H3 G44S benomyl hypersensitivity (suppressor S71 Y317X mutation). Additionally, mutations in the C-terminal region of Sgo1p were also found in other four suppressors. Together, C-terminal region of Sgo1p is inhibitory for the interaction of Sgo1p and H3. It is likely that C-terminal region need to be processed for Sgo1p to be mature or be activated for tension sensing function. The failure to observe the pericentric restoration of mutant Sgo1p in ChIP analyses may also be explained in that these suppressors actually bypass the requirement to be pericentric localized. In that case, Sgo1p is retained or recruited to the pericentric region by H3 at Gly44 and is further processed by currently unknown mechanism, the processed Sgo1p signals the generation of tension between two sister-chromatids, and leads to cell's metaphase to anaphase transition.

TABLE B-1. Yeast strains used in this study

Strain	Relevant genotype	Source or reference
yMK1361	*MATa ade2-1 can1–100 his3–11,15 leu2–3,112 trp1–1::sgo1*::TRP1 *ura3-1 hht1-hhf1::KAN hht2-hhf2::KAN hta1-htb1::Nat hta2-htb2::HPH* pQQ18 [*ARS CEN LEU2 HTA1-HTB1 HHT2-HHF2*]	This study
yJL170	*MATa ade2-1 can1–100 his3–11,15 leu2–3,112 trp1–1::sgo1*::TRP1 *ura3-1 hht1-hhf1::KAN hht2-hhf2::KAN hta1-htb1::Nat hta2-htb2::HPH* pMK439G44S [*ARS CEN LEU2 HTA1-HTB1 hht2-G44S-HHF2*]	This study
yJL258	*MATa ade2-1 can1–100 his3–11,15 leu2–3,112 trp1–1 ura3-1 hht1-hhf1::KAN hht2-hhf2::KAN hta1-htb1::Nat hta2-htb2::HPH* pQQ18 [*ARS CEN LEU2 HTA1-HTB1 HHT2-HHF2*] pJL51 [2µm URA3 HA-SGO1]	This study
yJL431	*MATa ade2-1 can1–100 his3–11,15 leu2–3,112 trp1–1::sgo1*::TRP1 *ura3-1 hht1-hhf1::KAN hht2-hhf2::KAN hta1-htb1::Nat hta2-htb2::HPH* pMK439G44A [*ARS CEN LEU2 HTA1-HTB1 hht2-G44A-HHF2*]	This study
yJL299	*MATa ade2-1 can1–100 his3–11,15 leu2–3,112 trp1–1::sgo1*::TRP1 *ura3-1 hht1-hhf1::KAN hht2-hhf2::KAN hta1-htb1::Nat hta2-htb2::HPH* pQQ18 [*ARS CEN LEU2 HTA1-HTB1 HHT2-HHF2*] pJL53 [ARS URA3 SGO1]	This study
yJL303	*MATa ade2-1 can1–100 his3–11,15 leu2–3,112 trp1–1::sgo1*::TRP1 *ura3-1 hht1-hhf1::KAN hht2-hhf2::KAN hta1-htb1::Nat hta2-htb2::HPH* pMK439G44S [*ARS CEN LEU2 HTA1-HTB1 hht2-G44S-HHF2*]	This study

TABLE B-2. Plasmid constructs used in this study

Plasmid	Main features	Source or reference
pJL51	2µm URA3 p*ADH*1-3x*HA-SGO*1-t*ADH*1	This study
pJL52	ARS1 CEN4 URA3 p*ADH*1-3x*HA*-t*ADH*1	This study
pJL53	ARS1 CEN4 URA3 p*ADH*1-3x*HA-SGO*1-t*ADH*1	This study

Fig. B-1

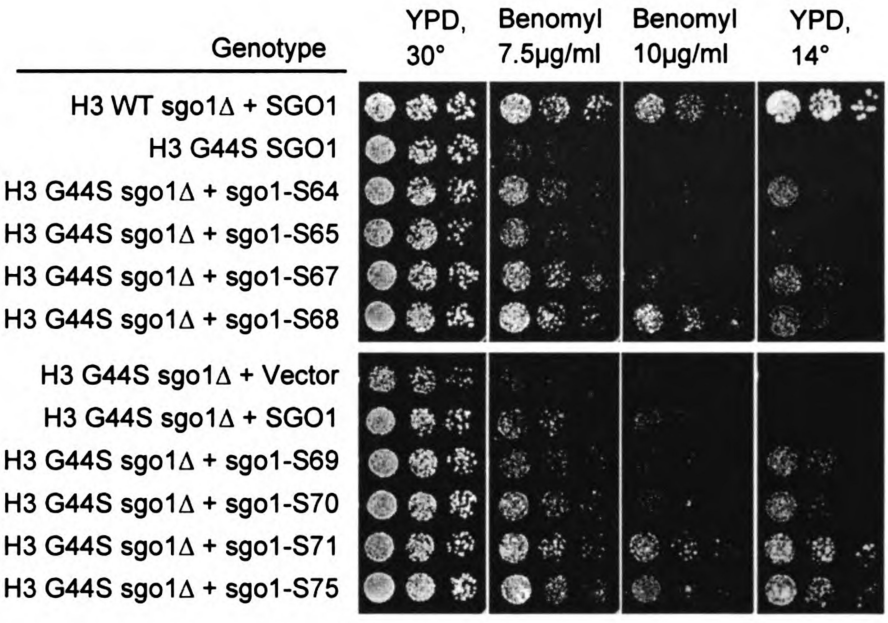

FIG. B-1. Screen for intra-genic mutations of *SGO1* that rescue the benomyl hypersensitivity of H3 G44S. Spot assay were performed to verify the suppression of H3 G44S benomyl hypersensitivity by intra-genic mutants of *sgo1*. *ARS CEN4* driven plasmids with either wildtype *SGO1* or bearing random error-prone PCR amplified *sgo1* ORF were transformed into *sgo1*Δ cells, 6 fold serial dilutions of cells were spotted into plates containing rich medium YPD with the absence or presence of benomyl as shown in the top.

Fig. B-2

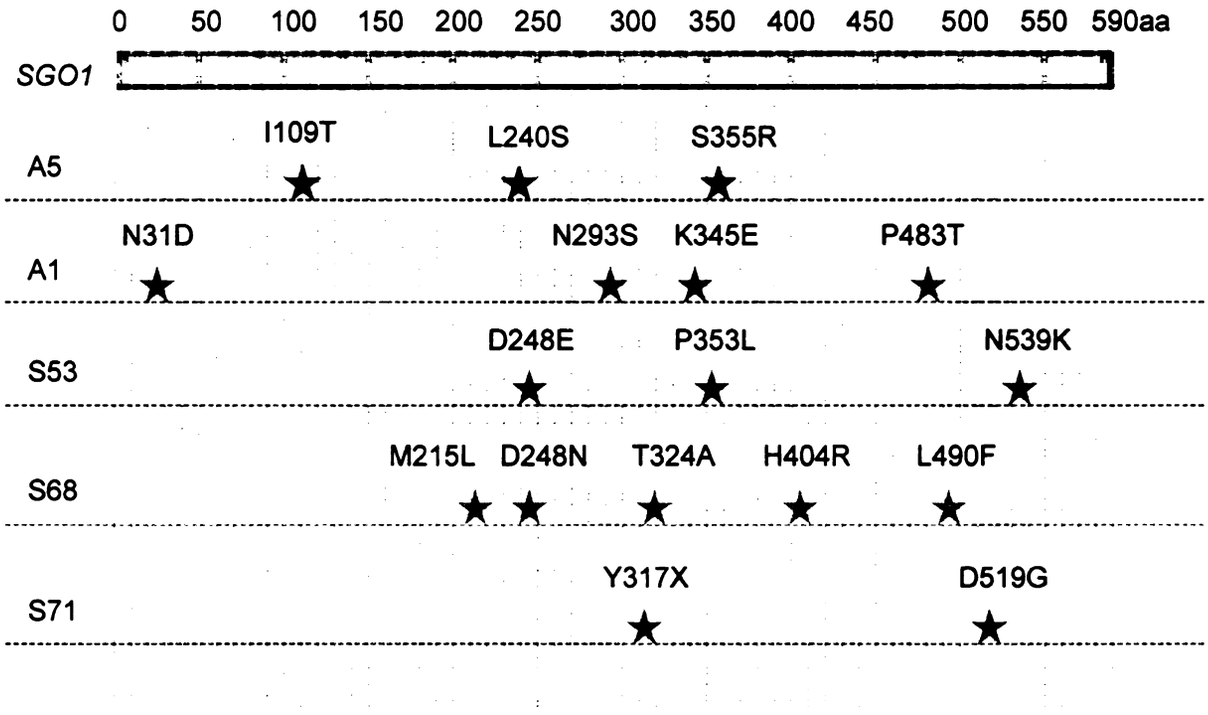

FIG. B-2. Schematic list of mutations identified in the intra-genic suppressor screen.

Fig. B-3

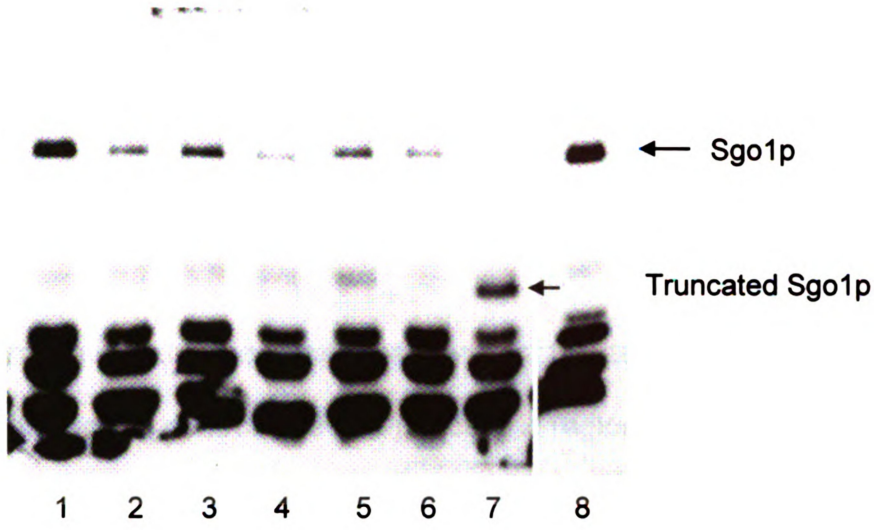

1: H3 G44S sgo1Δ + sgo1-A5
2: H3 WT sgo1Δ + SGO1
3: H3 G44S sgo1Δ + SGO1
4: H3 G44S sgo1Δ + sgo1-S53
5: H3 G44S sgo1Δ + sgo1-S64
6: H3 G44S sgo1Δ + sgo1-S68
7: H3 G44S sgo1Δ + sgo1-S71
8: 2μ Sgo1p positive control

FIG. B-3. Western Blot analysis against Sgo1p fused HA tag shows no major increase of Sgo1p level among intra-genic suppressors when compared to wildtype Sgo1p (lane 2, 3). Arrow indicates the size of Sgo1p, in suppressor S71 (lane 7) a truncated Sgo1p was detected. Cell were grow to log phase, whole cell extracts were prepared by boiling cell pellets in 2X SDS loading dye and vortex for 5 minutes at room temperature, extracts equal to 0.2 OD600 cells were loaded. Strains used lane 2: yJL299; lane 3: yJL303; lanes 4 to 7 were from suppressors Sis-S53, Sis-S64, Sis-S68, and Sis-S71 respectively.

FIG. B-4. Chromatin immunoprecipitation analysis of the association of intra-genic mutants of Sgo1 at centromere and pericentric region. (A) ChIP analysis of H3 G44S sgo1 intra-genic suppressor S53 at CEN3, CEN16 and pericentric region 0.3kb left or 1.7kb right from CEN16. Star marks internal common PCR control at DED1 locus. Top bands are PCR signals from positions shown in top of each image. Strain used in lane 2 is yJL299, lane 3 is yJL303, and lanes 4, 5 are Sis-S53. (B) ChIP analysis of H3 G44S sgo1 intra-genic suppressors A5, S68, S71 at centromere of chromosome 16 and pericentric region 1.7kb right from CEN16. Strain used in lane 3 is yJL299, lanes 4, 5 are yJL303, and lanes 6, 7, 8 are suppressors Sis-A5, Sis-S68, Sis-S71 respectively.

Fig. B-4

A

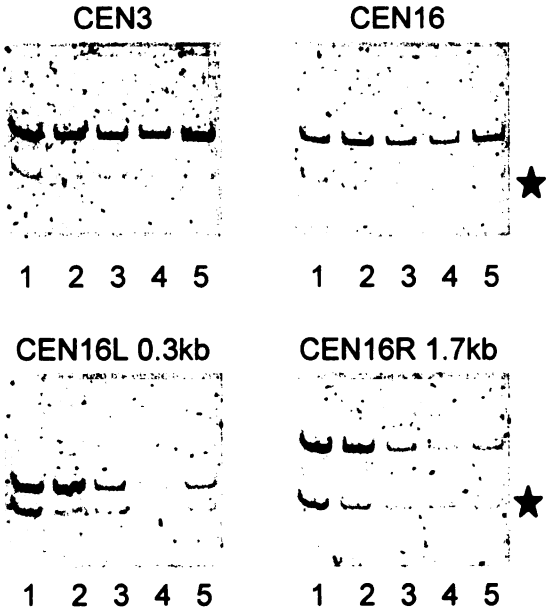

1: H3 G44S sgo1Δ + sgo1-S53 INP
2: H3 WT sgo1Δ + SGO1
3: H3 G44S sgo1Δ + SGO1
4: H3 G44S sgo1Δ + sgo1-S53
5: H3 G44S sgo1Δ + sgo1-S53

B

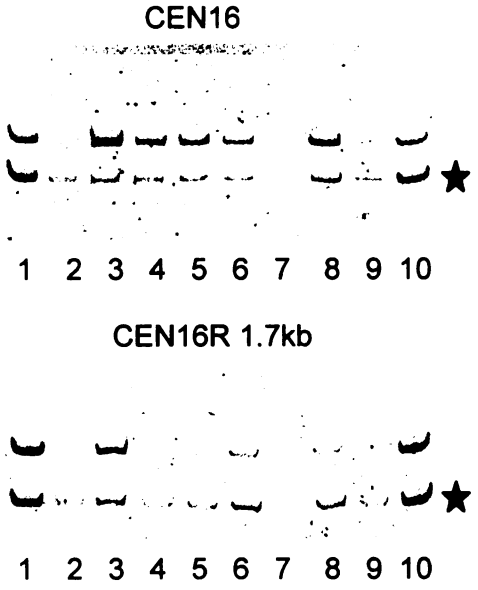

1: H3 WT sgo1Δ + SGO1 INP
2: H3 WT sgo1Δ + SGO1 no Ab control
3: H3 WT sgo1Δ + SGO1
4: H3 G44S sgo1Δ + SGO1
5: H3 G44S sgo1Δ + SGO1
6: H3 G44S sgo1Δ + sgo1-A5
7: H3 G44S sgo1Δ + sgo1-S68
8: H3 G44S sgo1Δ + sgo1-S71
9: H3 G44S sgo1Δ + sgo1-S71 no Ab control
10: H3 G44S sgo1Δ + sgo1-S71 INP

REFERENCES

1. **Gietz, D., A. St Jean, R. A. Woods, and R. H. Schiestl.** 1992. Improved method for high efficiency transformation of intact yeast cells. Nucleic Acids Res **20:**1425.

2. **Kuo, M. H., and C. D. Allis.** 1999. In vivo cross-linking and immunoprecipitation for studying dynamic Protein:DNA associations in a chromatin environment. Methods **19:**425-33.

3. **Luo, J., X. Xu, H. Hall, E. M. Hyland, J. D. Boeke, T. Hazbun, and M. H. Kuo.** 2009. Histone H3 Exerts Key Function in Mitotic Checkpoint Control. Mol Cell Biol **30:**537-549.

4. **Sherman, F.** 1991. Getting started with yeast. Methods Enzymol **194:**3-21.